# ADDIS ABABA UNIVERSITY

# ADDIS ABABA INSTITUTE OF TECHNOLOGY

## SCHOOL OF CIVIL AND ENVIRONMENTAL ENGINEERING

# Effects of hydrated lime as a filler on properties and performance of mastics and hot mix asphalt


**By**

**IBRAHIM HAMID KELAY**


**A Thesis**

**Submitted in Partial Fulfillment of the Requirements for the Degree of Master of Science in Road and Transportation Engineering**

**Advisor**

**Habtamu Melese (PHD, PE)**

**June, 2018**

**Addis Ababa, Ethiopia**

ADDIS ABABA UNIVERSITY

ADDIS ABABA INSTITUTE OF TECHNOLOGY

SCHOOL OF CIVIL AND ENVIRONMENTAL ENGINEERING

# Effects of hydrated lime as a filler on properties and performance of mastics and hot mix asphalt

By

Ibrahim Hamid Kelay

A Thesis Submitted in Partial Fulfillment of the Requirement for the Degree of Master of Science

In

Civil Engineering (Road and Transport Engineering)

**Approved by Board of Examiner**

| | | |
|---|---|---|
| Habtamu Melese (PHD.PE) | _____ | _____ |
| Advisor | Signature | Date |
| _____ | _____ | _____ |
| Internal Examiner | Signature | Date |
| _____ | _____ | _____ |
| External Examiner | Signature | Date |
| _____ | _____ | _____ |
| Chairman | Signature | Date |

# DECLARATION

I certify that research work titled "Effects of hydrated lime as a filler on properties and performance of mastics and hot mix asphalt" is my own work. The work has not been presented elsewhere for assessment and award of any degree or diploma. Where material has been used from other sources it has been properly acknowledged.

Ibrahim Hamid

# ABSTRACT

Flexible or asphalt concrete pavement is the paving system most widely adopted all over the world. It has been recognized that there are many different types of factors affecting the performance and durability of asphalt concrete pavement, including the service conditions, such as: variation of temperature from mild to extremes and repeated excessive axle loading as well as inadequate quality of the raw materials. All of these when combined together are going to accelerate the occurrence of distresses in flexible pavement such as permanent deformation and fatigue cracking.as a result proper mix design and appropriate material is a crucial for compromising the distress occurred at the service life of the pavements.

This study is about the effect of hydrated lime as filler on paving grade bitumen under various conditions. The basis of the thesis is to find out change in the rheological properties of the bitumen by modifying it with different fillers type and percentage. The types of fillers used in this research are hydrated lime and crushed Stone dust. Fillers help in filling the voids and change the physical and chemical properties. Fillers modify the properties, increase the performance of, and provide improved durability to various construction materials. The effects of fillers are therefore of vital importance. When bitumen is combined with filler, mastic is formed. This mastic can be viewed as the component of the asphalt mixture that binds the aggregates together and also the component of the asphalt that undergoes deformation when the pavement is stressed under traffic loading. The characteristics of the filler can significantly influence the properties of the mastic, and thus the filler properties can have significant effects on asphalt mixture performance.

Therefore, the main objective of this research is to investigate experimentally effect of using hydrated lime as a fillers on property and performance of asphalt mastic and hot asphalt concrete mixtures.

Different percentage of hydrated lime and crushed stone fillers (25%, 35% & 45% based on Filler to asphalt ratio) is used to modify the bitumen (Penetration grade 60-70). Various physical tests were conducted on virgin and modified bitumen (Mastic) for aged and Unaged samples to evaluate its rheological properties and the results were analyzed and compared.

The research evaluated the rheological tests conducted using dynamic shear rheometer (DSR) on mastics prepared from hydrated lime and crushed stone (as controlled Specimen). The major tests performed on DSR were Amplitude sweep test (AST) conducted for determining The visco- elastic region LVE for mastic, Frequency sweep test (FST) conducted to Construct master curve(for complex modulus and phase angle) and backspace diagram. AST & FST conducted for intermediate and high temperature ($10^oC$, $21.1^oC$, $37.8^oC$ & $54.4^oC$). Multiple stress and creep recovery (MSCR) test conducted to determine rutting parameter Recovery compliance ($J_{nr}$) and Performance Grade (PG) used for checking asphalt binder environmental temperature resistance. MSCR and PG test were conducted at higher temperatures ($52^oC$, $58^oC$, $64^oC$, $70^oC$ & $76^oC$).

The Research conclude that both fillers (Hydrated lime and crushed stone dust fillers) have an effect on asphalt mastic rheology and asphalt concrete properties. When the filler to asphalt ratio increased, the stiffness of asphalt mastic and asphalt concrete increased. As compared to crushed stone filler, asphalt mastic prepared with Hydrated lime had higher stiffness value and improve rutting performance of asphalt mastic at high temperature. Master curves developed from frequency sweep test showed that hydrated lime improves the shear modulus at high temperature and low frequency.

**Key Words:** Asphalt Mastics, Performance, Superpave

## ACKNOWLEDGEMENTS

I would like to express my profound gratitude to my advisor Dr. Habtamu Melese for providing me invaluable support, guidance and encouragement throughout this study. I am truly grateful for his advice in my personal and professional development. I would also like to thank the stuff of the Highway department lab for their kind assistance with several issues.

# Table of Contents

Abbstract ……..……..……..…….....III
Acknowledgment ……..……...……....V
Table Of Content ….……..…...VI
List Of Table……...…. VIII
List Of Figure……...…….……..…..*IX*
Abrevation ……..……....X
**CHAPTER 1. INTRODUCTION**..... 1
1.1. Background..... 1
1.2. Statement of the Problem..... 2
1.3. Objectives of the Study..... 2
1.4. Scope of the study..... 3
**CHAPTER 2. LITERATURE REVIEW**..... 4
2.1 Mineral Filler..... 4
2.2 Hydrated Lime..... 7
2.2.1 Introduction..... 7
2.2.2 Effect of Hydrated lime on Mix..... 7
2.2.3 Effect of Hydrated Lime on bitumen Rheology..... 8
**2.3 Bitumen Rheology**..... 10
2.3.1 General..... 10
2.3.2 Bitumen Constitution..... 10
2.3.3 Rheological properties of bitumen..... 11
2.4 Dynamic Oscillatory Testing Using a DSR..... 15
**CHAPTER 3. RESEARCH METHODOLOGY**..... 18
3.1 Experimental design..... 18
3.2 Materials and Laboratory Testing..... 18
3.2.1 Material Selection..... 19
3.2.2 Preparation of mastics..... 20
3.2.3 Laboratory Testing..... 21
3.3 Research Work Plan and Flow Chart..... 33
3.3.1. Research work plan..... 33
3.3.2. Experimental flow chart..... 34
CHAPTER 4. RESULT AND ANALYSIS..... 35
4.1. Dynamic Shear Rheological (DSR) Analysis of Asphalt Mastics..... 35
4.1.1. Amplitude Sweep Test (AST) Results..... 35

4.1.2. Frequency Sweep Test (FST) Results ..... 41
4.1.3. Performance Grade (PG) Test Results ..... 49
4.1.4. Multiple stress Creep Recovery (MSCR) Test Results ..... 52
CHAPTER 5. CONCLUSION AND RECOMMENDATION ..... 59
**5.1.** Conclusion ..... 59
**5.2.** Recommendation ..... 611
REFERENCES ..... 622
**APPENDIX A- MATERIAL QUALITY TEST RESULT** ..... 655
**APPENDIX B –AMPLITUDE SWEEP TEST (AST) TEST RESULT** ..... 666
**APPENDIX C – FREQUENCY SWEEP TEST (FST) TEST RESULT** ..... 6969
**APPENDIX D – STATICALLY ANALYSIS USING ANOVA (USING MS-EXCEL)** ..... 733
**APPENDIX D – PERFORMANCE GRADE (PG) TEST RESULT** ..... 755
**APPENDIX F - MSCR TEST RESULT** ..... 766

# List of Table

**Table 3.1:-** Tests that are conducted for the Asphalt Binder .....12

**Table 3.2:-** Tests that are conducted for the aggregate .....19

**Table 3.3:-** Recipe of mastics for DSR Test .....20

**Table 3.4:-** Matrix of bitumen-filler mastics .....21

**Table 3.5:-** Ratio of filler to bitumen in bitumen filler system .....21

**Table 3.6:-** Summary of the AASHTO MP-1 Specification .....23

**Table 3.7:-** Traffic Designation AASHTO M-332. .....30

**Table 3.8:-** Target Shear Stress and Strain Values for PG test .....30

**Table 3.9:-** Work plan for the research .....33

**Table 4.1:-** Summary of LVE region strain .....40

**Table 4.2:-** shift factor for complex modulus master curve on asphalt mastics for reference temperature 21.1$^{o}$C .....48

**Table 4.3:-** shift factor for phase angle master curve on asphalt mastics for reference temperature 21.1$^{o}$C .....48

**Table 4.4:-** Summary of ANOVA hypothesis test .....49

**Table 4.5:-** PG determination for Unaged 25%HL mastics .....50

**Table 4.6:-** PG determination for RTFO-Aged 25%HL mastics .....51

**Table 4.7:-** PG determination for RTFO-Aged 25%HL mastics .....51

**Table 4.8:-** Summary of MSCR testing temperature .....39

**Table 4.9:-** Summary of $J_{nr}$ and PR (%) Results .....57

# List of Figure

**Figure 2.1:-** Flow properties of bitumen as a function of temperature (at a given loading time . 12
**Figure 2.2:-** Idealized response of elastic, viscous, and viscoelastic materials under constant stress loading [Anderson] ..... 13
**Figure 2.3:-** Idealized response of viscoelastic materials under constant stress loading ..... 14
**Figure 2.4:-** the relationship between complex modulus (G*), storage modulus (G'), loss modulus (G'') and phase angle (δ) [Anderson]. ..... 15
**Figure 2.5**:- Testing arrangement in DSR (Airey, 1997) ..... 16
**Figure 2.6:-** Principles involved in DSR test (Airey, 1997) ..... 17
**Figure 4.7:-** Effect of crushed stone Filler (CSF) and temperature on asphalt mastic ratio 25% CSF ..... 35
**Figure 4.8:-** Effect of Hydrated Lime Filler (HL) and temperature on asphalt mastic ratio 25% HL ..... 36
**Figure 4.9:-** Effect Hydrated Lime filler ratio on asphalt mastic at temperature 37.8$^{o}$C ..... 36
**Figure 4.10:-** Effect of Crushed stone filler ratio on asphalt mastic at temperature 37.8oC ..... 37
**Figure 4.11:-** Effect of Filler and filler ratio on asphalt mastic at temperature 37.8oC ..... 37
**Figure 4.12:-** Effect of Temperature on LVE region of asphalt mastic ..... 38
**Figure 4.13:-** Effect of ageing on LVE region for 35% HL asphalt mastic at 21.1°C ..... 39
**Figure 4.14:-** Effect of aging on LVER For 25% HL mastics ..... 39
**Figure 4.15:-** Effect of filler type and content on stiffness of asphalt mastics at temperature 54.4oC ..... 40
**Figure 4.16:-** Effect of temperature and frequency on G* asphalt mastic at 25%HL ..... 42
**Figure 4.17:-** Shifting for complex modulus master curve for 25%HL mastic ..... 42
**Figure 4.18:-** Effect of temperature and frequency on $\delta$ asphalt mastic at 25% HL ..... 43
**Figure 4.19:-** Shifting for phase angle master curve for 25% HL ..... 43
**Figure 4.20:-** Complex modulus and phase angle master curve for 25% HL ..... 43
**Figure 4.21:-** Stiffness master curve for mastics with Hydrated Lime ..... 44
**Figure 4.22:-** Phase angle master curve for mastics with Hydrated Lime ..... 45
**Figure 4.23:-** Black space diagram for 25% HL ..... 46
**Figure 4.24:-** Effect of aging on stiffness of asphalt mastic (binder PG 60/70) ..... 47
**Figure 4.25:-** Effect of aging on stiffness of asphalt mastic (25% HL) ..... 47
**Figure 4.26:-** Effect of loading on MSCR total strain for 25%HL mastics at 70$^{o}$C ..... 53
**Figure 4.27:-** Effect of Temperature on MSCR-3.2kPa total strain for 25%HL mastics ..... 54

**Figure 4.28:-** Effect of Temperature on MSCR-0.1kPa total strain for 25%HL mastics..... 54
**Figure 4.29:-** Effect of filler content on MSCR 3.2kPa total strain for mastics at 64oC ..... 55
**Figure 4.30:-** Effect of filler content on MSCR 0.1 kPa total strain for mastics at 64oC ..... 55
**Figure 4.31:-** Effect of filler type on MSCR 0.1 kPa total strain for 25% HL & CSF mastics at 64oC ..... 56
**Figure 4.32:-** Effect of filler type on MSCR 0.1 kPa total strain for 25% HL & CSF mastics at 64oC ..... 56
**Figure 4.33:-** Effect of filler type on MSCR total strain for 25% HL & CSF mastics at 64$^{o}$C..... 566
**Figure 4.34:-**Non recoverable creep compliance Jnr-3.2kpa ..... 577
**Figure 4.35:-** Effect of temperature and filler content on $J_{nr}$ at 3.2kPa..... 58
**Figure 4.36:-** Non recoverable creep compliance $J_{nr\text{-}3.2kpa}$ & $J_{nr\text{-}0.1kpa}$ ..... 58

# CHAPTER 1. INTRODUCTION

## 1.1. Background

The increase in traffic volume over the past decades required the laying down of higher quality roadways. Researchers worldwide try to develop better composites, both affordable and more resistant, and a lot of money is invested on the development of new performance tests that better simulate field conditions. The quality level of highways is directly associated with the proper selection of materials (aggregates, binder, and additives), mix design, proper construction procedures, and adequate structural design of the pavement layers. If these factors are optimized, the distresses on the structure will be reduced, thereby significantly affecting the costs associated with rehabilitation and replacement of the structures. One of the major concerns in the mix designing is the type and amount of filler used, which is known to highly affecting the mix design, especially the optimum asphalt content.

Mineral fillers serve a dual purpose when added to asphalt mixtures. The proportion of mineral filler that is finer than the thickness of the asphalt film blends with asphalt cement binder to form a mortar or mastic that contributes to improved stiffening of the mix. Particles larger than the thickness of the asphalt film behave as mineral aggregate and hence contribute to the contact points between individual aggregate particles (Puzinauskas 1969).

Furthermore, they affect the workability, moisture sensitivity, stiffness and ageing characteristics of hot mix asphalt (HMA) (Mogawer et al. 1996). Also, fillers vary in gradation, particle shape, surface area, void content, mineral composition, and physico-chemical properties. Therefore, their influence on the properties of HMA mixtures also varies. The maximum allowable amount should be different for various types of filler.

The filler also influences the optimum asphalt content (OAC) in bituminous mixtures by increasing the surface area of mineral particles and, simultaneously, the surface properties of the filler particles modify significantly the rheological properties of asphalt such as penetration, ductility, and also those of the mixture, such as resistance to rutting. In order to improve the pavement performance, it is necessary to ensure that adequate behavior of the bituminous mixtures is achieved, which depends essentially on their composition.

Therefore, selecting the proper type of filler in asphalt mixtures would improve the filler's properties and, thus, enhance the mixture's performance (Kandhal 1981).

## 1.2. Statement of the Problem

In recent years, Ethiopia has experienced an increase the severity and extent of Pavement distress on the roads due to increments of traffic volume. Tire pressure and axle load increases mean that the bituminous layer near the pavement surface is exposed to higher stresses. High density of traffic in terms of commercial vehicles, overloading of trucks and significant variations in daily and seasonal temperature of pavements have been responsible for development of distress symptoms like raveling, undulations, rutting, cracking, bleeding, shoving and potholing of bituminous surfaces. In fact to mitigate the problem the roads has treated by a periodic and routine maintenance under concerned body. However, after serving some time the distress begin to appear and problem is still continuing.

Suitable material combinations and bituminous binders have been found to result longer life for wearing courses depending upon the percentage of filler and type of fillers used. Now a day crushed stone filler is the main filler type used in different construction projects of the countries however this filler type has less filler to filler interaction property and low affinity to bitumen and gives less strength and stiffness to asphalt mixture. Therefore, better filler material that enhance and improve the rheological properties of mastics and stiffness of the mix is needed to resist failure or distress when subjected to traffic loading or other environmental factors.

## 1.3. Objectives of the Study

The main objective of the study is to determine the effect of hydrated lime as filler on asphalt binder rheology and mastic property of HMA in order to evaluate the distress caused by traffic loading and weather conditions (Temperature).

**The specific objectives are**

- To evaluate the effect of crushed stone dust and hydrated lime filler on the rheology property of the bitumen.
- To determine visco-elastic ranges of modified binders using Amplitude Sweep Test.
- To evaluate rheological properties of the binders by developing master curves from Frequency Sweep Test
- To evaluate permanent deformation using Multiple Stress Creep Recovery Test.
- To determine Performance Grades of the binders for comparison.

## 1.4. Scope of the study

A detailed laboratory testing would be performed on samples of the asphalt mastics from the different fillers type crushed stone; hydrated lime and different filler content with percentage on mastics (25%, 35% & 45%) on the 60/70 penetration grade binder. The study more focuses on the rheological characteristics of asphalt binder and mastic (asphalt binder plus filler). The rheological tests are conducted using a Dynamic Shear Rheometer (DSR) apparatus for intermediate and high temperature. However rheological tests conducted using Bending Beam rheometer (BBR) for low temperature and Pressure aging Vessels (PAV) for long term aging is not done due to absence of apparatuses in the country.

# CHAPTER 2. LITERATURE REVIEW

## 2.1 Mineral Filler

The term mineral filler refers to the fraction of the mineral aggregate, which mostly passes the 75μm sieve. Many different materials such as limestone dust, volcanic ash, silt, powdered shale, Portland cement, mineral sludge, hydrated lime, rock flour, diatomaceous earth and fly ash, referred to as filler types, can be described in this way (Tunnicliff, 1962). Usually asphalt mixtures have been designed to include mineral filler. Different filler types may be used interchangeably, and different quantities of one type may satisfy a single mixture design situation. The filler is important because of the surface area involved, and that properties of an asphalt pavement may be improved by the use of filler include strength, plasticity, amount of voids, resistance to water action and resistance to weathering (Tunnicliff, 1962). Traxler and Miller (1936) classified filler characteristics as follows:

- Primary characteristics of fundamental importance: particle size, size distribution, and shape.
- Primary mineralogical characteristics of less importance: texture, hardness, strength, specific gravity and wettability
- Secondary characteristics dependent on one or more primary characteristics: void content, average void diameter and surface area.

Kavussi and Hicks (1997) mentioned that in the early times, the evaluation of mineral filler in asphalt mixtures, relied on routine laboratory tests, most from soil mechanics.

These tests involved liquid limit, plasticity index, cementation (to test coagulation or cohesion properties), shrinkage test, and water-bitumen preferential test (to reject hydrophilic fillers). As researchers became more experienced with mineral fillers, tests such as particle density, shape, surface texture, size distribution, surface area, air permeability, bulk density, fractional voids in dry compacted filler, pore diameter and permeability of packed filler to water were recognized to be the importance to evaluate filler. In order to provide satisfactory engineering properties to an asphalt mixture, a filler should not possess high porous particles and at the same time, having a hydrophobic surface, with high affinity to bitumen. Under these conditions, it might absorb the lighter oily fractions of the bitumen

present in the mixture, tending to stiffen it. Additionally, it should not have an adverse chemical reaction with bitumen, and not possess hydrophilic surface in order to ensure good adhesion between binder and aggregates.

### 2.1.1 The Role of Mineral Filler in Asphalt Mixtures

How then does the mineral filler fraction affect the performance of HMA? First, it is well known that the addition of mineral filler causes a stiffening effect. This stiffening effect depends on the temperature, stiffening increases with increasing temperature a desirable trend. Mineral fillers, in essence, lower the temperature dependency of binders, making them less viscous at elevated temperature with relatively little effect on stiffness at low temperatures. To this extent mineral fillers are desirable, low-cost asphalt modifiers.

However, an excessive amount of filler can lead to unwanted stiffening. For this reason, and recognizing that too little mineral filler is also undesirable, the SHRP volumetric mix design criteria limit the filler content (dust: asphalt ratio) to a range between 0.60 and 1.20 by volume. [Anderson, D.A, 1987].

Filler type and particle size directly affect the engineering properties of the asphalt mixtures, In addition to filling the voids, the fillers' components interact with the binder present in the mix, potentially making it stiff and brittle. The change in mix properties is strongly related to the properties of the filler. (R Muniandy, 2013).

Fillers tend to increase the resilient modulus of asphalt mixes (Anderson 1987) .However, most of the strength of HMA is attributed to the surface contact between the aggregate particles. Excessive amount of fillers will result in an increase in the bitumen content and can result in a weak asphalt mix (Kandhal et al 1998).

Asphalt paving mixtures have been designed to include mineral filler since about 1890 (Tunnicliff, 1967). The filler plays an important role in determining the properties and behavior of the mixture. The role of mineral filler in the paving mixture can be divided into two parts. The filler serves as an inert material for filling the voids between coarser aggregate in the mixture. On the other hand, the filler serves as an active material, the activity taken place in the properties at the interface between the filler and the bitumen, because of its fineness and surface characteristics.

Mineral fillers are added to asphalt paving mixtures to fill the voids of the aggregate and reduce the voids in the mixture. However, addition of mineral fillers has dual purpose when added to asphalt mixtures (Richardson 1915). A portion of the mineral filler that is finer than the asphalt film thickness mixed with asphalt binder forms a mortar or mastic and contributes to improved stiffening of mix. This modification to the binder that may take place due to addition of mineral fillers could affect asphalt mixture properties such as rutting and cracking.

The other portion of fillers larger than the asphalt film thickness behave as a mineral filler and serves to fill the voids between aggregate particles, thereby increasing the density and strength of the compacted mixture. In general, filler have various purposes among which, they fill voids and hence reduce optimum asphalt content and increase stability, meet specifications for aggregate gradation, and improve bond between asphalt cement and aggregate [Brown et al 1989].

The workability and practical performance of asphalt mixtures depend largely on the proportion and type of filler used. Generally, the addition of filler results in a decrease in percentage of air voids in asphalt mixtures. The difference in densification is one of the reasons why mixtures containing different quantities of filler possess different mechanical properties. Anderson (1987) indicated the mineral filler may affect asphalt paving materials in a number of ways such as: stiffen and extend the bitumen, alter the moisture resistance, affect the ageing characteristics, and affect the workability and compaction characteristics of the asphalt mixtures.

The most important effect of filler is its stiffening effect. Mineral fillers are also important in changing the viscosity of the binder. They tend to make binder less viscous at elevated temperatures in such a way they can be regarded as modifiers. Having a high content of filler, however, will result in undesirable stiffness which can affect the workability of the mix. The stiffening effect of fillers tends to decrease at lower temperatures instead the mineral fillers tend to improve the fracture properties of the asphalt binder (Lee et al 1995). Hugo, B., et. al. evaluated the potential benefits of using calcareous fillers to improve aging resistance of bitumen. They concluded that calcareous fillers greatly influenced the properties of bitumen provided that filler content does not exceeds a critical concentration determined by the type of filler and binder to be used.

Wojciech, G., and Jaroslaw, W., studied the structure of lime stone mineral filler and evaluated their stiffening properties in fill-bitumen mastic. They concluded that specific surface area, average grain diameter, grain diameter and grain morphology greatly influenced the stiffening properties in filler-bitumen materials.

The quality of mastics, the combination of asphalt binder and filler, influences the overall mechanical performance of asphalt mixtures as well as placement workability. Generally the effect of the filler is based on a volumetric filler effect or an interactive role between the filler and the bitumen due to the fineness and surface characteristics of the filler. [Christopher, 2004].

Some fillers may be added in relatively large quantities without stiffening the binder. These fillers can extend the binder making the mix appear to have an excessive asphalt content. On the other hand, too little mineral filler may reduce the effective viscosity of the mastic and lead to premature rutting of the pavement. Clearly neither too little nor too much mineral filler is desirable. Unfortunately, the maximum or minimum allowable filler content depends on a number of factors such as the source and gradation of the filler and the gradation of the mixture. Stiffening and extension of the asphalt by mineral filler can also affect the design asphalt selected during mix design.

## 2.2 Hydrated Lime

### 2.2.1 Introduction

Hydrated lime is mainly composed of calcium hydroxide $Ca(OH)_2$. It is obtained by hydrating quicklime (essentially calcium oxide, CaO) using specific equipments. Quicklime is manufactured by burning limestone of very high purity (made of calcium carbonate, $CaCO_3$) at temperatures around 900°C in dedicated kilns (Boynton, 1980). The same cycle can be performed on dolomite ($CaCO_3.MgCO_3$) in order to obtain dolomitic lime (CaO.MgO) and then hydrated dolomitic lime ($Ca(OH)_2.Mg(OH)_2$).

### 2.2.2 Effect of Hydrated lime on Mix

Hydrated Lime is now seen as a multifunctional additive that improves the durability of asphalt mixes (Lesueur, 2010). Unfortunately, measuring the durability of asphalt mixtures

in the laboratory is not possible, because of the many distresses and failure modes that asphalt mixtures can experience.

Research performed by J.Epps(1992) show that the addition of hydrated lime to HMA increases stiffness. This helps to distribute and reduce the stresses and strains within the pavement structure created by traffic loads and generally reduce permanent deformation potential.

Still, test methods are available in order to evaluate the resistance of pavement materials to the action of detrimental agents such as water, freeze–thaw cycles, temperature and Ultra-Violet light exposure (ageing) and/or traffic. More precisely, HL is seen to improve (Lesueur, 2010; Little & Epps, 2001; Little & Petersen, 2005; Sebaaly et al., 2006; Sebaaly, 2007)

- ✓ The resistance to moisture damage and frost,
- ✓ The resistance to chemical ageing and
- ✓ The mechanical properties, in particular, modulus, strength, rutting resistance, fatigue and thermal cracking.

Mineral filler such as hydrated lime filler can serve as an active filler and show physiochemical activity in the aggregate-mastic interface. Ishai and Craus (1977) investigated the effect of the filler on aggregate-bitumen adhesion properties in sand asphalt mixtures.

## 2.2.3 Effect of Hydrated Lime on bitumen Rheology

The hydrated lime actually stiffens the asphalt film and reinforces it. Furthermore, the lime makes the HMA less sensitive to moisture effects by improving the aggregate-asphalt bond. This synergistically improves rut resistance. As the HMA ages due to oxidation, hydrated lime reduces not only the rate of oxidation but also the harm created by the products of oxidation. This effect keeps the asphalt from hardening excessively and from becoming highly susceptible to cracking (through fatigue and temperature (thermal) cracking). [Berger & Huege, 2004].

The quality of mastics, the combination of asphalt binder and filler, influences the overall mechanical performance of asphalt mixtures as well as placement workability. Generally the effect of the filler is based on a volumetric filler effect or an interactive role between the

filler and the bitumen due to the fineness and surface characteristics of the filler. (Christopher, 2004).

Some of the Creep Tests performed at Texas by Little (1994) also show that hydrated lime promotes high temperature stability, thereby increasing resistance to permanent deformation. Studies by Little (1996) and Lesueur, Little, and Epps (1998) evaluated the changes in rheology, aging kinetics, oxidative hardening created by adding hydrated lime to HMA. It showed the improvements in resistance to permanent deformation, fatigue cracking and low temperature fracture. Johannson (1998) conducted extensive research on bitumen ageing and adding of hydrated lime to bitumen. His findings showed that although the filler effect of lime increases low temperature stiffness, fracture toughness is also increased substantially. He also saw that hydrated lime reduces the effects of age-hardening more so at high temperatures than at low temperatures.

Hopman (1998) did some of the most powerful research work demonstrating a lime-bitumen interaction which showed similar results as reported by Lesueur, Little, and Epps (1998). Hopman used light absorption measurements and gel permeation chromatography to show a significant change in generic composition of the bitumen after the addition of lime which indicated the lime is active filler.

In a study by Plancher et al (1976) hydrated lime decreased age hardening of the binder, using laboratory ageing at high temperatures (130$^{o}$C and 163$^{o}$C). They concluded that lime treatment:

- ✓ Reduces the viscosity increases upon ageing
- ✓ Removes reactive polar compounds
- ✓ Reduces the formation of carbonyl-type oxidation products upon ageing
- ✓ Reduces the ratio of asphaltenes formed to oxidation products formed upon ageing
- ✓ Reduces asphaltenes formation.

Plancher el al propose that the beneficial effect of lime treatment in reducing bitumen oxidative hardening is due to two synergistic effects: (a) lime reduces the formation of oxidation products by the removal of oxidation catalysts or promoters and (b) lime reduces the sensitivity of the bitumen to these oxidation products by removing reactive polar

molecules that would otherwise interact with the oxidation products to cause an increase in viscosity.

In a study by Petersen et al (1987) it was shown that lime treatment of bitumen reduced age hardening, increased the high-temperature stiffness of unaged bitumen, reduced the stiffness of aged bitumens at higher temperatures, and increased the bitumen tensile-elongation at low temperatures. These effects should benefit asphalt pavements by increasing asphalt durability, reducing rutting, shoving and other forms of permanent pavement deformation, improving fatigue resistance in aged pavements and improving pavement resistance to low-temperature transverse cracking. In this study the ageing was performed using a thin film accelerated test with ageing temperature of 113°C and ageing time of 3 days. Petersen at al summarises that the net result of the combined effects of lime treatment should result in longer lasting pavements with improved performance during the life of the pavement.

## 2.3 Bitumen Rheology

### 2.3.1 General

Bitumen is a fractional residue distillated from crude oil and is composed of a mixture of organic molecules that vary widely in composition from non-polar saturated hydrocarbons to highly polar and highly condensed aromatic ring systems (Petersen, 1984). Predominant hydrocarbons with appreciable amounts of compounds containing oxygen, sulfur, and nitrogen as well as minor amounts of metals such as vanadium, nickel, iron, magnesium, calcium and other elements exist in a bitumen constitution (Romberg et al., 1959). Because the types of compounds and their molecular weights cover wide ranges, it is difficult to specify the precise composition from tests on the entire bitumen. Read and Whiteoak (2003) summarised that most bitumens distillated from a variety of crude oil contain: carbon 82-88%, hydrogen 8-11%, sulphur 0-6%, oxygen 0-1.5%, nitrogen 0-1%.

### 2.3.2 Bitumen Constitution

Bitumen consists of a large variety of molecular structures. Therefore, a thorough identification and classification of all these structures is an extremely difficult task. As an

alternative, the bitumen constituents can be classified on polarity and solubility. On this basis, bitumen is comprised of three fractions:

- ✓ Asphaltenes,
- ✓ Resins, and
- ✓ Oils (Aromatics and Saturates).

Asphaltenes are highly polar, high molecular weight hydrocarbons surrounded by moderately polar aromatic molecules and dispersed in a continuous non-polar oily phase. Resins are semi-solid fractions acting as a peptising agent, which keep the asphaltene molecules from coagulation (Kerbs, R. D., and Walker, R. D, 1971). The proportion of resins to asphaltenes governs to a degree the solution (SOL) or gelatinous (GEL) type character of the bitumen. Aromatics, which consist of the lowest molecular weight naphthenic aromatic compounds in the bitumen, present the major proportion of the dispersion medium for the peptised asphaltenes (Whiteoak, C. D, 1990).

They consist of non-polar carbon chains in which unsaturated ring systems dominate, and they have a high dissolving ability for other high molecular weight hydrocarbons. Saturates comprise straight and branch-chain aliphatic hydrocarbons, together with alkylnaphthenes and some alkyl-aromatics. They are non-polar viscous oils, which are white in colour (Whiteoak, C. D, 1990).

To conclude, asphaltenes constitute the body of the bitumen, aromatics affect the adhesive and ductile properties, and saturates and resins influence the viscosity and flow (Hastead, W. J., 1985). The asphaltenes content has a large effect on the rheological characteristics of a bitumen. Increasing the asphaltenes content produce a harder, more viscous bitumen with a lower penetration, high softening point and, consequently high viscosity. Asphaltenes constitutes 5 to 25% of the bitumen.

### 2.3.3 Rheological properties of bitumen

**1. General**

The mechanical response of bitumen is dependent on time and temperature. Considering only the temperature effect on the viscosity of bitumen, the principal viscosity properties are shown in Fig-2.1.

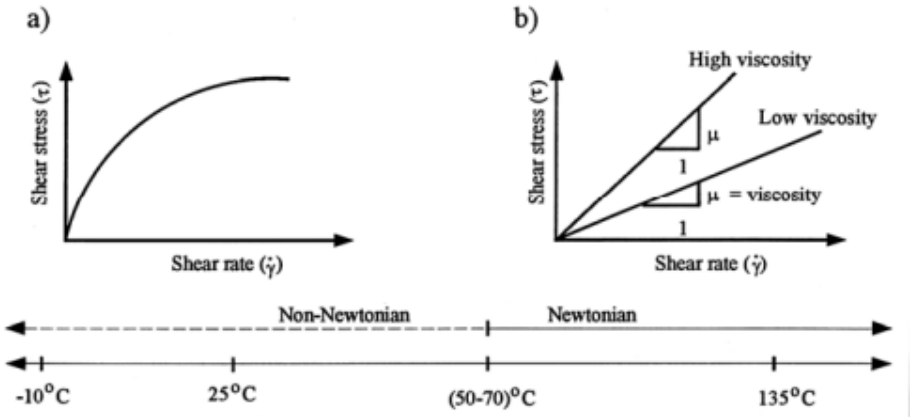


**Figure 2.1:-** Flow properties of bitumen as a function of temperature (at a given loading time

Viscous liquids like hot bitumen are sometimes called plastic because once they start flowing, they do not return to their original position. This is why in hot weather, some asphalt pavements flow under repeated wheel loads and wheel path ruts form.

However, it is a common agreement that rutting in asphalt pavements during hot weather is also influenced by aggregate properties. As stated by (McGennis et al 1994), it is probably more correct to say that the asphalt mixture is behaving like plastic. At low temperatures or very rapid loading times, bitumen behaves like elastic solids. If too much load is applied, elastic solids may break. Even though bitumen is an elastic solid at low temperatures, it may become too brittle and crack when excessively loaded. This is the reason why low temperature cracks sometimes develop in asphalt pavements during cold weather.

## 2. Linear viscoelastic model

A viscous materials is one that is semi-fluid in nature. When stressed, it will deform or tend to deform, any deformation being unrecovered when the loading is removed. Elastic materials also deform or tend to deform when stressed. However. When the loading is removed, any deformation is fully recovered. Bitumens are visco-elastic materials. The degree to which their behaviour is viscous and elastic is a function of both temperature and period of loading (usually referred to as 'loading time')'at high temperatures or long times of loading, they behave as viscous liquids whereas at very low temperatures or short times of loading they behave as elastic (brittle) solids. The intermediate range of temperature and loading times, more typical of conditions in service, results in visco-elastic behaviour.

(Anderson et al 1994) used the simple creep test to explain and characterize the stress-strain response of a material. In this test, a load of constant magnitude is applied to a material at

time $t_0$, at time $t_i$, the load is removed. The inherent differences between elastic, viscous, and viscoelastic behavior is shown in Fig-2.2.

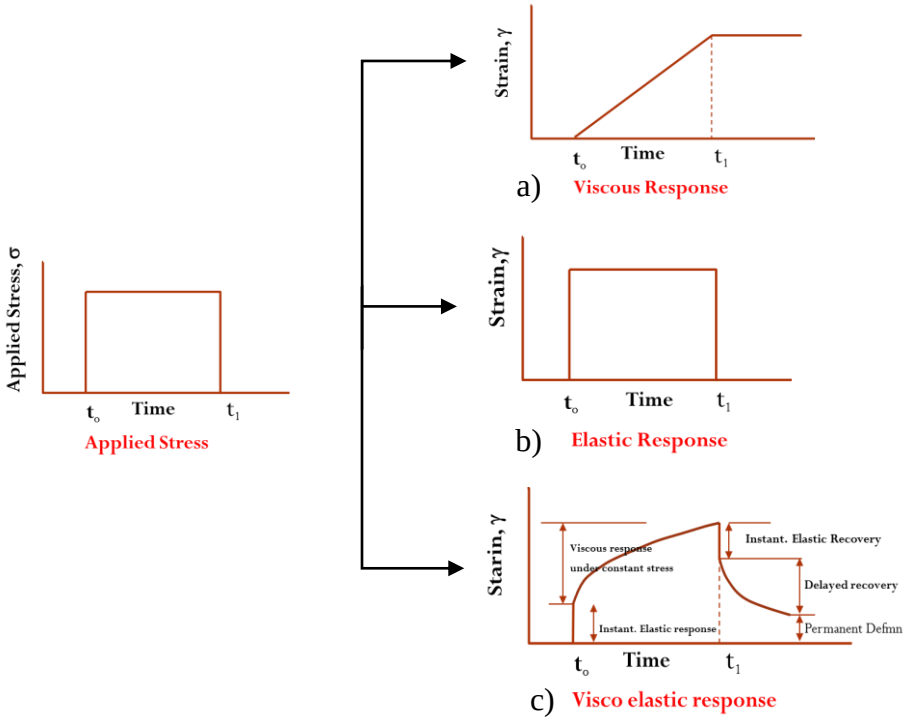


**Figure 2.2:-** Idealized response of elastic, viscous, and viscoelastic materials under constant stress loading [Anderson]

Bitumen is often characterized as a viscoelastic material. A viscoelastic material (Figure 2.2 c) has both elastic and viscous components of response, followed by a gradual time-dependent deformation. This time dependent deformation may further be divided into a purely viscous component and a delayed elastic component. Upon removing the load at $t_i$, the viscous flow ceases, and none of this deformation is recovered. The delayed elastic deformation is, however, recovered, but not immediately as with purely elastic deformation. Instead, once the load is removed, the delayed elastic deformation is slowly recovered, at a decreasing rate, as is shown in Figure- 2.2 c).

The description of elastic, viscous, and viscoelastic response given above is only valid for linear responses. (Anderson et al 1994) argue that linear methods of characterization and analysis are more than adequate for engineering design problems. Nonlinear response, especially for viscoelastic materials such as bitumen, is said to be extremely difficult to characterize in the laboratory and to model in practical engineering problems.

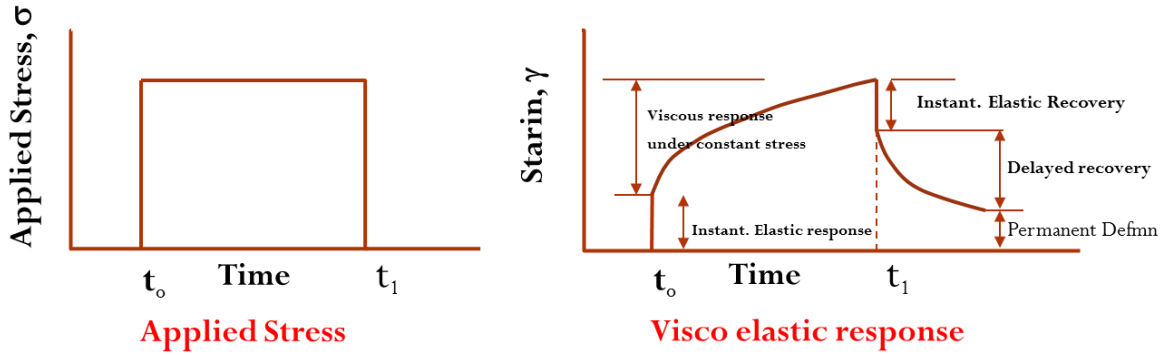


**Figure 2.3:-** Idealized response of viscoelastic materials under constant stress loading

## 3. Dynamic mechanical analysis

There are many methods and ways of characterizing viscoelastic properties. (Bahia and Anderson) claim that dynamic (oscillatory) testing is the best technique to measure and explain the viscoelastic properties of bituminous materials. In the shear mode, the complex modulus, G*, and phase angle, δ, are measured. G* represents the total resistance to deformation under a given load. δ represents the relative contribution of an in-phase elastic component and an out-of-phase viscous component to the measured complex modulus. Bahia and Anderson explain that the elastic in-phase component can be related directly to energy stored in a sample for every loading cycle, while the viscous out-of-phase component can be related directly to energy lost per cycle in permanent flow. Bahia and Anderson explain further that the relative distribution of these components is a function of the composition of the material, loading time and temperature.

Both the complex modulus and the stiffness modulus are simply indicators of the resistance of bitumen to deformation under a given set of loading conditions. (Anderson et al () describe how the dynamic mechanical properties are directly related to the creep properties, but in a mathematically complex way. (Anderson et al 1994) further describes the typical parameters or output which is obtained from dynamic testing. The primary response in dynamic testing is the complex dynamic modulus, which is computed (in strain-controlled mode) using the following equation.

$$G^*(\omega) = |\tau(\omega)| / |\gamma(\omega)| \quad \text{---------- (1)}$$

Where

$G^*(\omega)$ = complex dynamic shear modulus at frequency ω, Pa

$|\tau(\omega)|$ = absolute magnitude of the dynamic shear stress response, Pa, &

| γ(ω) |= absolute magnitude of the applied dynamic shear strain, m/m.

The phase angle, δ indicates the lag in the stress response compared with the applied strain. For purely elastic materials, the phase angle will be 0°, whereas for purely viscous materials, the phase angle will be 90°. The phase angle was in SHRP pointed out as an important parameter in describing the viscoelastic properties of material such as bitumen.

Anderson et al (1994) describe three other parameters from dynamic testing which are often used: the storage modulus G′ (ω); the loss modulus G′′(ω); and the loss tangent, or tan δ. These parameters can be visualized as seen in Figure 2.4 1.13.

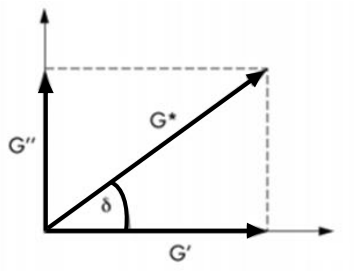


$G' = G^* \cos \delta$
$G'' = G^* \sin \delta$
$G^* = \sqrt{G'^2 + G''^2}$

**Figure 2.4:-** the relationship between complex modulus (G*), storage modulus (G′), loss modulus (G′′) and phase angle (δ) [Anderson].

they describes how the storage modulus and the loss modulus sometimes are misinterpreted as the elastic and viscous modulus; in reality, the elastic component of the response only represents part of the storage modulus, and the viscous response only part of the loss modulus. In addition to the elastic and viscous response, most real viscoelastic materials exhibit a significant amount of delayed elastic response that is time-dependent but completely recoverable. In interpreting the storage and loss moduli, Anderson et al points out how it should be kept in mind that both these parameters reflect only a portion of the delayed elastic response.

## 2.4 Dynamic Oscillatory Testing Using a DSR

### Introduction of Dynamic Shear Rheometer (DSR)

DSR is the acronym for Dynamic Shear Rheometer and is used to measure the dynamic shear modulus and phase angle of bituminous binders at intermediate and high pavement temperatures. In the DSR dynamic oscillatory testing, the shear stresses and shear strains vary with time from positive to negative in a sinusoidal fashion. The DSR provides stress-strain moduli at different rate of loading expressed in terms of frequency at different test

temperatures (Anderson et al., 1994). The DSR equipment used in bituminous binders' characterization can be divided into two categories: (1) controlled stress, when the rheometer applies a stress to the specimen and measures the resulting strain, and (2) controlled strain, when the rheometer applies a strain to the specimen and measures the resulting stress.

A 1-mm by 25-mm or 2-mm by 8-mm, hockey puck-shaped, sample of bituminous binder squeezed between two parallel metal plates is placed in a temperature controlled chamber, as shown in Figure 2. The chamber for controlling the test specimen temperature by heating or cooling maintains a constant specimen environment. The medium in the environment chamber can be liquid or gas. Due to the extreme temperature dependency of bituminous binders, it is necessary to control the temperature for the rheological testing of bituminous binders to a much finer degree than for most other viscoelastic materials. A change in temperature of 1$^{o}$C can result in a modulus change of up to 25 percent for some binders (Anderson et al., 1994).

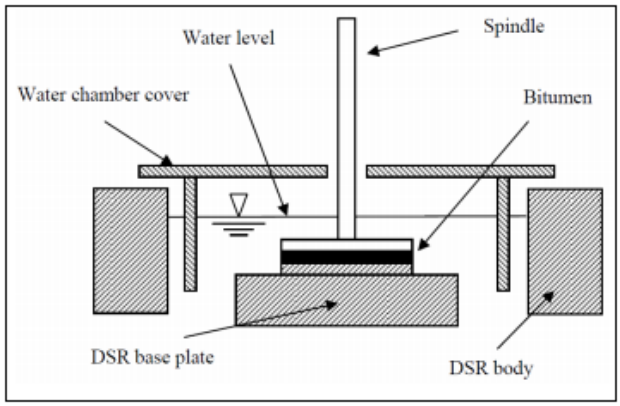


**Figure 2.5**:- Testing arrangement in DSR (Airey, 1997)

Two types of spindles (upper plate) used in the DSR testing are 25-mm diameter parallel plate geometry, and 8-mm diameter parallel geometry. It is essential to select spindle geometry due to the effect of compliance of parallel plate geometry on rheological measurements for the extremely high stiffness binders under dynamic loading at low temperatures. Anderson et al. (1994) suggested that 25-mm parallel plates should be used when the complex modulus ranges from $10^3$to $10^5$Pa; 8-mm parallel plates should be used

when the complex modulus ranges from$10^5$to $10^7$Pa; torsion bar or bending beam rheometer should be used when the complex modulus is greater than $10^7$Pa.

During the test, the sample of bituminous binder is sheared between two parallel plates. One of the parallel plates is oscillated with respect to the other at selected frequencies and rotational deformation amplitude (or torque amplitude). As shown in Figure 3, the spindle (upper plate) is caused to oscillate sinusoidally while the base plate is fixed during testing. The testing is carried out by oscillating the spindle about its own axis such that a radial line through point A moves to point B, then reverses direction and moves through point A to point C, followed by moving back from point C to point A (Airey, 1997).

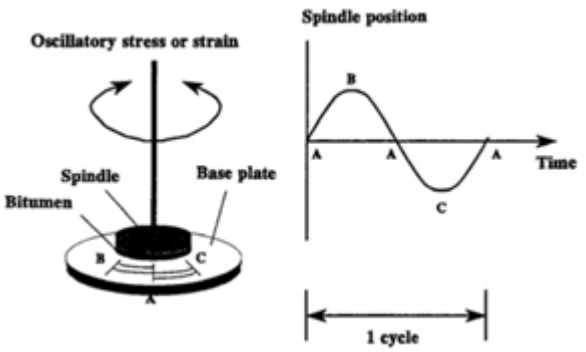


***Figure 2.6:-*** Principles involved in DSR test (Airey, 1997)

The complex modulus (G*) is an indication of the stiffness of the materials, high value of G* meaning the materials is more stiff and vice versa. Complex shear modulus (stiffness) increases with the increase of the frequency, while for high frequencies the phase angle (δ) decreases, meaning that the material gets into the more stiffen. This shows that the asphalt binder and asphalt mastic is plastic region at high frequencies. In contrast the stiffness of asphalt mastic decrease with decrease frequency, while for low frequency the phase angle increase, meaning that the material gets into the more elastic region.

# CHAPTER 3. RESEARCH METHODOLOGY

The goal of this study was to determine the property and overall performance asphalt mastics with different content of Hydrated lime. The effectiveness of this filler were evaluated by comparing test results conducted on crushed aggregate stone mastics. The test used in this study to compare performance tests were conducted on Dynamic shear rheometer (DSR). All tests on asphalt binder were conducted according to respective ERA, AASHTO and ASTM testing standards.

## 3.1 Experimental design

In this study, the effects of filler (hydrated lime) on the mastic property and HMA performance were evaluated in the laboratory. The research evaluated various materials (i.e., aggregates, binders, and hydrated lime) using multiple test methods and conditioning procedures. Samples of the filler materials (hydrated lime and crushed stone) were mixed separately with bitumen in various percentages ranging from 25% to 45%. Series of tests were carried out on the samples to determine their suitability as filler materials with respect to [ AASHTO, 1997] specifications.

These ingredient materials were subjected to various laboratory tests in order to determine their physical properties whether they can meet common specification limits. These quality assurance tests conducted on the aggregates include: gradation, Los Angeles abrasion, soundness, flakiness, aggregate crushing value, asphalt affinity, specific gravity and water absorption tests. The tests carried out on the asphalt cement sample include: penetration, flash point, ductility, durability, purity and specific gravity. Then the results obtained from the tests are compare with the common specifications.

## 3.2 Materials and Laboratory Testing

Two Filler type (hydrated lime and Crushed stone) with three different percentages (25%, 35%, & 45%) and asphalt binders with penetration grad (PG 60-70) were selected to conduct the laboratory tests. The binder & mastic used for tests were Unaged and Aged (short-term aged using the rolling thin film oven (RTFO) according to ASTM 2872 (2012) to simulate

short term aging that the asphalt binder experiences during production and placement in the field).

## 3.2.1 Material Selection

### 1. Asphalt binder

Binder grade used from the project location Adama-Awash overlay project site at Welenchti is 60/70 to evaluate effect of mineral filler (hydrated lime) on the stiffness of mastics and performance of hot mix asphalt (HMA) and the bitumen subjected to various tests in the laboratory to determine its physical properties. Hence some quality test has been conducted for the asphalt binder listed below.

Table 3.1: **- Tests that are conducted for the Asphalt Binder**

| I. No | Test description | Test method | ERA Spec. | Test result |
|---|---|---|---|---|
| 1 | Ductility,5cm/min at 25°c | AASHTO T-51 | Min. 100 | 100+cm |
| 2 | Penetration,100gm, 5sec at 25°c | AASHTO T-49 | 60-70 | 62 |
| 3 | Flash point, °c | AASHTO T-48 | 232°C (450°F) | 307°C(586°F) |
| 4 | Specific Gravity | AASHTO T228 | - | 1.015 |
| 5 | Softening point | AASHTO T-053 | | 50.3°C(123oF) |

### 2. Aggregate (mineral filler)

The mineral aggregates used in the research were subjected to various tests in order to assess their physical characteristics and suitability in the road construction. The aggregates are obtained from ECWC Construction site at Adama -Awash overlay project site located 7 Km away from Welenchity town .Hence Welenchiti town located at 125 Km from Addis Ababa along Ethio -Djibouti road.

Table 3.2: **- Tests that are conducted for the aggregate**

| I. N | Test description | Test Method | Specification (ERA, 2002) | Test Result |
|---|---|---|---|---|
| 1 | Particle shape, Flakiness, % | BS 812, Part 105 | < 45 | 17 |
| 2 | Los Angeles Abrasion, % | AASHTO T96 | < 30 | 14 |
| 3 | Aggregate Crushing Value, ACV, % | BS 812, Part 110 | < 25 | 19 |
| 4 | Water absorption, % | ASTM C 127 | < 2 | 1.9 |
| 5 | Specific Gravity (Bulk)<br>i. Coarse Aggregate<br>ii. Fine Aggregate | <br>AASHTO T85<br>AASHTO T84 | <br>-<br>- | <br>2.60<br>2.70 |

### 3. Hydrated lime

The hydrated lime used for this research is taken from local lime factories produce lime Dekasos Senkele Lime factory located at ambo town 125 km away from Addis Ababa.

## 3.2.2 Preparation of mastics

Mastics are asphalt mixtures composed of binder and aggregates smaller than 75 microns (passing through No. 200 sieve). The mastics used in this research were blended in such a way that the filler/asphalt (F/A) ratio will be ranges between 0.6-1.2 in mass.

**Table 3.3:-** Recipe of mastics for DSR Test

| Mastics | F/A by mass | Mass of material in gm. | | | Total Mass of Mastic (gm) |
|---|---|---|---|---|---|
| | | **Bitumen** | **Crushed stone** | **Hydrated Lime** | |
| Crushed aggregate + Asphalt bitumen | 0.4 | 75 | 25 | | 100 |
| | 0.6 | 65 | 35 | | 100 |
| | 0.8 | 55 | 45 | | 100 |
| Asphalt bitumen + Hydrated Lime(HL) | 0.4 | 75 | | 25 | 100 |
| | 0.6 | 65 | | 35 | 100 |
| | 0.8 | 55 | | 45 | 100 |

### 1. Filler Concentration by Mass

A combination of 60/70 penetration grade bitumen (virgin bitumen) with two filler types and three filler concentrations of 25%, 35% and 45% by mass were included in the testing program, as shown in Table 4. The filler concentration by mass is considered in order to easily compare with the filler proportion in asphalt mixture design because the filler proportion in asphalt mixture design is normally shown by mass content. The choices of using 25%, 35% and 45% to prepare the bitumen-filler mastics are based on the filler content for a HMA mixture.

$$\textbf{Filler concentration by mass} = \frac{\text{Mass FILLER}}{\text{Mass bitumen} + \text{Mass Filler}} \quad \ldots\ldots\ldots\ldots\ldots\ldots\ldots\ldots\ldots\ldots \text{(3.3)}$$

The determination of ratio of filler to bitumen based on mass is given by:

$$\textbf{Ratio of filler to bitumen by mass} = \frac{\textbf{Mass Filler}}{\textbf{Mass bitumen}} \quad \ldots\ldots\ldots\ldots\ldots\ldots\ldots\ldots\ldots\ldots\ldots\ldots\ldots\ldots \text{(3.4)}$$

Table 3.4:- **Matrix of bitumen-filler mastics**

| Materials / Filler contents | Base(virgin) bitumen | Bitumen-Filler Mastics | |
|---|---|---|---|
| | 60/70 Pen. Grade | Crushed stone | Hydrated lime |
| 0% | ✓ | | |
| 25% | | ✓ | ✓ |
| 35% | | ✓ | ✓ |
| 45% | | ✓ | ✓ |

Table 3.5: - **Ratio of filler to bitumen in bitumen filler system**

| Selection of filler content in the investigation | | Filler proportion in Super pave Mixture bitumen |
|---|---|---|
| Filler content by mass | Ratio of Filler to Bitumen | Ratio of Filler to Bitumen |
| 25% | 0.4 | 0.6 – 1.2 |
| 35% | 0.6 | |
| 45% | 0.8 | |

## 2. Preparation of Asphalt mastics Sample

For the preparation of asphalt mastics first asphalt binder (virgin) heated at Elevated temperature from 110oC – 160oC to make asphalt fluid and less viscous. The filler weighted based on the proportions of the filler to asphalt mastic was blend to asphalt binder at mixing temperatures of 160°C. The mixing process was carefully performed for 20min to form homogenous mixture.

Six mastics were prepared by blending each mineral filler with the asphalt binder using filler-to-asphalt ratio and the sample was conditioned by aged using Rolling Thin Film Oven Test (RTFOT) according to standard method AASHTO T 240-06 or ASTM d 2872-04 to simulate the effect of heat and air on a moving film asphalt during mixing and construction process on Hot mix Asphalt(HMA).

## 3.2.3 Laboratory Testing

The objective of this study was to investigate the influence of hydrated Lime filler on the rheological properties and Performance of asphalt binders. To achieve this, conventional (Empirical) and Rheological (Superpave) tests were conducted in the laboratory on the neat and mastic binders. The data obtained from these tests were analyzed to evaluate the effects of HL and crushed stone filler on bitumen.

# 1. Conventional Tests

## 1.1 Penetration test

A standard method of test for penetration of bituminous materials on AASHTO T 49-06 or ASTM D 5- 05. The penetration test can be considered as an indirect measurement of the viscosity of the bitumen at 25$^{o}$C, to specify different grades of bitumens. In the penetration test, a needle penetrates a sample of bitumen under a load of 100 grams at a temperature of 25$^{o}$C for a known loading time of 5 seconds. The penetration test used as a measure of consistency .Higher penetration indicates softer consistency and vice versa.

## 1.2 Softening point test

A standard method of test for softening point of bitumen (Ring and Ball) on AASHTO T53-06 or ASTM D36-95. The ring and ball softening point test is usually conducted to determine the consistency of bitumens by measuring the equi-viscous temperature at the beginning of the fluidity range of bitumens. In this test, a steel ball (weight 3.5 g) is placed on a bitumen sample contained in a brass ring that is suspended in a water or glycerine bath, in which the bath temperature is raised at 5$^{o}$C per minute. Water is used for bitumen with a softening point of 80$^{o}$C or below. Meanwhile, glycerine is used for softening points greater than 80$^{o}$C [Read and Whiteoak, 2003]. The softening point is useful in the classification of bitumens as one element in establishing the uniformity of shipments or source of supply, and is indicative of the tendency of the material to flow at the elevated temperature.

## 1.3 Ductility

A standard method of test for Ductility of bituminous materials on AASHTO T 51-06 or ASTM D 113-99. The ductility of a bituminous material is measured by the distance to which it will elongate before breaking when two ends of briquette specimen of the material which are pulled apart at a specified speed (5 cm/min) and specified temperature (25 ± 0.5$^{o}$C). The ductility test is used to describe the ductility and tensile behavior of bituminous binders. The test, which is normally performed at ambient temperature, is believed to reflect the homogeneity of the binder and its ability to flow.

### 1.4 Flash point and fire point

A standard method of test for flash and fire point by Cleveland open cup on AASHTO T 48-06 or ASTM D 92-05a. This method is used to determine the flash and fire points of all petroleum products, except fuel oils and those having an open cup flash below 79 °C. The flash and fire points indicate the materials combustibility. The fumes from the material at the flash point temperature are explosive.

### 1.5 Specific gravity

A standard method of test gravity of semi-solid bituminous materials on AASHTO T 228-06 or ASTM D 70-03.Specific gravity of bitumen we used is 1.017.

## 2. Performance Test

The performance of asphalt pavements are not easily characterized by physical properties as they are subjected to complex environmental and loading conditions. In addition, various modified binders cannot necessarily be characterized by empirical properties. It is important to understand the stress-strain behaviour of bituminous binders over a wide range of temperatures and loading time conditions. Thus, fundamental tests were introduced and developed to investigate mechanical properties and viscoelasticity of binders under different environmental conditions.

The Strategic Highways Research Program (**SHRP**), developed in the United States of America, was a coordinated effort to produce binder specifications which were classified based on a performance-grade system in accordance with fundamental testing results [Petersen et al., 1994; Anderson et al., 1994].

Table 3.6:- **Summary of the AASHTO MP-1 specification**

| Test | Performance parameter | Asphalt condition state | Specification | Specification limit | Test Temperature (°C) |
|---|---|---|---|---|---|
| RV | Flow ability | Neat | Viscosity | 3 Pa.s | 135 |
| DSR | Rutting resistance | Neat | G*/sinδ@10rad/sec | 1.0 kPa (min) | High |
| DSR | Rutting Resistance | RTFO aged | G*/sinδ@10rad/sec | 2.2 kPa (min) | High |
| DSR | Fatigue cracking resistance | PAV- aged | G*/sinδ@10rad/sec | 5000kPa (max) | Intermediate |
| BBR | Thermal cracking resistance | PAV aged | Creep Stiffness, S @ 60sec | 300 Mpa | Low +10°C |
| | | | m-value @ 60 sec | 0.30 | Low +10°C |
| DDT | Thermal cracking resistance | PAV-aged | Failure strain @ 1.0 mm/min | 1.0% | Low+10°C |

# 2.1 Dynamic Shear Rheometer (DSR)

## 2.1.1 Basic principle

The DSR is a tool to characterize the elastic, viscoelastic and viscous properties of materials including bitumens over a wide range of temperatures and frequencies (times of loading).

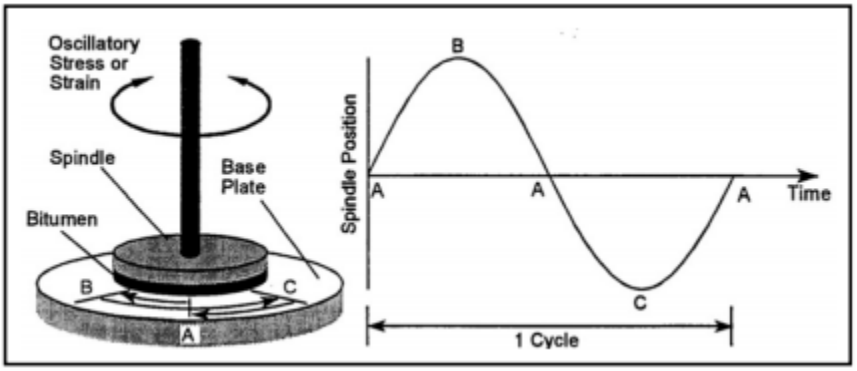


**Figure 3.1:-** Illustration of the DSR set-up [Airey, 1997]

The principles involved in DSR testing are illustrated in Fig. 3.1, where the bitumen is sandwiched between a spindle and a base plate. The base plate is fixed. A torque is applied to the top plate so that it oscillates back and forth. One cycle is completed when the top plate goes from point A to point B, then reverses direction and moves past point A to Point C, followed by a further reversal and movement back to Point A. This oscillation comprises one smooth, continuous cycle which can be continuously repeated during the test. DSR tests can be carried out in either controlled stress or controlled strain testing modes. In the controlled stress mode, a specific magnitude of shear stress is applied to the bitumen by application of a torque to the spindle and the resultant spindle rotation is measured, from which the magnitude of shear strain is calculated. In the controlled strain mode, the magnitude of spindle rotation is specified and the required torque to achieve is measured, from which the magnitude of shear stress is calculated [Airey, 1997].

In this study, two testing (parallel plate) geometries are used with the DSR: an 8 mm diameter plate with a 2 mm testing gap and a 25 mm diameter plate with a 1 mm testing gap. The selection of the testing geometry is based on the operational conditions, with the 8 mm plate geometry generally being used at low to intermediate temperatures (4 to 40$^{o}$C) and the 25 mm geometry at high temperatures (46 to 88$^{o}$C). It is also possible to use the same testing geometry over a wide temperature range, although the precision of the

results may be limited as a result of compliance errors and reduction in the precision with which the torque can be measured at low stress levels [Airey 2002a, 2002b; Airey and Hunter, 2003].

### 2.1.2 Testing procedure

The rheological properties of the original bitumen, and bitumen filler(crushed and hydrated) mastics blends, unaged and aged samples, were determined using dynamic mechanical methods consisting of temperature and frequency sweeps in an oscillatory-type testing mode performed within the linear viscoelastic region. The oscillatory tests were conducted on a Bohlin Gemini dynamic shear rheometer (DSR) using two parallel plate testing geometries consisting of 8 mm diameter plates with a 2 mm testing gap and 25 mm diameter plates with a 1 mm testing gap (Fig. 3.2). In this study, the samples were prepared using silcon mould method.

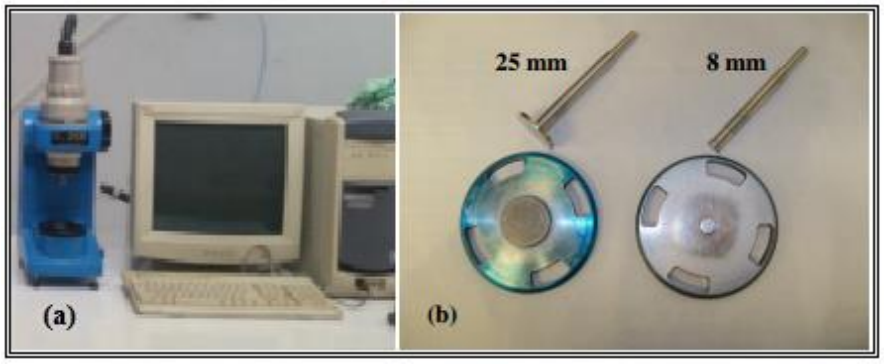


**Figure 3.2**:- (a) DSR and (b) 8 mm and 25 mm parallel plate

For the silicone mould method, softening point ring apparatus was used due to absence of silicone mould the hot bitumen is poured into 23 mm diameter softening ring with a height of 6.4mm. Once the bitumen mastic has cooled for 10-20 min, removed from the mold and centered on the upper plate of the DSR. The upper plate is then lowered to the required gap plus 50 μm, depending on the test temperature the geometry of the plate would be either 8 mm or 25 mm and testing gap is set at a height of 50 μm plus 2 mm or 1 mm respectively. The bitumen mastic that has been bulged out between the plates was then trimmed flush to the edge of the plates using a hot spatula or blade. After trimming, the gap was closed by a further 50 μm to achieve the required testing gap as well as a slight bulge around the circumference of the testing geometry.

### 2.1.3 Dynamic Shear Rheometer (DSR) Testing

The rheological properties of the binder and mastics were measured using the Dynamic Shear Rheometer (DSR), by conducting four types of tests: dynamic shear oscillation at single frequency or Amplitude sweep test AST (1.596 Hz), dynamic frequency sweep oscillation (0.1 - 25Hz) Performance grade PG test at (1.596Hz) and repeated shear creep loading and recovery or Multiple stress creep recovery (MSCR) test at constant stress (100 pa and 3000 Pa). The behavior of the materials was evaluated in terms of complex shear modulus - G*, rutting parameter - G*/sinδ, and phase angle – δ for the three types of tests.

### 1. Amplitude Sweep Test (AST)

The amplitude sweep test was carried out following the test standard AASHTO T 315 single frequency (10 rad/sec or 1.596 Hz) at specific test temperatures (10.0$^{o}$C, 21.1$^{o}$C, 37.8$^{o}$C & 54.4$^{o}$C).The 10 rad/sec angular frequency is equivalent to a frequency (f) of 1.59 cycles per second (1.59 Hz), as per the relationship $\omega = 2\pi f$ (Peterson et al., 1999; Uddin, 2003). The 10 rad/sec angular frequency corresponds, with sinusoidal loading, to a 0.1 second loading time, where loading time (t) is determined from the relationship $t = (2\pi f)^{-1}$.The 0.1-second loading time represents the loading time within a pavement structure resulting from the pass of a vehicle tire traveling at approximately 50 mph (80km/hr.).

AST were conducted to determine the visco elastic region for material (asphalt mastics). The linear viscoelastic range, which is the region of behavior in which the shear modulus is independent of shear stress or strain. The limit of linear viscoelastic behavior is the point beyond which the complex modulus decreases to 95% of the measured value at zero-strain, as shown in Figure 3.3 (Peterson, et al., 1999).

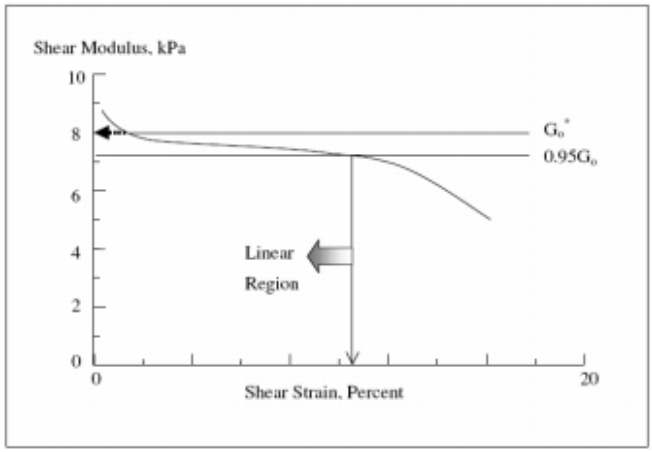


**Figure 3.3:-** Linear visco elastic region of asphalt binder (Peterson et al., 1999).

## 2. Frequency Sweep Test (FST)

The frequency sweep tests were conducted using four temperatures (10.0°C, 21.1°C, 37.8°C, and 54.4 °C) over wide frequency ranges (0.1 - 25Hz). Frequency sweep means that the stress or strain frequency applied is stepwise increased and at any frequency step the two resulting values of G* and δ are measured, within an assigned frequency range (Druta, 2006).

Frequency sweep test conducted to construct master curve and black space diagram.

### 2.1 Master curve

In constructing master curves for the asphalt binders, dynamic shear rheometer data are collected over a range of temperatures and frequencies. A standard reference temperature must be selected. (On this case $T_{ref}$ = 21.1°C) Then, the data at all other temperatures (10.0°C, 37.8°C & 54.4°C) are shifted relative to this reference temperature until a smooth curve is generated. The master curves of the complex modulus and phase angle with the change in frequency can be constructed in this manner. Shift factors can be used to compare the rheological complexity of the sample. For instance, a rheologically simple material exhibits the same shift factor for both the complex modulus and phase angle master curve, while for a rheologically complex material these are expected to be different.

#### 1.1 Sigmoidal Functions for Modeling Master Curves

Pellinen and Witczak (2002) proposed using a sigmoidal function [Equation (3.1)] for modeling the dynamic modulus master curve. The sigmoidal function is fitted to the dynamic modulus test data using regression analysis.

$$\log|E^*| = \delta + \frac{\alpha}{1+e^{\beta-\gamma\log f_r}} \quad \text{..... (3.1)}$$

$$\phi = -90 * \delta\alpha - \frac{\exp^{(\beta+\delta(\log f_r))}}{[1+e^{(\beta+\delta(\log(f_r)))}]^2} \quad \text{..... (3.2)}$$

**Where ,** log |E*| = log of the dynamic modulus,
ϕ=phase angle
$f_r$ = reduced frequency, and
**α, β, γ, δ** = fitting parameters.

This fitting function provides an analytically simple form that can be used to easily determine the physical characteristics of a material at any temperature and loading time.

The parameters **α** and **α+δ** represent the minimum and maximum dynamic modulus values, respectively. For example, the maximum dynamic modulus (**α+δ**) represents the maximum stiffness of asphalt mixture, which at high temperature relies mainly on aggregate interlock, but at intermediate and low temperatures depends also on the binder stiffness. The parameters **β** and **γ** describe the shape of the sigmoidal function (Pellinen et al. 2002).

The fitting parameters; β, δ, and γ are estimated using a numerical optimization technique. The optimization process is done with the aid of the Solver function in MS Excel.

Coefficients of the model have meaningful physical significance (Figure 3.4). For instance, the coefficients of β and γ determine the shape of the sigmoidal function model. A sigmoidal functional curve will move to the left and become stiffer with the increase of β and γ, respectively. The coefficient δ+α and δ represent the minimum and maximum values of the creep compliance, respectively. The coefficient δ+α represents the equilibrium (glassy) compliance at very small times.

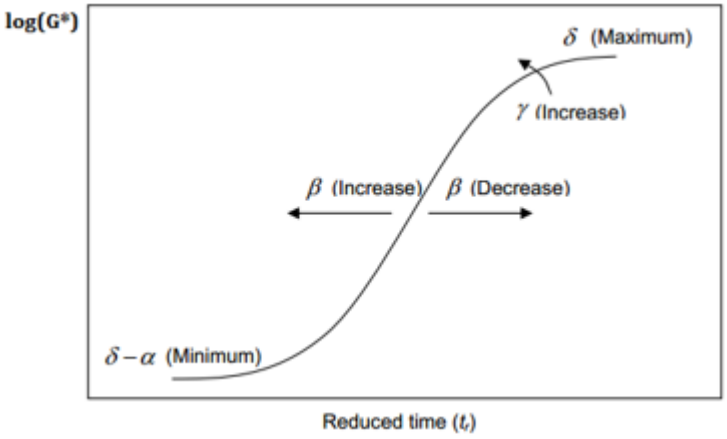


**Figure 3.4: -**Effect of the sigmoidal function coefficient on Master curve (Pellinen and Witczak (2002)

## 2.2 Black space diagram

A Black space diagram is a plot of log G* versus δ over all test temperatures and frequencies. This plot is very sensitive to morphology. Unlike the master curve, the Black space diagram does not require any shifting, thus temperature - independent curves can be constructed when the material obeys time -temperature superposition.

## 3. Multiple stress creep recovery (MSCR)

The repeated shear creep test is performed using the Dynamic Shear Rheometer (DSR) by applying a controlled shear stress (at 0.1 KPa and 3.2 kPa) using a haversine load for 1 second followed by a 9-second rest period. During each cycle, the asphalt binder reaches a peak strain and then recovers before the shear stress is applied again. The permanent strain is then accumulated for 10 cycles (or 100 seconds). Since asphalt pavements are designed to be flexible, they must quickly return to their original configuration after loading. Rutting, pushing, and shoving are just a few of the failure mechanisms associated with inelastic or permanent deformation. Repeated loading without complete binder recovery is also a cause of fatigue cracking (durta, 2006).

**Multiple Stress Creep and Recovery (MSCR) Test**

The creep recovery (elastic) properties of the asphalt binder were evaluated using multiple stress creep and recovery (MSCR) tests following the AASHTO T 350 test method. This test involves applying two shear stress levels (0.1 kPa and 3.2 kPa). The average non - recoverable creep compliance ($J_{nr\ (0.1)}$ and $J_{nr\ (3.2)}$) values are computed respectively using Equations 3.3 and 3.4. The percent difference in non-recoverable compliance ($J_{nr\text{-}diff}$) between 0.1 kPa and 3.2 kPa is determined using Equation 3.5.

$$\mathbf{J_{nr\text{-}(0.1)}} = \sum_{N=1}^{10}[Jnr\ (0.1, N)]/10 \quad \text{..... (3.3)}$$

$$\mathbf{J_{nr\text{-}(3.2)}} = \sum_{N=1}^{10}[Jnr\ (3.2, N)]/10 \quad \text{..... (3.4)}$$

$$\mathbf{J_{nr\text{-}diff}} = \frac{Jnr\ (3.2) - Jnr\ (0.1)}{Jnr\ (0.1)} * 100 \quad \text{..... (3.5)}$$

**Where,**

$J_{nr\ (0.1),} = (\varepsilon_{10} - \varepsilon_1)/0.1$

$J_{nr\ (3.2),} = (\varepsilon_{10} - \varepsilon_1)/3.2$

$\varepsilon_1$=the strain at the end of creep portion

$\varepsilon_{10}$=the strain at the end of recovery portion

$J_{nr\ (0.1)}$ =average non-recoverable creep compliance at 0.1kpa

$J_{nr\ (3.2)}$ =average non-recoverable creep compliance at 3.2kpa

$J_{nr}$ (0.1, N) = non-recoverable creep compliance at 0.1kpa

$J_{nr}$ (0.1, N) = non-recoverable creep compliance at 3.2kpa

$J_{nr\text{-}diff}$ =percent difference in non-recoverable compliance b/n 0.1kpa and 3.2kpa

N = Number of cycle

Table 3.7:-**Traffic Designation AASHTO M-332**

| Traffic Designation | Traffic level (ESALs) | Load rate (km/h) | Jnr3.2 (kpa-1) |
|---|---|---|---|
| Standard Traffic "S" | <10 million | >70 | 4.0 |
| Heavy Traffic "H" | 10 – 30 million | 20-70(slow) | 2.0 |
| Very Heavy Traffic "V" | >30 million | <20 | 1.0 |
| Extremely Heavy Traffic "E" | >30 million | < 20 (standing) | 0.5 |

## 4. Binder Performance Grade (PG)

The performance grade of the asphalt binder was classified following the AASHTO M 332[3] specification. According to the standard test procedure, AASHTO T 315, test is conducted at high temperature with increment of 6°C temperature for performance grading system and with input strain 12% strain for original and 10% strain for RTFO aged samples were used. It was believed that the permanent deformation parameter G*/sinδ is a good indication for rutting on the pavement. But studies shows that there is poor relationship between G*/sinδ and rutting depth (Anderson, 2011). therefore, in this research G*/sinδ is only used for checking asphalt binder environmental temperature resistance.

The minimum limits of G*/sinδ for both unaged and RTFO aged binder tests 1.0KPa and 2.2Kpa respectively, and a maximum limit of G*sinδ for PAV-aged binder tests are 5.0Kpa.

Table 3.8:-**Target Shear Stress and Strain Values for PG test**

| Asphalt Tasted | Target shear strain , % | Target Shear stress, KPa |
|---|---|---|
| Neat binder | 12 | 0.12 |
| RTFOT-Aged | 10 | 022 |
| PAV-Aged | 1 | 50 |

### 2.1.4 DSR parameter for pavement distress

## 1. Rutting Parameter

The work of Bahia and Anderson (1995a) and Roberts, et al. (1996) served as the source of the following discussion on the rutting parameter development. The magnitude of the complex modulus and the degree of phase angle are required to determine the relationship between asphalt stiffness and the type of deformation: recoverable and non-recoverable.

This is especially true when considering rutting resistance at high service temperatures. A higher G* and a lower δ are desired for rutting resistance. An asphalt with a high G* is stiffer and provides increased resistance to deformation. An asphalt exhibiting a lower δ has a greater elastic component, thus allowing more of the total deformation to be recovered.

Rutting is assumed to be the primary result of deformations within the surface layer. Rutting is considered a stress-controlled, cyclic loading phenomenon. Work is being done to deform the surface layer with each loading cycle. A portion of the work is recovered in the elastic rebound of the surface layer, while the remaining work is dissipated through permanent deformation and heat (John P. Zaniewski, Michael E. Pumphrey, 2004).

The relationship G*/sinδ was chosen as the parameter for SHRP specifications with respect to rutting. It can be seen in the preceding equation that an increase in G* and decrease in sin δ will both decrease the amount of work dissipated per loading cycle within a pavement's surface layer. This relationship follows the rationale that a binder with a high G* value is stiffer, which increases its resistance to deformation, and a binder with a low sinδ value is more elastic, whereby its ability to recover part of the deformation is increased.

## 2. Fatigue Cracking Parameter

Fatigue cracking is the primary pavement distress at intermediate service temperatures (Roberts, et al., 1996). Pavement fatigue cracking is considered a strain controlled distress in thin pavement layers, less than 2 inches, because deformations in the asphalt layers are typically the result of poor subsurface layer support and not so much the effect of decreases in pavement stiffness (Huang, 1993). Pavement fatigue cracking is considered a stress-controlled distress in thick pavement layers, greater than 6 inches, as the pavement is the main load-carrying constituent. A combination of both stress-controlled and strain-controlled distresses exists with intermediate thickness HMA pavements (John P. Zaniewski, Michael E. Pumphrey, 2004).

Fatigue cracking occurs primarily in thin pavement layers; therefore, the distress is modeled as a strain-controlled phenomenon (Bahia and Anderson, 1995a and Roberts, et al., 1996).

The work done during a loading cycle can be dissipated by cracking, crack propagation, heat, and plastic flow. All of these dissipation mechanisms are damaging to pavement

structures; therefore, it is necessary to limit the amount of energy dissipated. (John P. Zaniewski, Michael E. Pumphrey, 2004). The G*sin relationship was therefore selected as a parameter for the SHRP specification. By limiting the G*sin parameter, decreasing G* and/or sinδ, the energy dissipated per cycle is limited as well. This limiting parameter follows the rationale that a binder with a low G* is softer, which allows it to deform without developing high stresses, and a binder with a low sinδ will be more elastic, which enables the pavement structure to return to its original condition without dissipating energy.

## 2.3 Rolling Thin Film Oven Test (RTFOT)

A standard method of test for Effect of heat and air on a moving film of asphalt (Rolling Thin Film Oven Test). It is used to age the asphalt binders simulating short-term in-field aging conditions occurring during construction of HMA. Approximately 35 g of the binder is poured into each bottle, and this is placed in a rack inside the oven at 163°C. The rack is rotated for 75 minutes and the open orifice on the top of the bottle encounters an air jet during each rotation. The standard procedure for this test is shown in ASTM D2872.

# 3.3 Research Work Plan and Flow Chart

## 3.3.1. Research work plan

The research work plan shows the total no of tests conducted in laboratory in this thesis and also the Number of replication for each test.

Table 3.9:- **Work plan for the research**

| I/N | Description | | | Number of Tests | | |
|---|---|---|---|---|---|---|
| | Sample type | Sample condition | Test | Test Replicate | Temperature Replicate | No of tests |
| 1 | Neat Binder | Unaged | Conventional Tests | | | 9 |
| | | | PG Determination | 2 | 4 | 8 |
| | | | AST @ 10.0, 21.1, 37.8 & 54.4°C | 2 | 4 | 8 |
| | | | FST @ 10.0, 21.1, 37.8 & 54.4°C | 2 | 4 | 8 |
| | | | RTFOT @ 163°C | 2 | 1 | 2 |
| | | Aged | PG Determination | 2 | 4 | 8 |
| | | | AST @ 10.0, 21.1, 37.8 & 54.4°C | 2 | 4 | 8 |
| | | | FST @ 10.0, 21.1, 37.8 & 54.4°C | 2 | 4 | 8 |
| | | | RTFOT @ 163oC | 1 | 1 | 1 |
| 2 | 25% CSF/HL Mastics | Unaged | AST @ 10.0, 21.1, 37.8 & 54.4°C | 4 | 4 | 16 |
| | | | FST @ 10.0, 21.1, 37.8 & 54.4°C | 4 | 4 | 16 |
| | | | PG Determination | 4 | 1 | 4 |
| | | | RTFOT @ 163°C | 2 | 1 | 2 |
| | | Aged | AST @ 10.0, 21.1, 37.8 & 54.4°C | 4 | 4 | 16 |
| | | | FST @ 10.0, 21.1, 37.8 & 54.4°C | 4 | 4 | 16 |
| | | | PG Determination | 4 | 1 | 4 |
| | | | MSCR @ 52, 58, 64, 70 & 76°C | 4 | 4 | 16 |
| 3 | 35% CSF/HL Mastics | Unaged | AST @ 10.0, 21.1, 37.8 & 54.4°C | 4 | 4 | 16 |
| | | | FST @ 10.0, 21.1, 37.8 & 54.4°C | 4 | 4 | 16 |
| | | | PG Determination | 4 | 1 | 4 |
| | | | RTFOT @ 163oC | 2 | 1 | 2 |
| | | Aged | AST @ 10.0, 21.1, 37.8 & 54.4°C | 4 | 4 | 16 |
| | | | FST @ 10.0, 21.1, 37.8 & 54.4°C | 4 | 4 | 16 |
| | | | PG Determination | 2 | 1 | 2 |
| | | | MSCR @ 52, 58, 64, 70 & 76°C | 4 | 4 | 16 |
| 4 | 45% CSF/HL Mastics | Unaged | AST @ 10.0, 21.1, 37.8 & 54.4°C | 4 | 4 | 16 |
| | | | FST @ 10.0, 21.1, 37.8 & 54.4°C | 4 | 4 | 16 |
| | | | PG Determination | 4 | 1 | 4 |
| | | | RTFOT @ 163oC | 2 | 1 | 2 |
| | | Aged | AST @ 10.0, 21.1, 37.8 & 54.4oC | 4 | 4 | 16 |
| | | | FST @ 10.0, 21.1, 37.8 & 54.4oC | 4 | 4 | 16 |
| | | | PG Determination | 4 | 1 | 4 |
| | | | MSCR @ 52, 58, 64, 70 & 76oC | 4 | 4 | 16 |
| **Total No of Tests** | | | | | | **328** |

## 3.3.2. Experimental flow chart

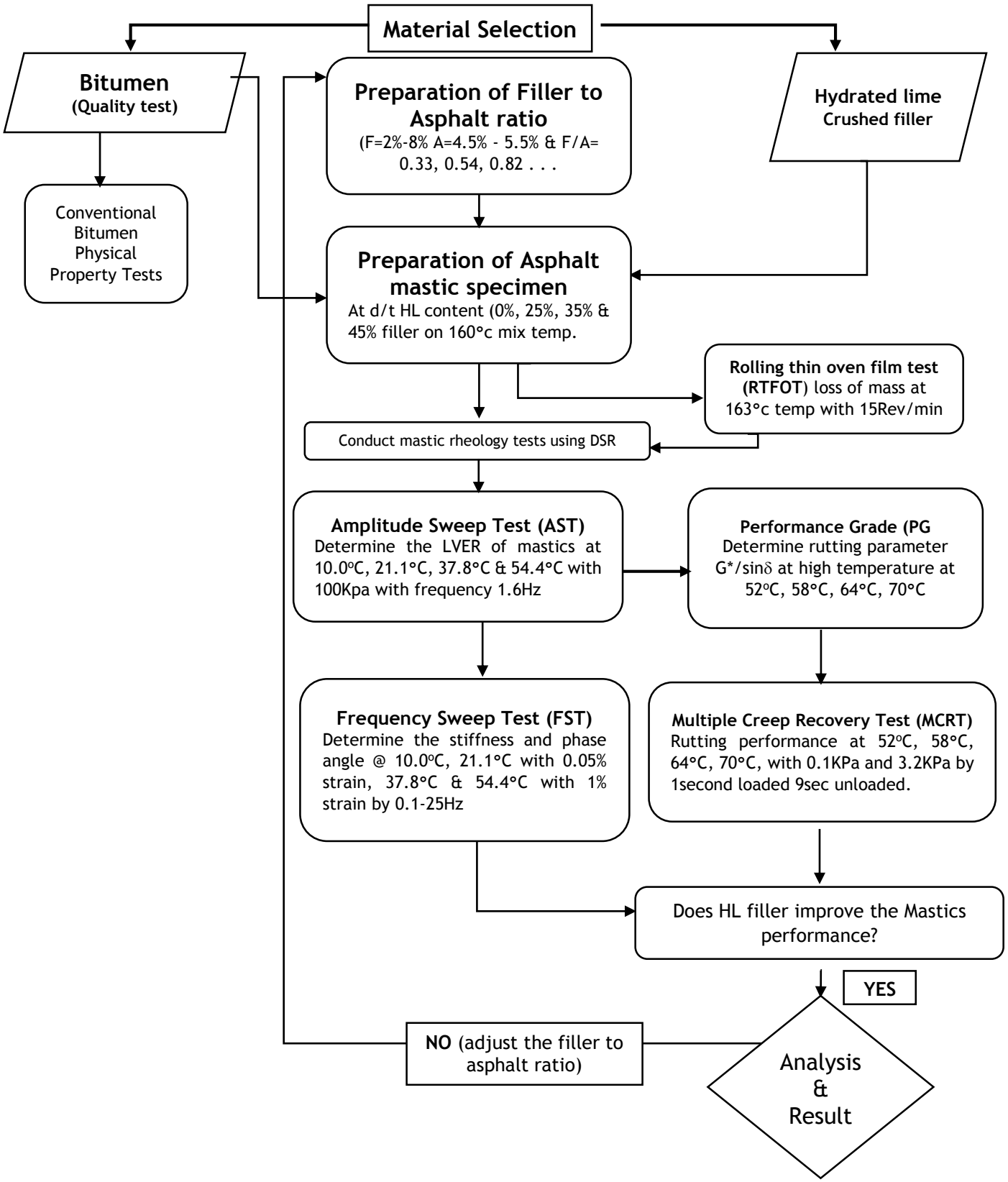


**Figure 3.5:-** Flow chart for experimental work

# CHAPTER 4. RESULT AND ANALYSIS

## 4.1. Dynamic Shear Rheological (DSR) Analysis of Asphalt Mastics

### 4.1.1. Amplitude Sweep Test (AST) Results

### 1. Effect of Temperature and Mineral Filler on Mastic of LVE

From The test results indicate that both stiffness and strain for the given asphalt mastic dependent on the temperature and types of mineral filler have. As shown in the figure below as the temperature decreases, there is an increase in complex modulus that indicates that asphalt mastic more stiff at low temperature. In contrast, as temperature increases, the stiffness of the mastic material decreases. As shown in the figure 4.1 and 4.2 the reduction of G* as the temperature increase from 10.0°C, 21.1°C, 37.8°C and 54.4°C. This indicates that asphalt mastic affected by temperature. Amplitude sweep tests results are presented in **Appendix B**.

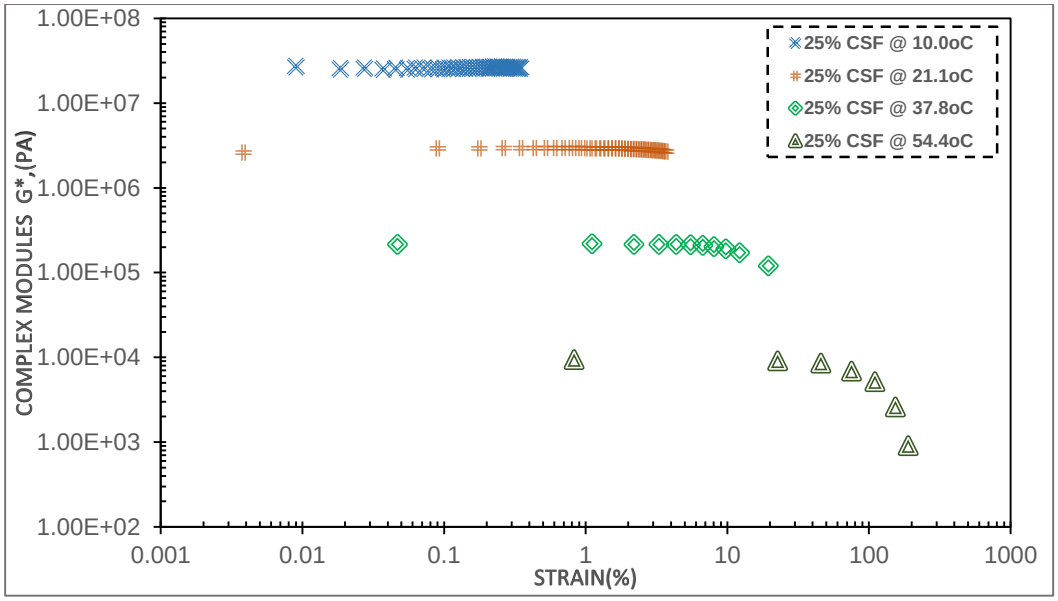


**Figure 4.7:-** Effect of crushed stone Filler (CSF) and temperature on asphalt mastic ratio 25% CSF

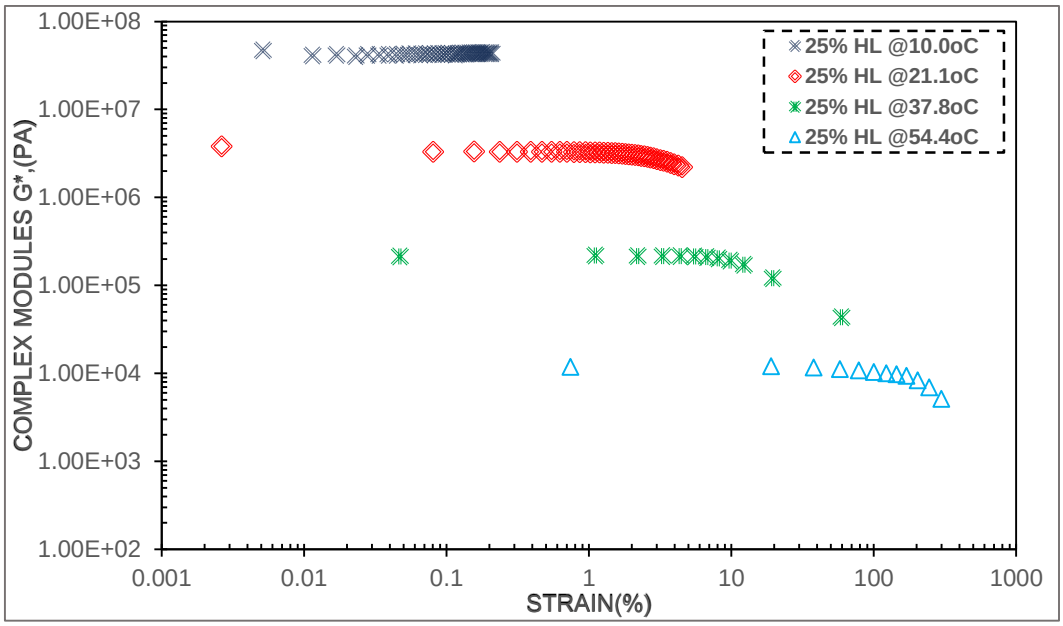


**Figure 4.8:-** Effect of Hydrated Lime Filler (HL) and temperature on asphalt mastic ratio 25% HL

## 2. Effect of Filler content on mastics of LVE and Stiffness

On the other hand Fillers has a significant effect on stiffness and strain value relative to virgin binder, therefore hydrated lime has higher complex modules value than crushed stone filler and virgin bitumens. In figure 4.3 figure 4.4, G* increases slightly for as the percentage of filler content increases at constant temperature. Hence from graphs shows below G* has more significant response (change) for temperature than filler type, therefore mastic is more susceptible to temperature rather than filler type.

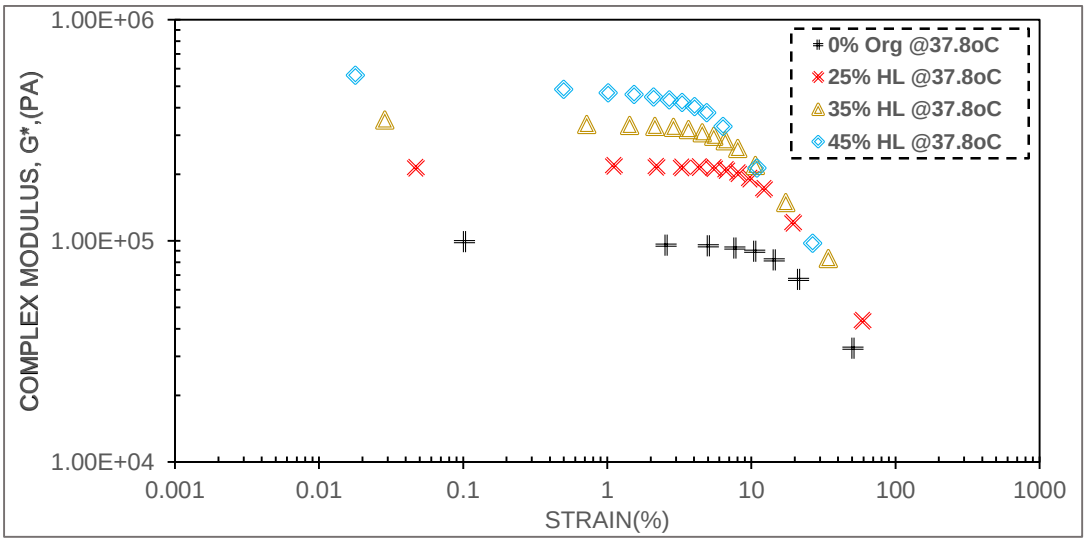


**Figure 4.9:-** Effect Hydrated Lime filler ratio on asphalt mastic at temperature 37.8$^{o}$C

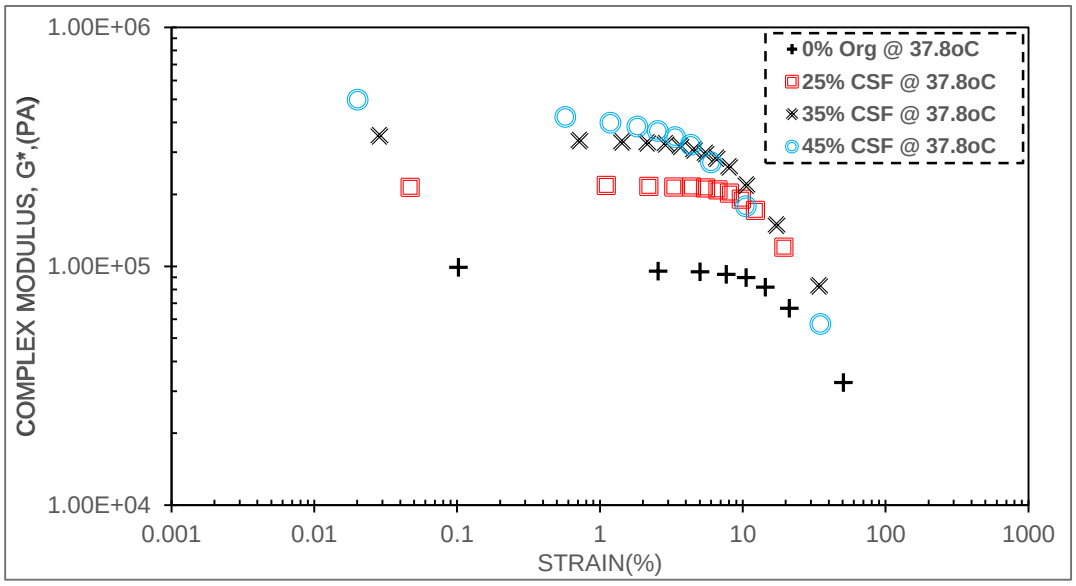


**Figure 4.10:-** Effect of Crushed stone filler ratio on asphalt mastic at temperature 37.8oC

## 3. Effect of filler type on mastics of LVE

Filler type is one of the major effect on stiffness and rheological property of bitumen. From figure 4.5 presented below hydrate lime has more stiffness G* than crushed stone and virgin bitumen.

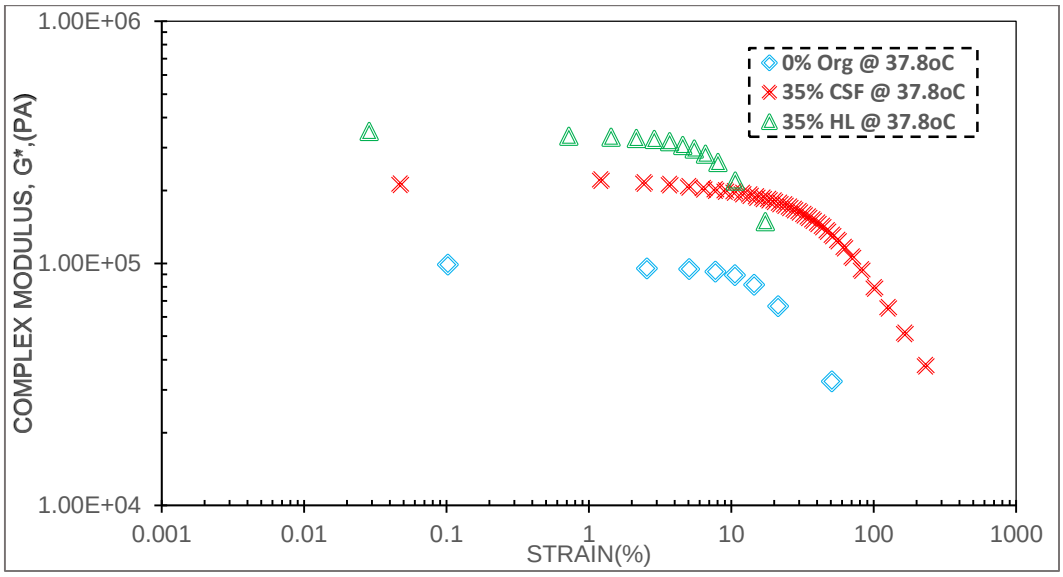


**Figure 4.11:-** Effect of Filler and filler ratio on asphalt mastic at temperature 37.8oC

In analyzing the AST data, which was explained earlier, was used to determine the linear Visco Elastic region (LVE). As shown in Figures 4.4, the linear strain limit was therefore

somewhat arbitrarily established as the stress or strain at which the complex modulus decreased to 95 percent of its initial value.

It should be noted that at temperatures below 20˚C and especially at high frequencies, no decrease in complex modulus could be observed over the entire range of the applied stresses. This was due to the high stiffness of the bitumen and the low strain values that could be generated by the rheometer. This meant that at these temperatures and frequencies, even at the highest possible generated stress, the sample was still within its linear region. Therefore, defining the LVE region at low temperatures (e.g. 10˚C) for some of the bitumens was not possible. The LVE limits of the mastics at all conditions of frequency and temperature are presented in Tables 4.1

The data from these stress sweeps was analyzed and the linear stress or strain limits plotted against temperature. These graphs are shown in Figures 4.1 to 4.7. It can be seen from Figures 4.6 to 4.7 that generally the LVE strain limit increases with temperature for all the bitumens

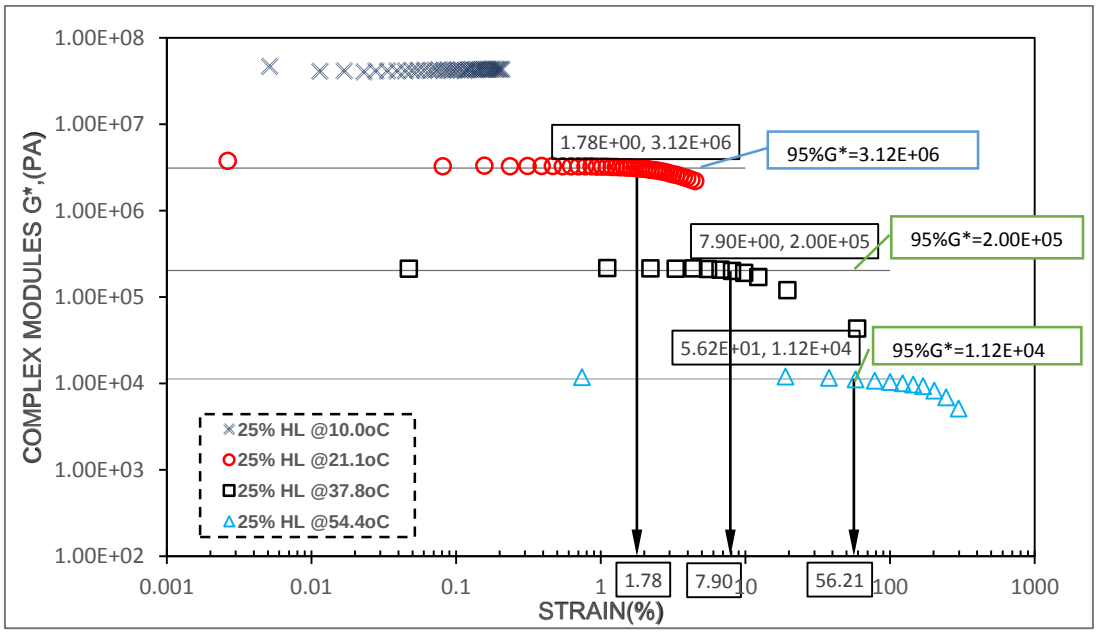


**Figure 4.12:-** Effect of Temperature on LVE region of asphalt mastic

## 4. Effect of Aging on LVE of asphalt mastics

Aging has the effect on the asphalt mastic stiffness and strain. As shown on the Figure 4.7 below the stiffness value of Unaged asphalt mastic is lower than RTFO aged asphalt

mastic, which decreases LVER. The result shows from the graph there is an increasing in complex modulus by 3.94 times and reduction of LVE ranges by 137.8%.

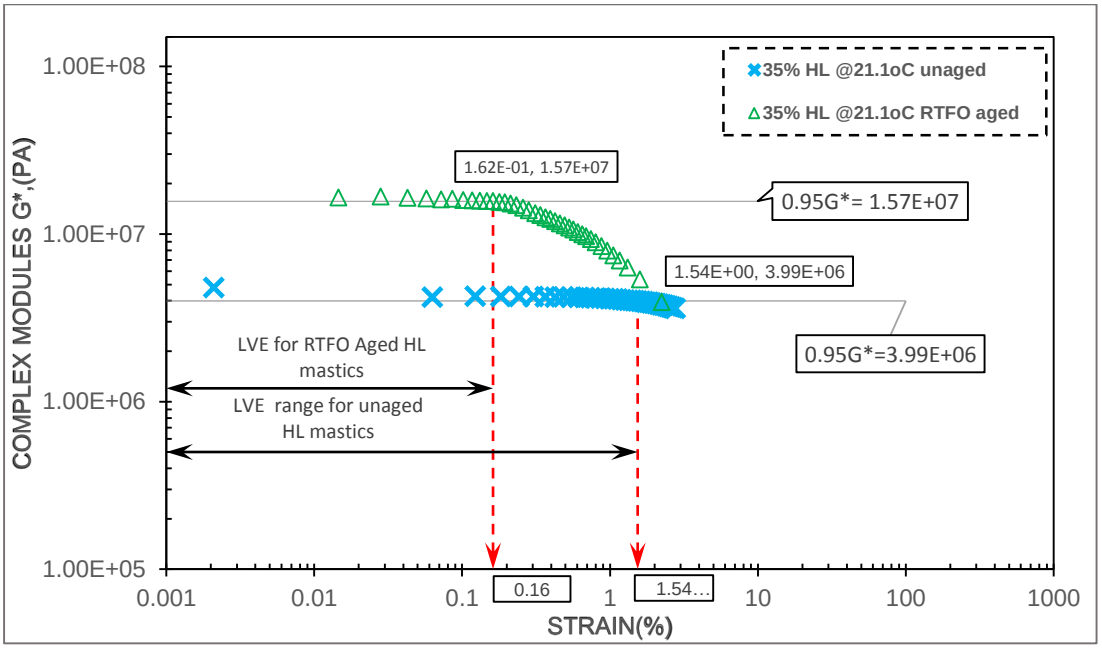


**Figure 4.13:-** Effect of ageing on LVE region for 35% HL asphalt mastic at 21.1°C

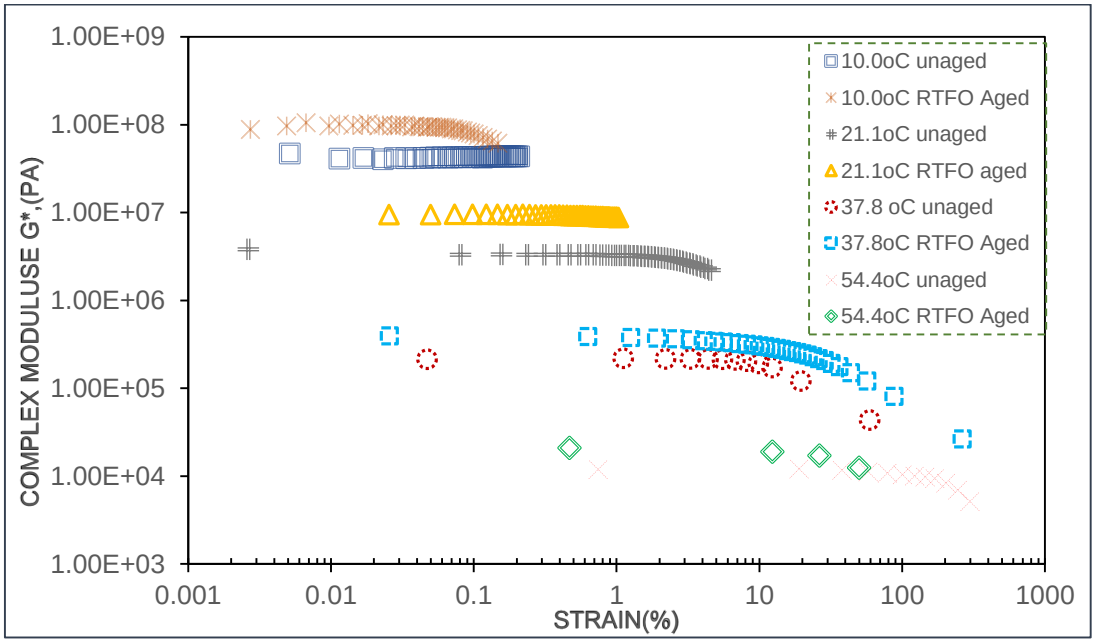


**Figure 4.14:-** Effect of aging on LVER For 25% HL mastics

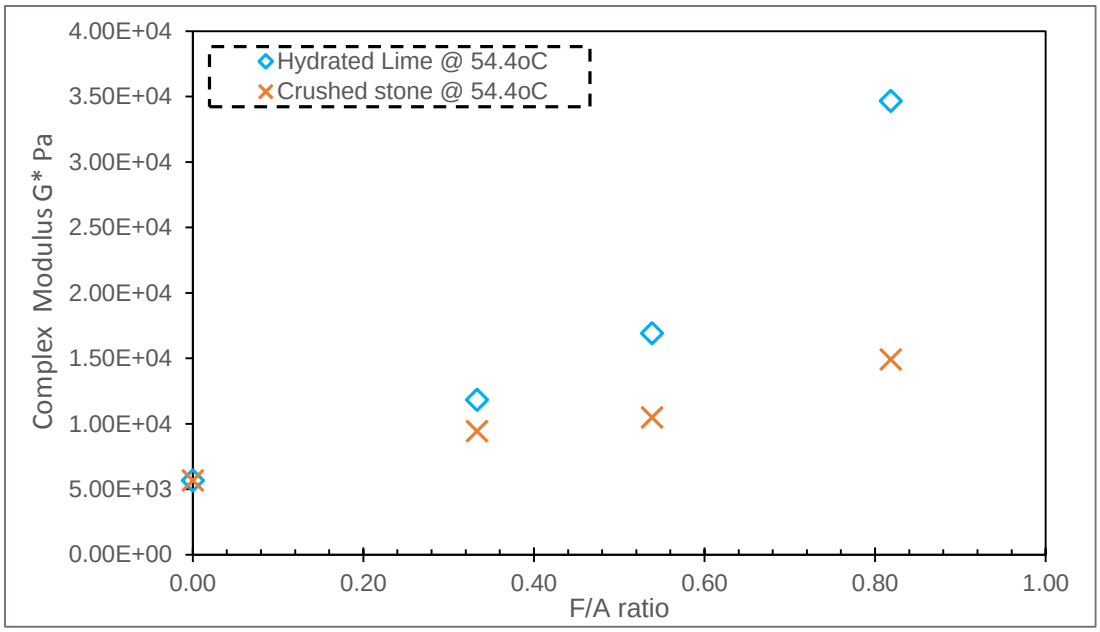


**Figure 4.15:-** Effect of filler type and content on stiffness of asphalt mastics at temperature 54.4oC

Table 4.1:- **Summary of LVE region strain**

| Filler type | Test temperature(°C) | LVE region strain (%) | |
|---|---|---|---|
| | | Unaged | Aged |
| Neat binder | 10 | - | - |
| | 21.1 | 0.31 | 1.3 |
| | 37.8 | 6.06 | 4.9 |
| | 54.4 | 62.49 | 42.3 |
| 25% Hydrated lime | 10 | - | - |
| | 21.1 | 1.78 | 0.77 |
| | 37.8 | 7.91 | 2.38 |
| | 54.4 | 56.21 | 5.06 |
| 35% hydrated lime | 10 | - | - |
| | 21.1 | 1.54 | 0.16 |
| | 37.8 | 3.60 | 1.13 |
| | 54.4 | 19.11 | 1.72 |
| 45% hydrated lime | 10 | - | - |
| | 21.1 | 0.79 | 0.12 |
| | 37.8 | 1.46 | 0.65 |
| | 54.4 | 28.30 | 12.3 |

## 4.1.2. Frequency Sweep Test (FST) Results

### 1. Effect of Temperature and Frequency on stiffness of mastic

Measurements from the temperature-frequency sweep tests were used to construct master curves for the binders. A master curve provides the relationship between stiffness and reduced frequency; the reduced frequency is in turn obtained by developing a relationship between the test temperature and the horizontal shift of data at different frequencies from different temperatures. In this case, data from the four different test temperatures were horizontally shifted to form a single smooth curve at 21.1°C reference temperature.

As seen from the graphs, complex shear modulus (stiffness) values have increased with the increase in frequency, while they decreased with the increase of the temperature. The increase in the filler volume fraction, also increased the shear modulus values for all types of mastics.

In general, the increase in shear moduli due to the increase of the frequency is based on the fact that the material is in the plastic region (viscous) at low frequencies (high values for phase angle), as shown in Figures 4.10 and 4.12, while for high frequencies the phase angle decreases, meaning that the material gets into the more elastic region. These figures show the rheological behavior of mastics at 25% volume fraction (phase angle variation) function of frequency sweep at all four testing temperatures.

For all test temperatures, the shear modulus increases (phase angle decreases) with increasing test frequency. This implies that the asphalt binder stiffness decreases with viscoelastic-liquid behavior when tested at higher temperature and lower frequency ranges (figures 4.10 & 4.12). Frequency sweep tests results are presented in **Appendix C**.

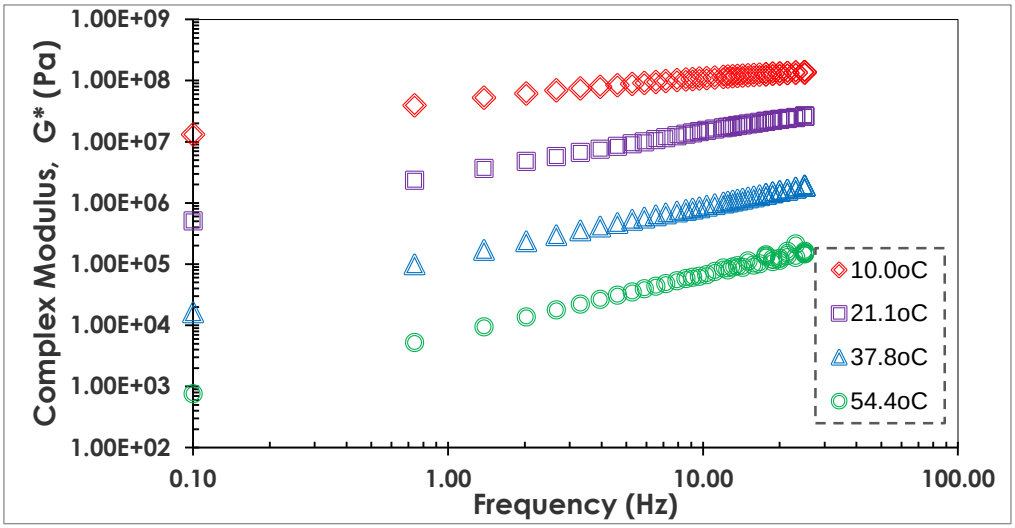


**Figure 4.16:-** Effect of temperature and frequency on G* asphalt mastic at 25%HL

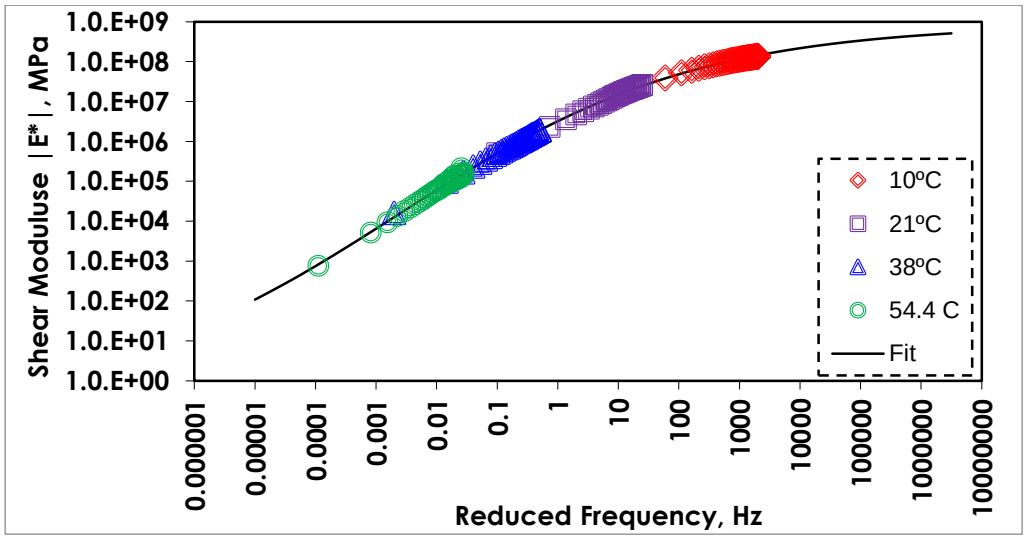


**Figure 4.17:-** Shifting for complex modulus master curve for 25%HL mastic

In constructing the master curves using the time-temperature superposition principle, test data collected from the DSR at different temperatures and loading times, in terms of stiffness or shear complex modulus G*, are compared to a reference temperature, which usually is 21.1 °C. The data at any other temperatures are then shifted with respect to time until various curves overlap almost perfectly to form a single master curve. Typically, the shear complex modulus or stiffness modulus of asphaltic mixes increases with decreasing temperature and increasing loading frequency. As shown in figure 4.11 and 4.13 master curve for complex modulus and phase angle at different temperatures are shifted to a single temperature curve ($T_{ref}$ =21.1°C). These figures shows stiffness of asphalt mastics increases and phase angle decreases as the reduced frequency increase.

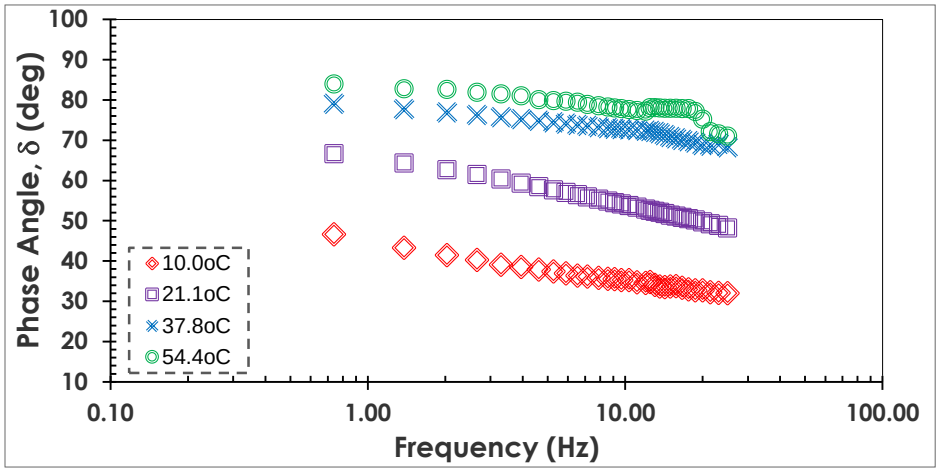


**Figure 4.18:-** Effect of temperature and frequency on δ asphalt mastic at 25% HL

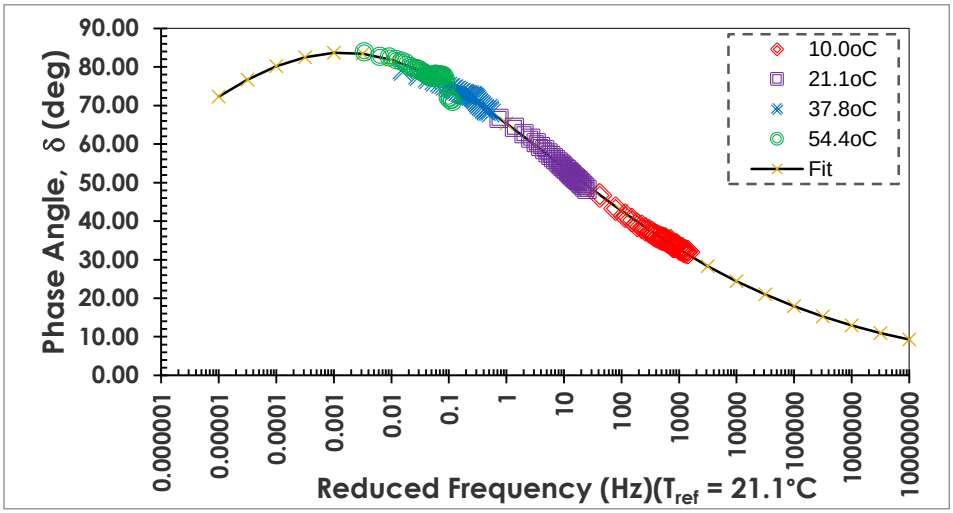


**Figure 4.19:-** Shifting for phase angle master curve for 25% HL

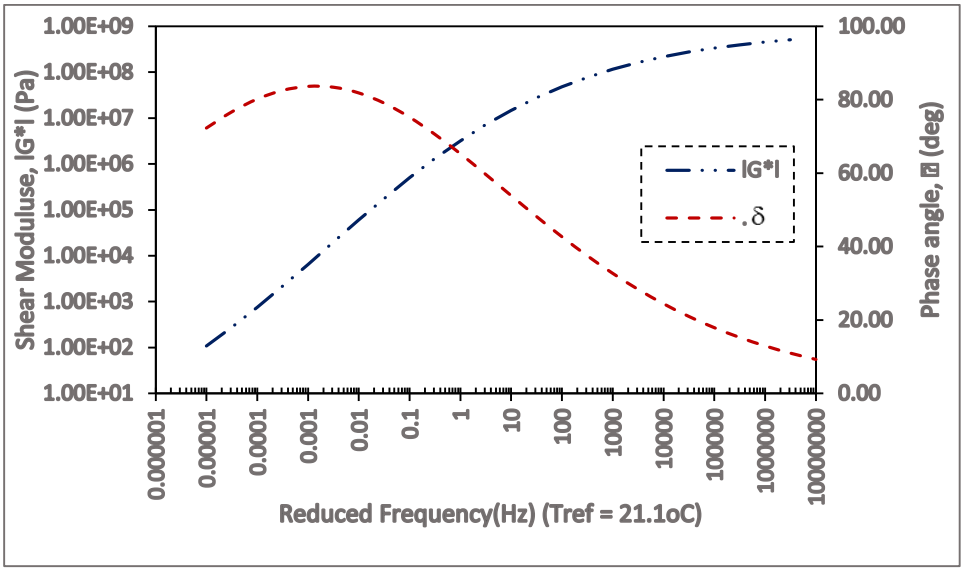


**Figure 4.20:-** Complex modulus and phase angle master curve for 25% HL

It can be seen from above figure 4.14 that as the reduced frequency decreases, the shear modulus decreases continuously which reflects the decrease in the resistance to shear deformation; which in turn results in a decrease in elasticity or ability to store energy. At lower temperature and higher reduced frequency, the Asphalt binder and asphalt mastics exhibited higher viscoelastic properties (higher stiffness and lower phase angle).

According to Figure 4.14, the linear viscoelastic response of an asphalt mastic can be categorized into three zones of behaviour:

- Low temperatures or short loading times (high frequencies), where bitumen behaves as an elastic solid and shear stiffness approaches 1 GPa (glassy region),
- Intermediate temperatures or loading times, where bitumen gradually changes from elastic behaviour to fluid behaviour. Within this transition region, behaviour of bitumen is composed of both elastic and viscous responses, and
- High temperatures or long loading times (low frequencies), where bitumen behaves as a viscous fluid.

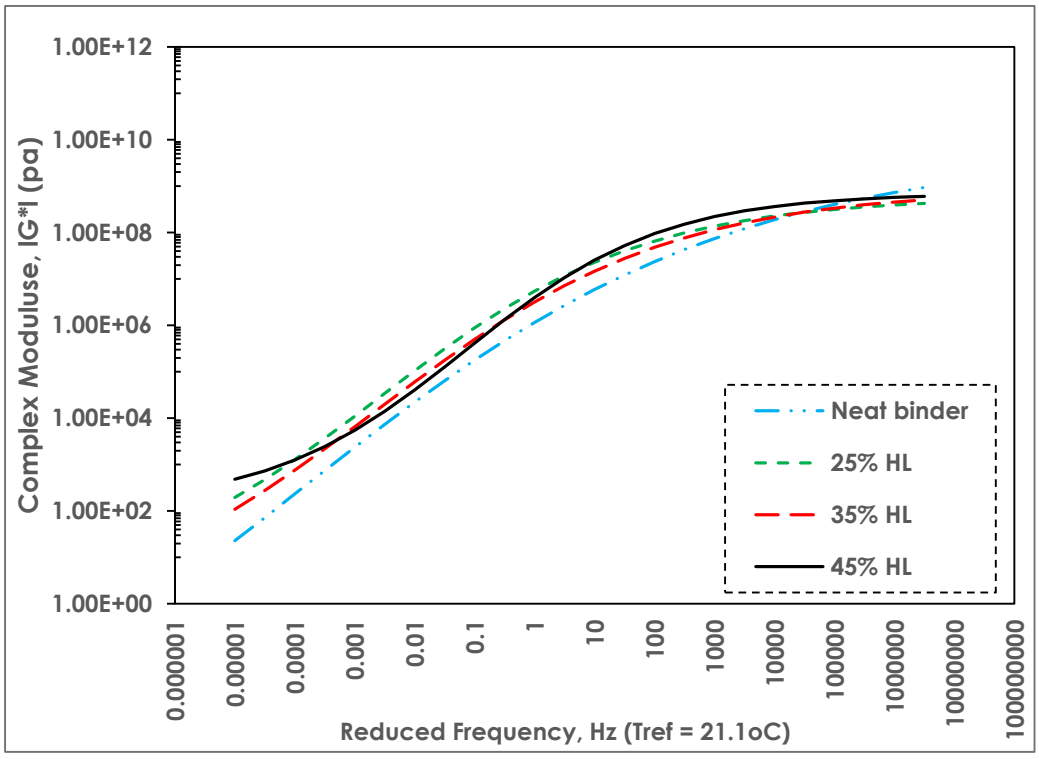


**Figure 4.21:-** Stiffness master curve for mastics with Hydrated Lime

A comparison of complex modulus master curves for all the HL asphalt mastics is presented in Figure 4.15. The figure shows that the mastic's with higher filler content has the lowest

complex modulus values at high frequencies and low temperatures. The Hydrate lime mastics with 45% filler ratio had the largest change in complex modulus as a function of loading frequency having the highest complex modulus values of all the mastics and neat binder at high frequencies and lowest values at low frequencies.

At high temperature and low frequency the smaller value of shear modulus is pronounced and at low frequency and high temperature the modulus increases appreciably as modifier increases. However, at high frequency and low temperature the effect of the modifier makes no difference (for frequency more than10Hz) since frequency relates to loading rate (speed), from the graph the effect of modifier is evident at typically operating frequency/speed (0.01 to 10Hz).

From above graphs we can summarize that hydrated lime filler appreciably improves the complex shear modulus of the virgin binder at higher temperatures. Rutting is a serious problem at high temperature due to slow moving traffic and as observed the filler improves the pavement performance against this distress by increasing the stiffness of the binder.

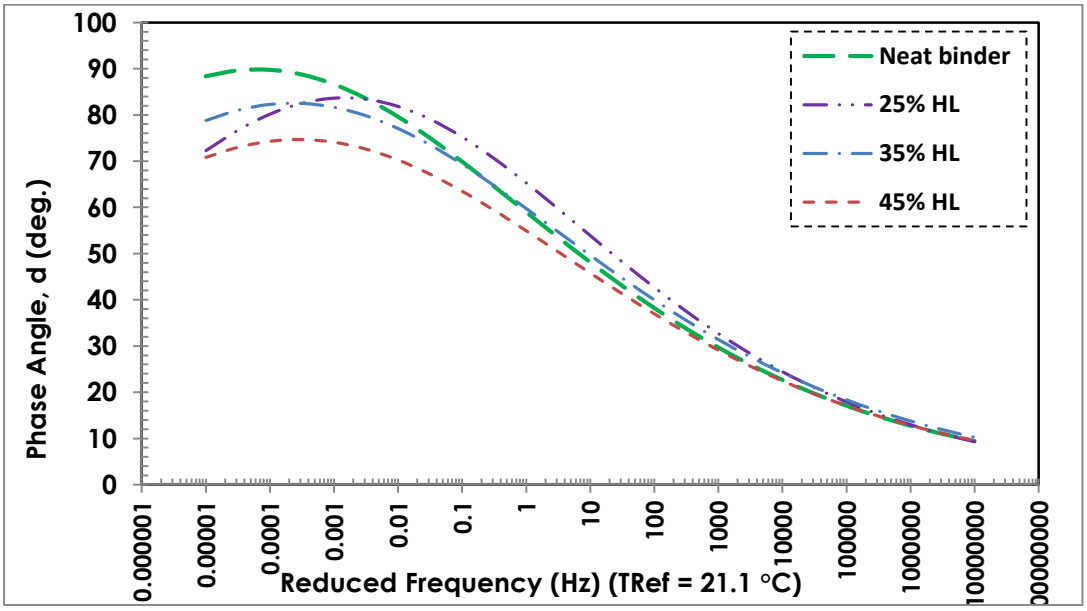


**Figure 4.22:-** Phase angle master curve for mastics with Hydrated Lime

Figure 4.16, presents a comparison of the phase angle master curves for the three mastics with one neat binder. It demonstrate that the decrease in phase angle at high temperature and low frequency as content of modifier increases, Thus the decrease in phase angle indicates the increase in elastic modulus.

It can be seen in the figure that all the mastics tend to converge towards the same phase angle versus loading frequency relationship at high frequencies (low temperatures). This can be attributed to the high elastic response of binders at low temperatures and high frequencies irrespective of filler type and content.

## 2. Black space diagram

Black diagram is also a common data presentation diagram for the understanding of the rheological characteristics of bituminous binders. The complex modulus and phase angle measurement obtained from a dynamic test are plotted in the graph of the Black diagram. The effects of temperature and loading time are eliminated from the plot, which allow the dynamic data to be presented in a plot without requiring the shifting of raw data.

The black space diagram is a simple rheological plot of shear modulus and phase angle in semi-log space (Figure 4.17). From figure below the mastic resulted in smooth black diagram, which exhibits viscoelastic-liquid properties.

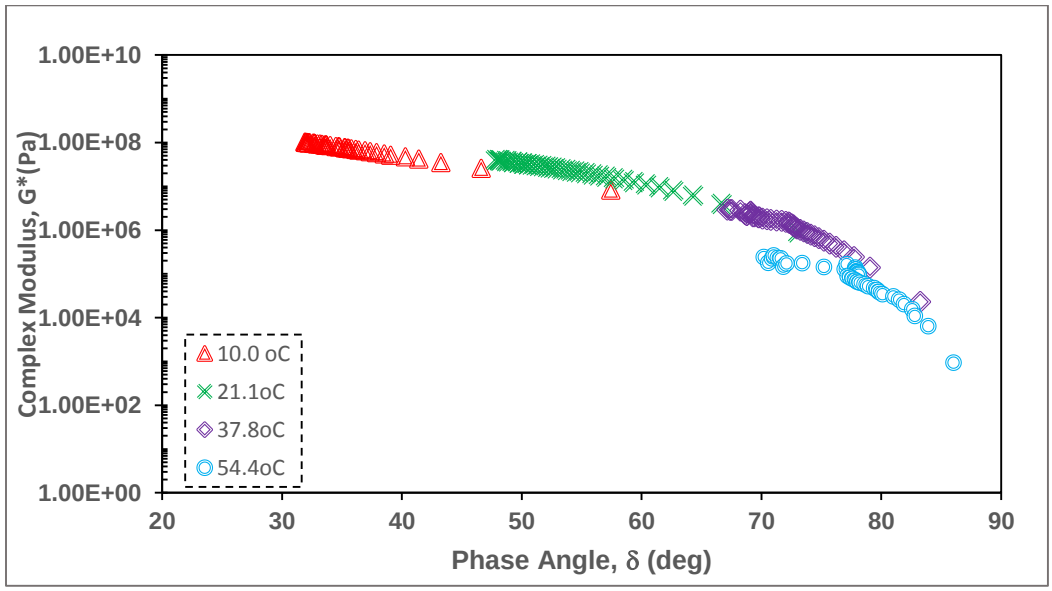


**Figure 4.23:-** Black space diagram for 25% HL

## 3. Effect of Filler on Aging of asphalt mastics

Asphalt binder or asphalt mastic needs to be soft enough in order to resist cracking at low temperatures, and stiff enough to avoid rutting at high temperatures. As we have seen in the figure 4.18 below Aging of binder has increases (complex modulus) stiffness at high temperature and low reduced frequency and decrease the elasticity and softening effect of

binder at low temperature and high reduced frequency, this shows that the binder effect for fatigue cracking and low temperature has decrease.

As observed above in figure 4-18 and 4-19 the main rheological parameter, complex shear modulus (G*) behaves in different ways as a result of temperature, frequency, content of filer and ageing.

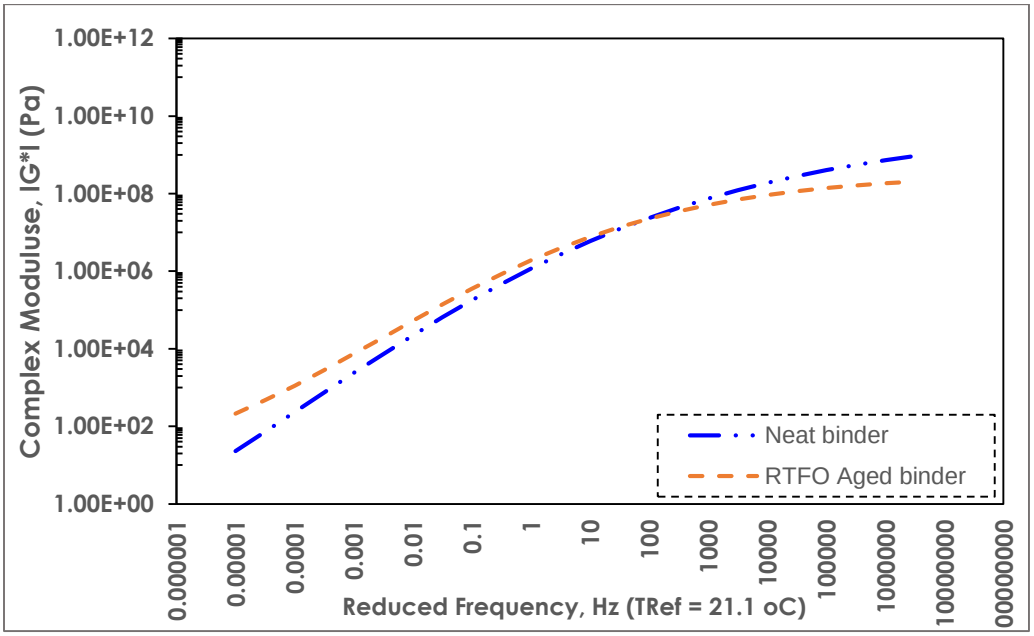


**Figure 4.24:-** Effect of aging on stiffness of asphalt mastic (binder PG 60/70)

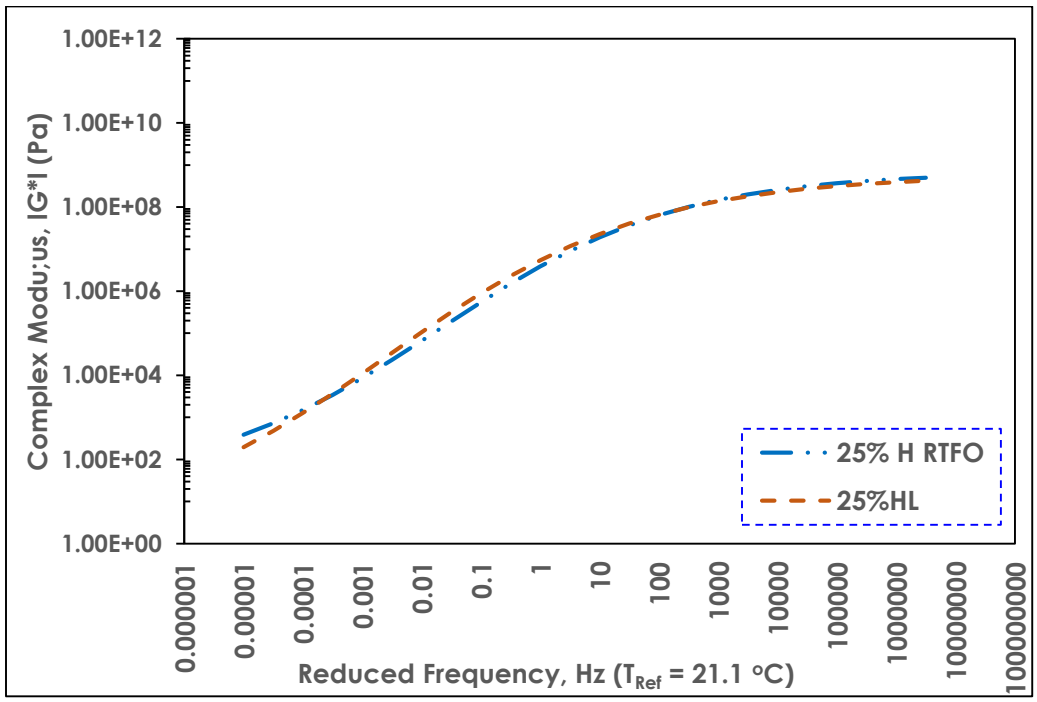


**Figure 4.25:-** Effect of aging on stiffness of asphalt mastic (25% HL)

Figure 4.19 presents a comparison of the complex modulus master curves for the 25% HL RTFOT aged and Unaged mastics. It can be seen in the figure that by addition of hydrated lime there is a significant reduction on stiffness due to aging effect on mastics. This can be attributed to the high elastic response of binders and asphalt mastics at low temperatures and high frequencies and enhance the binder elasticity (ductility behaviour) at low temperature to improve the influence of fatigue and low temperature cracking.

Table 4.2:- **shift factor for complex modulus master curve on asphalt mastics for reference temperature 21.1oC**

| Filler type | Sample type | α | β | δ | γ | $a_{10.0}$ | $a_{21.1}$ | $a_{37.8}$ | $a_{54.4}$ |
|---|---|---|---|---|---|---|---|---|---|
| Neat binder | 0% | 14.652 | -1.092 | -4.909 | 0277 | 1.150 | 0.00 | -1.497 | -2.723 |
| Hydrated lime | 25% HL | 8.596 | -1.179 | 0.164 | 0.458 | 1.188 | 0.00 | -1.812 | -3.135 |
| | 35% HL | 9.517 | -1.073 | -0.586 | 0.408 | 1.908 | 0.00 | -1.701 | -2.953 |
| | 45% HL | 6.741 | -0.697 | 2.100 | 0.611 | 1.940 | 0.00 | -1.417 | -2.499 |
| Crushed stone | 25% CSF | 8.264 | -0.563 | 0.625 | 0.426 | 1.942 | 0.00 | -1.394 | -2.980 |
| | 35% CSF | 7.632 | -0.962 | 0.878 | 0.500 | 1.860 | 0.00 | -1.580 | -3.242 |
| | 45% CSF | 9.149 | -1.099 | -0.238 | 0.427 | 1.691 | 0.00 | -1.754 | -2.763 |

Table 4.3:- **shift factor for phase angle master curve on asphalt mastics for reference temperature 21.1oC**

| Filler type | Sample type | α | β | γ | $a_{10.0}$ | $a_{21.1}$ | $a_{37.8}$ | $a_{54.4}$ |
|---|---|---|---|---|---|---|---|---|
| Neat binder | 0% | 12.481 | 1.343 | 0.383 | 1.145 | 0.000 | -1.055 | -0.357 |
| Hydrated lime | 25% HL | 10.374 | 1.018 | 0.359 | 1.756 | 0.000 | -1.671 | -2.341 |
| | 35% HL | 11.463 | 1.168 | 0.359 | 2.053 | 0.000 | -1.395 | -1.000 |
| | 45% HL | 10.377 | 1.137 | 0.384 | 2.234 | 0.000 | -1.615 | -1.487 |
| Crushed stone | 25% CSF | 11.298 | 1.293 | 0.337 | 1.252 | 0.000 | -1.267 | -0.765 |
| | 35% CSF | 11.803 | 1.163 | 0.319 | 1.710 | 0.000 | -1.299 | -0.913 |
| | 45% CSF | 12.793 | 1.234 | 0.338 | 2.066 | 0.000 | -1.360 | -1.321 |

## 4. Statistically analysis with ANOVA

After the laboratory procedures and data collection were conducted, statistical analysis was performed to evaluate the significance of addition of filler (hydrated lime) to asphalt binder using one-way analysis of variance (ANOVA).

On this study, the three independent variables(25%, 35% and 45%) consisted for ANOVA analysis and the null hypothesis is the addition of mineral filler on asphalt mastic has no effect. This mean there is no difference in the means stiffness of mastic with in three groups of treatment. Therefore the

Null hypothesis can be formulate as

H0: $\mu 1 = \mu 2 = \mu 3$ (claim)
H1: At least one mean is different from the others.

If there is no difference in the means, the between-group variance estimate will be approximately equal to the within-group variance estimate, and the F test value will be approximately equal to F critical. The null hypothesis will not reject. However, when the means differ significantly, the between-group variance will be much larger than the within group variance; the F test value will be significantly greater than F critical value; and the null hypothesis will be rejecting. Since variances are compared, Using 0.1 level of significance for this hypothesis analysis tests.

ANOVA was performed taking values of the complex shear modulus (G*) obtained at selected values $10^{-5}$ Hz, 1.0 Hz, and $10^{+6}$ Hz frequencies for the reference temperature of 21.1°C. Details of ANOVA hypothesis testing is presented in **Appendix D** of the research paper.

Table 4.4:- **Summary of ANOVA hypothesis test**

| Frequency, (Hz) | F factor | P factor | F critical | Null hypothesis |
|---|---|---|---|---|
| $10^{-5}$ | 5.237547 | 0.071764 | 4.19086 | Reject |
| 1.0 | 0.485082 | 0.710683 | 4.19086 | Accept |
| $10^{+6}$ | 11.68026 | 0.018997 | 4.19086 | Reject |

Therefore the statistical analysis supports the previous conclusion which says the modifier(hydrated filler) improves the binder at low frequency and high temperature and high frequency and low temperature, but not at intermediate low temperature. This implies the hydrated lime is better at maximum damaging effect of heavy traffic during high temperature with low speed of loading rate.

## 4.1.3. Performance Grade (PG) Test Results

Performance graded (PG) is used for specifying asphalt binders based on performance specification. It specifies binders on the basis of the climate and attendant pavement temperatures in which the binder is expected to serve. Performance graded (PG) binders are graded for the high end and low end temperatures for example PG 64-22. The first number, 64, is often called the "high temperature grade." This means that the binder would possess adequate physical properties to resist rutting at least up to 64°C. This would be the high pavement temperature corresponding to the climate in which the binder is actually expected

to serve. Likewise, the second number (-22) is often called the "low temperature grade" and means that the binder would possess adequate physical properties to resist thermal cracking at least down to -22°C. To simulate their actual aged condition in the field binders have been aged in the Rolling Thin Film Oven (RTFO) to simulate oxidative hardening that occurs during hot mixing and placing and in the Pressure Aging Vessel (PAV) to simulate hardening in service that could be expected after a few years in place

In this study low temperature grade characterization is not specified due to absence of pressure aging vessel (PAV) Bending beam rheometer (BBR) and Direct Tensile tester (DTT) equipment.

The rheological parameter, $G^*/\sin\delta$ was chosen as the parameter for SHRP specifications with respect to rutting and used to determine the maximum temperature that the asphalt binder could meet the minimum criteria of AASHTO M-320.

The tests are done after different aging conditions and the data are used to calculate the specification parameters as follows:

- Test original binder; $G^*/\sin\delta$ at 10 rad/s must be greater than or equal to 1 kPa.
- Test RTFO-aged binder; $G^*/\sin\delta$ at 10 rad/s must be greater than or equal to 2.2 kPa.
- Test PAV-aged binder; $G^* \sin\delta$ at 10 rad/s must be less than or equal to 5.0 MPa.

Table 4.5:- **PG determination for Unaged 25%HL mastics**

| Test Temperature | Phase Angle (δ) | Complex Modulus(G*) | Elastic Modulus(G′) | Viscous Modulus(G″) | G*/Sind ≥ 1kPa | Remark |
|---|---|---|---|---|---|---|
| (°C) | (°) | (Pa) | (Pa) | (Pa) | (Pa) | |
| 58.05 | 86.51 | 5.76E+03 | 3.51E+02 | 5.75E+03 | 5.77E+03 | Pass |
| 63.92 | 87.76 | 2.47E+03 | 9.65E+01 | 2.47E+03 | 2.47E+03 | Pass |
| 69.98 | 88.64 | 1.13E+03 | 2.68E+01 | 1.13E+03 | 1.13E+03 | Pass |
| 75.94 | 89.02 | 5.53E+02 | 9.46E+00 | 5.53E+02 | 5.53E+02 | Fail |
| Pass Fail Temperature (°C) | 71.34 | | | | | |
| Grade | 70 | | | | | |

Table 4.6:- **PG determination for RTFO-Aged 25%HL mastics**

| Test Temperature | Phase Angle (δ) | Complex Modulus(G*) | Elastic Modulus(G′) | Viscous Modulus(G″) | G*/Sind ≥ 2.2kPa | Remark |
|---|---|---|---|---|---|---|
| (°C) | (°) | (Pa) | (Pa) | (Pa) | (Pa) | |
| 64.08 | 86.90 | 4.58E+03 | 2.48E+02 | 4.57E+03 | 4.59E+03 | Pass |
| 69.97 | 87.61 | 2.29E+03 | 9.54E+01 | 2.29E+03 | 2.29E+03 | Pass |
| 75.95 | 88.35 | 1.06E+03 | 3.04E+01 | 1.06E+03 | 1.06E+03 | Fail |
| Pass Fail Temperature (°C) | 70.02 | | | | | |
| Grade | 70 | | | | | |

Table 4.7:- **Summary of performance grade determination test result**

| **Mastic** | **Unaged** | | **Aged (RTFO)** | | **Performance Grade AASHTO (M320)** |
|---|---|---|---|---|---|
| | Pass fail Temperature(°C) | Temperature Grade(°C) | Pass fail Temperature(°C) | Temperature Grade(°C) | |
| Neat binder | 65.5 | 64 | 67.3 | 64 | PG64-YY |
| 25%HL | 71.34 | 70 | 70.02 | 70 | PG70-YY |
| 35%HL | 73.4 | 70 | 74.5 | 70 | PG70-YY |
| 45%HL | 81.1 | 76 | 76.03 | 76 | PG76-YY |
| 25%CSF | 70.5 | 70 | 68.5 | 64 | PG64-YY |
| 35%CSF | 72.4 | 70 | 71.6 | 70 | PG64-YY |
| 45%CSF | 75.5 | 70 | 70 | 70 | PG70-YY |

In the table shows that the increment of filler content increase in performance grade (PG) of mastics. Hydrated lime filler has two grade increment at filler percentage of 45%. This shows that modifying bitumen with filler material increases the stiffness of the asphalt binder and better resistance for high temperature deformation. Performance Grade tests results are presented in **Appendix E**.

In the PG system, the high temperature parameter, G*/sinδ , is measured by applying an oscillating load to the binder at very low strain. In the above table shows there is a slight difference in pass fail temperature for the same filler content of different filler type. The PG high temperature parameter doesn't accurately represent the ability of modified binders to resist rutting and only showing the maximum temperature the pavement could serve based on the stiffness.. By using the higher levels of stress and strain in the MSCR test, the response of the asphalt binder captures not only the stiffening effects of the modifier, but also the delayed elastic effects.

## 4.1.4. Multiple stress Creep Recovery (MSCR) Test Results

The repeated shear creep test is performed using the Dynamic Shear Rheometer (DSR) by applying a controlled shear stress (0.1 kPa and 3.2kpa) using a haversine load for 1 second followed by a 9-second rest period. During each cycle, the asphalt binder reaches a peak strain and then recovers before the shear stress is applied again. The permanent strain is then accumulated for 10 cycles (or 100 seconds).

Repeated shear creep and recovery tests give extremely important practical information and, at the same time, useful data to one interested in the theory of the mechanical properties of asphalt binders or mastics. Since asphalt pavements are designed to be flexible, they must quickly return to their original configuration after loading. Rutting, pushing, and shoving are just a few of the failure mechanisms associated with inelastic or permanent deformation. Repeated loading without complete binder recovery is also a cause of fatigue cracking. Although the quality and gradation of the aggregate are important parts of the asphalt mix performance, the creep response of the binder/mastic is also a contributing factor. As creep is a time-dependent function, it is necessary to monitor recovery per unit time or to stipulate a time interval for an expected recovery. Since asphalt pavements are designed to be flexible, they must quickly return to their original configuration after loading.

For this study, repeated shear creep testing was conducted on hydrated lime and crushed stone filler mastics at temperatures 52°C, 58°C, 64°C, 70°C and 76 °C and three Filler content on mastics 25%, 35%, and 45%.

Table 4.8:- **Summary of MSCR testing temperature**

| Filler content | PG | Testing temperature (°C) | | | | |
|---|---|---|---|---|---|---|
| Neat binder (0%) | 64 | 52 | 58 | 64 | 70 | - |
| 25%HL | 70 | 52 | 58 | 64 | 70 | - |
| 35%HL | 70 | 52 | 58 | 64 | 70 | 76 |
| 45%HL | 76 | 58 | 64 | 72 | 76 | 82 |
| 25%CSF | 64 | 52 | 58 | 64 | 70 | |
| 35%CSF | 70 | 52 | 58 | 64 | 70 | |
| 45%CSF | 70 | 52 | 58 | 64 | 70 | |

## 1. Effect of loading on multiple stress creep recovery

Vehicle Loading is one of the parameter for rutting occurrence on pavement structure, figure 4.26 shown below as the loading increase the total (accumulated) strain was decreasing, this show that traffic loading has major influence on pavement distress like rutting and shoving at high temperature. therefor the accumulated strain increased up to

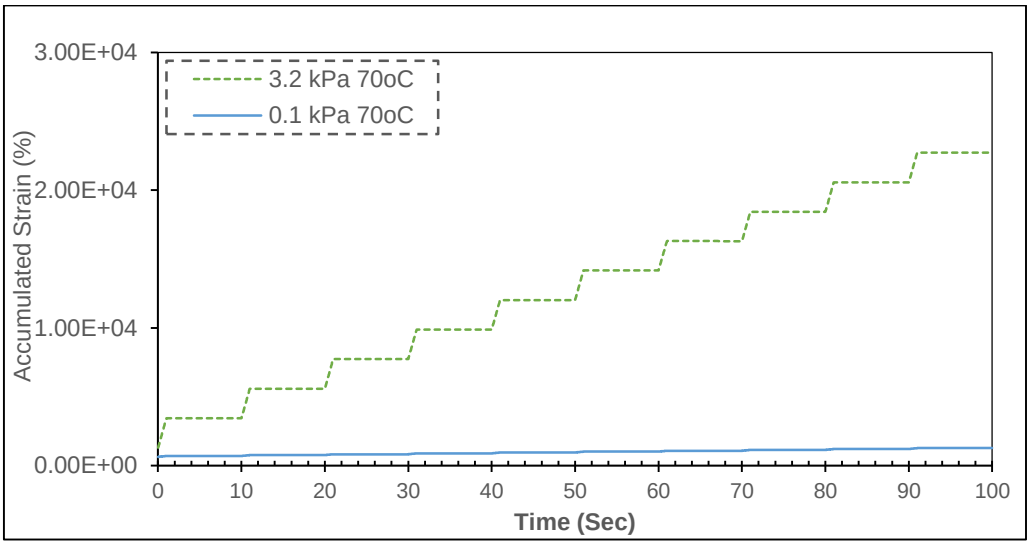


**Figure 4.26:-** Effect of loading on MSCR total strain for 25%HL mastics at 70°C

## 2. Effect of Temperature on Multiple stress creep recovery test

From the figures 4.27 below it is shown that the accumulated strain increase for the same percentage of filler content as increases the temperature increases. This refers that increasing temperature could influence the resistance of asphalt pavements to rutting. The test data shows that the total strain of hydrated lime mastics were increasing with increasing temperature at the same mass fraction of 45% hydrated lime mastic. The hydrated lime mastic total strain increased by 2.32 when the test temperature increase from 70°C to 76°C and 1.68 the test temperature increased from 76°C to 82°C.

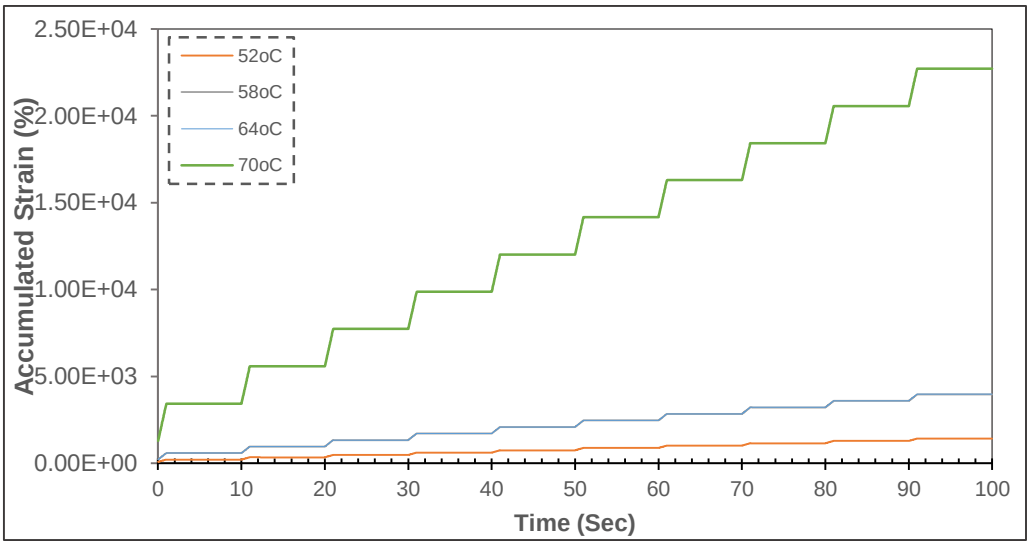


**Figure 4.27:-** Effect of Temperature on MSCR-3.2kPa total strain for 25%HL mastics

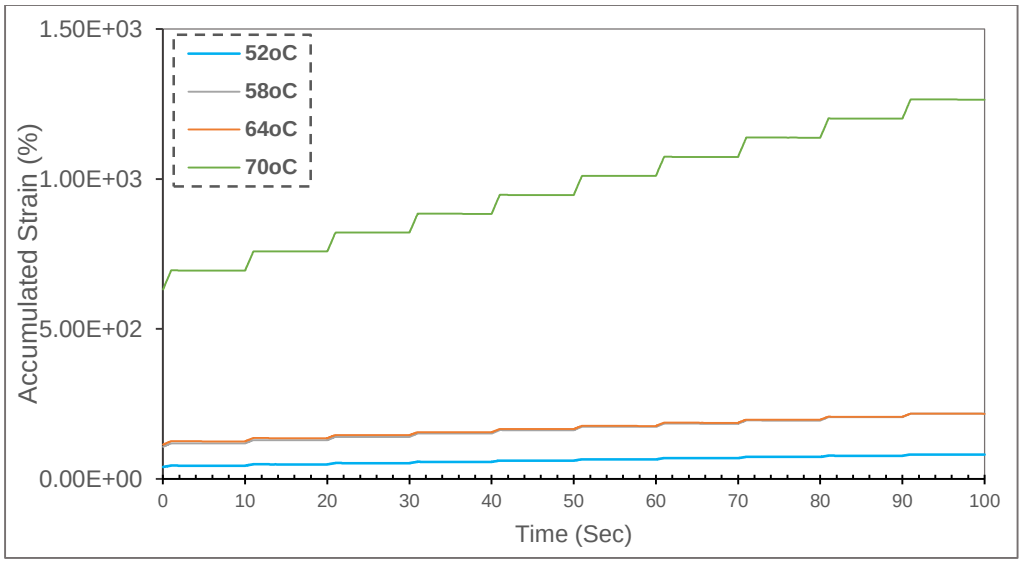


**Figure 4.28:-** Effect of Temperature on MSCR-0.1kPa total strain for 25%HL mastics

## 3. Effect of Filler content on multiple stress creep recovery

Figures 4.29 to 4.30 show that the total (accumulated) strain was influenced by the content of the mineral filler used, decreasing with the increase in the filler content in the mastics. Smallest values of total strain were obtained for mastics with 45% filler content, followed by the 35 and 25% filler content. This shows that high filler content could improve better the resistance of asphalt pavements to rutting phenomenon compared to lower content of mineral filler. From MSCR data shows that the total strains of hydrated lime mastics were reduce with increasing filler content compared to crushed stone mastic at constant temperature. Typically hydrated lime mastic strain reduced by 0.75, 0.73 and 0.24 times for

25%, 35% and 45% respectively at constant test temperature of 64°C after 10 cycles of shear creep loading and recovery.

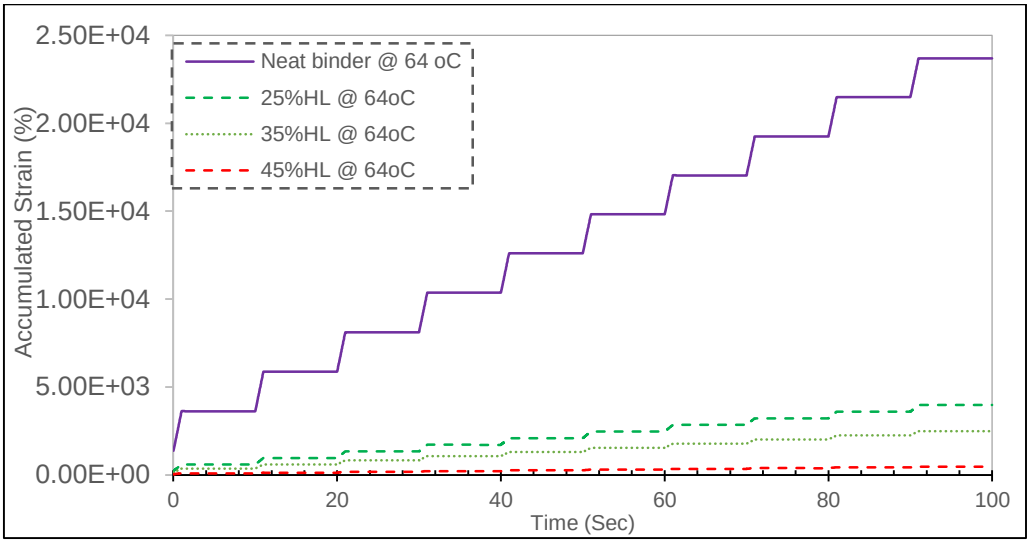


**Figure 4.29:-** Effect of filler content on MSCR 3.2kPa total strain for mastics at 64oC

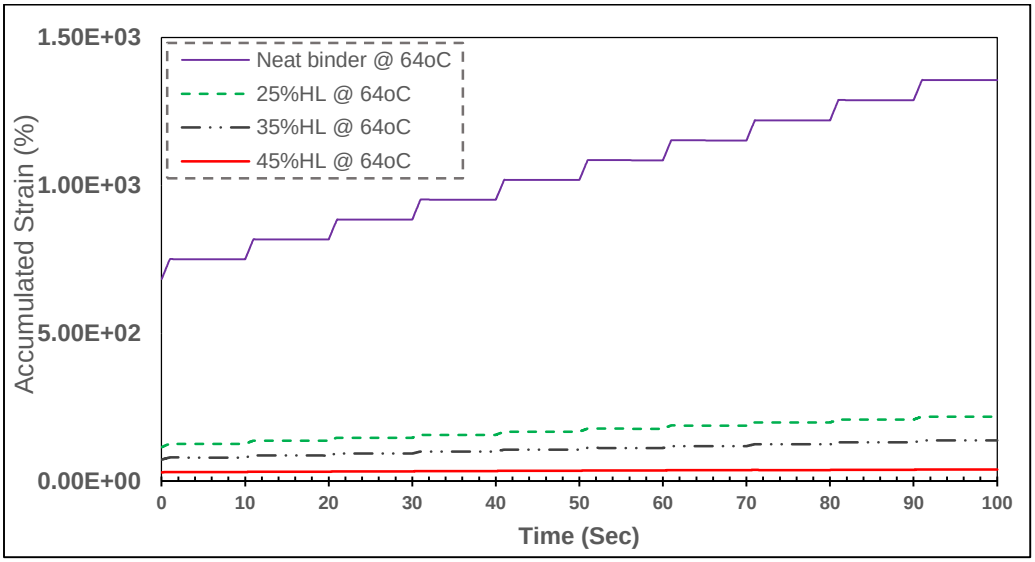


**Figure 4.30:-** Effect of filler content on MSCR 0.1 kPa total strain for mastics at 64oC

## 4. Effect of Filler type on multiple stress creep recovery

Figure 4.31 to 4.33 shows that hydrated lime filler mastic has small accumulated strain than crushed stone mastic for 0.1kPa and 3.2kPa. , the non-recoverable creep compliance Jnr refers to the ratio between accumulated strains and applied stress an indicator of rutting resistance for hydrated lime mastics is small compared to crushed stone. From the data shown below the accumulated strain for hydrated lime reduce by 0.78 than crushed stone for 25% filler content at temperature of 64°C. This shows the resistance for permanent

deformation for hydrated lime mastics is much higher than crushed stone at temperature 64°C.

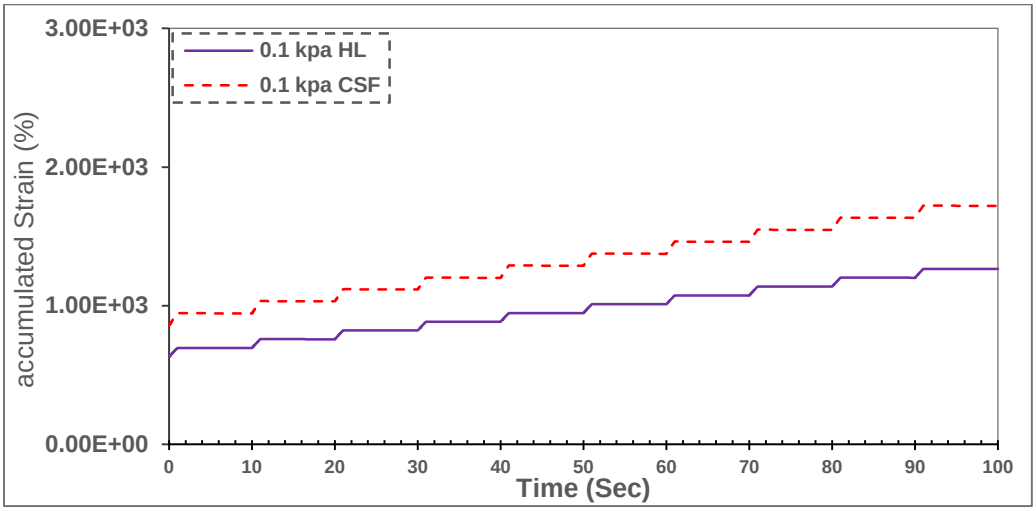


Figure 4.31:- **Effect of filler type on MSCR 0.1 kPa total strain for 25% HL & CSF mastics at 64oC**

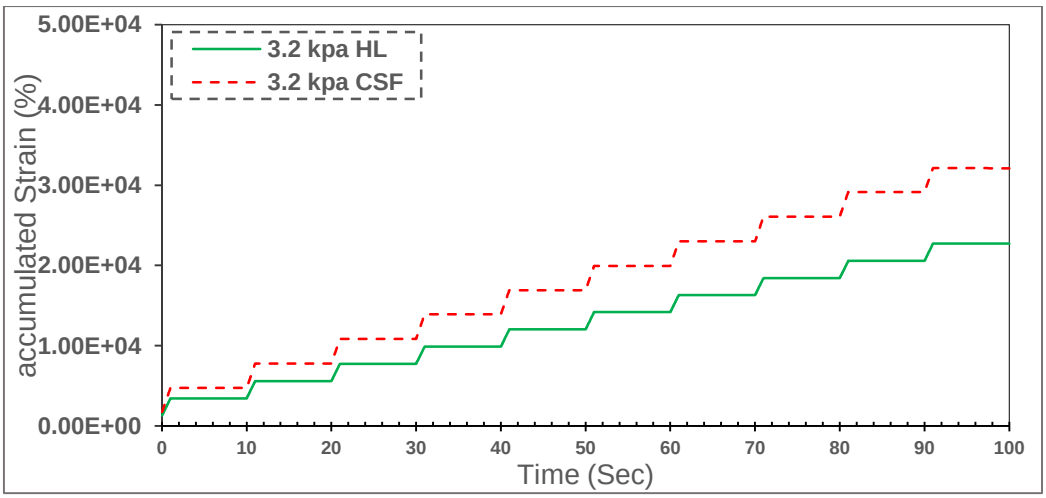


Figure 4.32:- **Effect of filler type on MSCR 0.1 kPa total strain for 25% HL & CSF mastics at 64oC**

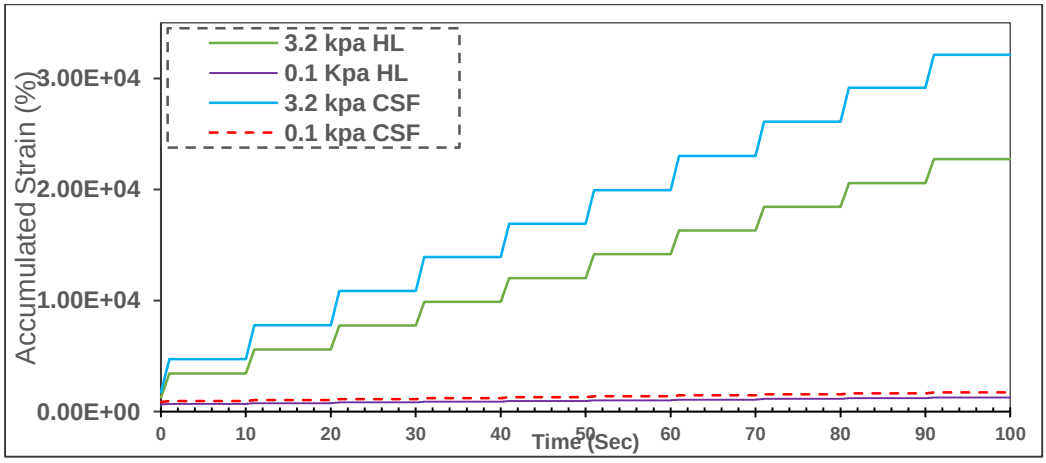


**Figure 4.33:-** Effect of filler type on MSCR total strain for 25% HL & CSF mastics at 64°C

Table 4.9:- **Summary of Jnr and PR (%) Results**

| Mastic type | Temperature (°C) | $J_{nr}$ (kPa$^{-1}$) | | $J_{nr\text{-}diff}$ (kPa$^{-1}$) | PR (%) | | PG designation |
|---|---|---|---|---|---|---|---|
| | | τ = 0.1 | τ = 3.2 | | τ = 0.1 | τ = 3.2 | |
| **Neat Binder** | 52 | 1.06 | 1.06 | 0.00 | 4.781 | 2.8 | PG52-YY(H) |
| | 58 | 1.70 | 1.84 | 8.24 | 5.71 | 1.92 | PG58-YY(H) |
| | 64 | 6.64 | 6.88 | 3.61 | 1.37 | 0.00 | -- |
| | 70 | 9.64 | 10.22 | 6.02 | 1.3876 | 0.00 | -- |
| **25% HL** | 52 | 0.407 | 0.410 | 0.74 | 9.49 | 3.48 | PG52-YY(E) |
| | 58 | 1.08 | 1.15 | 6.48 | 3.92 | 1.04 | PG58-YY(H) |
| | 64 | 1.01 | 1.15 | 13.86 | 5.51 | 0.61 | PG64-YY(H) |
| | 70 | 6.25 | 6.62 | 5.92 | 0.86 | 0.00 | -- |
| **35% HL** | 52 | 0.191 | 0.196 | 2.62 | 14 | 4.23 | PG52-YY(H) |
| | 58 | 0.43 | 0.51 | 18.6 | 8.4 | 1.57 | PG58-YY(V) |
| | 64 | 0.63 | 0.72 | 14.29 | 7.92 | 1.65 | PG64-YY(V) |
| | 70 | 3.76 | 4.07 | 2.24 | 2.86 | 0.19 | PG70-YY(S) |
| | 76 | 5.19 | 6.64 | 27.94 | 6.91 | 0 | -- |
| **45% HL** | 58 | 0.12 | 0.11 | 8.33 | 24.73 | 6.20 | PG58-YY(E) |
| | 64 | 0.09 | 0.13 | 44.44 | 40.47 | 12.61 | PG64-YY(E) |
| | 70 | 0.56 | 0.62 | 10.71 | 28.5 | 1.64 | PG70-YY(V) |
| | 76 | 0.98 | 1.43 | 45.92 | 4.06 | 1.18 | PG76-YY(H) |
| | 82 | 2.25 | 2.41 | 7.11 | 3.16 | 0.45 | PG82-YY(S) |

***N.B*** **–**the recovery stain should be less than strain at the end of creep to compute percent of recovery otherwise the material has on plastic region (viscous region) and does not recover after loading off. Therefore, Zero percent recovery means the material dose not recover after load removed.

Figure 4.34 and 4.35 shows the relationships between Jnr and temperature tested at 3.2 kPa shear stress levels. Asphalt binder with higher $J_{nr}$ value typically measure lower stiffness. It is shown in this figure that the increase in temperature reduced the stiffness properties of the asphalt binder. This shows that higher Jnr value has a lower shear modulus and less resistance of permanent deformation (rutting).

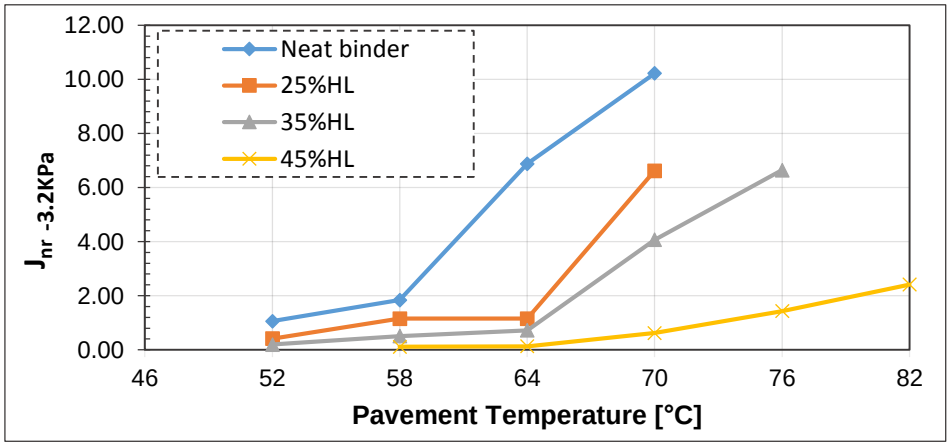


**Figure 4.34:-**Non recoverable creep compliance Jnr-3.2kpa

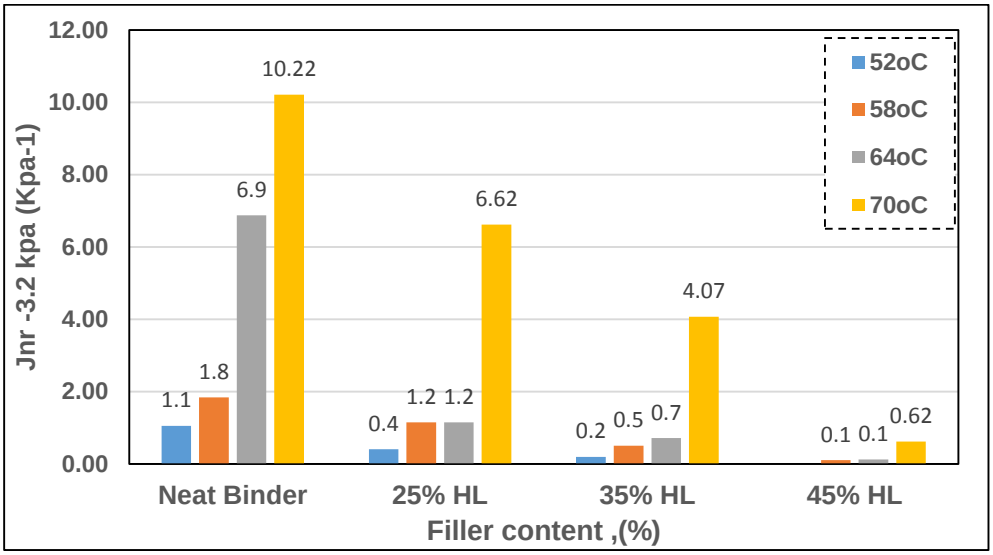


**Figure 4.35:-** Effect of temperature and filler content on $J_{nr}$ at 3.2kPa

Figures 4.36 shown below the rutting parameter (Jnr) decreases as the percentage of hydrated lime filler increase and increases as the temperature increases. This refers that addition of filler could stiffen the binder and improve the resistance of asphalt pavements to rutting at all temperatures especially at lower temperatures. For a given test temperatures, slightly higher Jnr (3.2) value was obtained compared to the Jnr (0.1). MSCR tests results are presented in **Appendix F.**

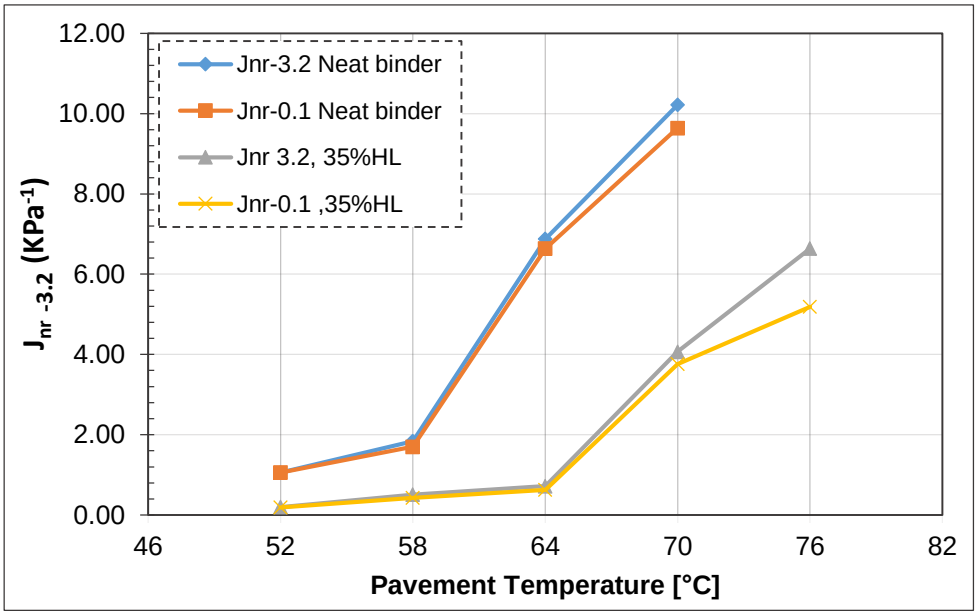


**Figure 4.36:-** Non recoverable creep compliance $J_{nr\text{-}3.2kpa}$ & $J_{nr\text{-}0.1kpa}$

# CHAPTER 5. CONCLUSION AND RECOMMENDATION

The main objective of the study is to determine the effect of hydrated lime as filler on asphalt binder rheology and mastic property of HMA in order to evaluate the distress caused by traffic loading and weather conditions (Temperature).

## 5.1. Conclusion

Based on the experimental result & analysis obtained the following conclusion could be drawn.

From test result obtained from AST the LVE range for all mastics are influenced by temperature and Aging. The stiffness of mastics increase as the temperature decreases and vice versa. However, the percentage of filler content in binder has increases the stiffness of mastics and making stiffer at high temperature than Neat binder itself.

From test result obtained from FST For all mastics in almost similar pattern shear stiffness decreases as temperature increases. At high temperature and low frequency the smaller value of shear modulus is pronounced but increases as filler increase. The stiffening effects of both mineral filler are relatively larger at shorter loading times and at high temperatures, beside hydrated lime filler more suitable at long loading time and at high temperature. Therefore, hydrated lime filler are used to protect permanent deformation or rutting at high temperature and slow speed than crushed stone filler. Hydrate lime filler reduce the aging effect on the neat binder, this help to remove unnecessary stiffening effect during Mixing and construction.

From complex modulus master curve result Hydrate lime mastics with 45% filler ratio had the largest change in complex modulus as a function of loading frequency having the highest complex modulus values of all the mastics and neat binder at high frequencies and lowest values at low frequencies. Therefore, hydrated lime filler are used to protect permanent deformation or rutting at high temperature and slow speed

From phase angle master curve result all the mastics tend to converge towards the same phase angle versus loading frequency relationship at high frequencies (low

temperatures).this shows that Binder elastic property more influence than filler type and content.

From MSCR the non-recoverable creep compliance(Jnr) decreases and the percent of recovery increases as the filler content Increase in the mastic, this show mastics elasticity increases as filler content increase this improve the performance of the binder at high temperature and low frequency. Thus Filer material for modifying binder is recommendable to minimize rutting

In general hydrated lime filler has better rheological performance than crushed stone filler at low frequency and high temperature, this helps to improve the rutting performance of asphalt mixture at high temperature.

## 5.2. Recommendation

Based on the results of this study, the following recommendations can be made to improve the filler effect on asphalt binder and to obtain a better asphalt mix.

The study showed that it is possible to improve the rheology and performance asphalt binder with addition of filler, hence, hydrated lime filler has better rheological performance than crushed stone filler and crushed stone filer is the main HMA component used in the country thus it is recommendable to use hydrated lime as a filler in Ethiopia around high temperature area and heavy traffic roads.

This study shows only the effect of filler on mastics at high and intermediate temperature using only Dynamic shear rheometer (DSR) with conditioning RTFOT (short term aging), however the result may not gave us a full rheological properties, therefore detail study should be conduct using test equipment DSR, Bending Beam Rheometer (BBR), Rotational Viscometer (RV), Direct Tension Tester (DDT) with two conditioning Pressure Aging Vessel (PAV) and Rolling thin Film oven test (RTFOT).

Ethiopian road authority (ERA) and the stack holders in road construction would adopt the new SHRP binder specifications were developed to address the shortcomings of the previous asphalt grading systems, for better simulation of actual field condition (Temperature, Loading etc..)

# REFERENCES


- AASHTO - American Association of State Highway and Transportation Officials, (2002), T315 "Determining the Rheological Properties of Asphalt Binder Using a Dynamic Shear Rheometer (DSR)."
- Airey, G.D. (1997). "Rheological Characteristics of Polymer Modified and Aged Bitumens", Ph.D. Thesis, Department of Civil Engineering, University of Nottingham, United Kingdom.
- American Association of State Highway and Transportation Officials (AASHTO), (1997) "Standard specification for mineral filler for bituminous paving mixtures", USA, Washington DC, M07 – 17.
- Anderson D. A., Goetz W.H., (1973) "Mechanical behavior and reinforcement of mineral filler asphalt mixtures", Proc., Association of Asphalt Paving Technologists, Vol. 42.
- Anderson, D.A. (1987). "Guidelines for Use of Dust in Hot-Mix Asphalt Concrete Mixtures" Journal of the Association of Asphalt Paving Technologists, Vol. 56,
- Anderson, D.A., Cristensen, D.W., Bahia, H.U., Dongre, R., Sharma, M.G., Antle, C.E., Button, J., (1994), "Binder characterization and evaluation, Volume 3." SHRP-A-369, Strategic Highway Research Program, National Research Council, Washington, D.C.
- Aragão, F rancisco, (2007), "Effects of aggregates on properties and performance of mastics and Superpave hot mix asphalt mixtures". Civil Engineering Theses
- Bahia, H.U and Anderson, D.A., "The new proposed rheological properties of asphalt binders: why are they required and how do they compare to conventional properties." Physical Properties of Asphalt Cement Binders, STP 1241. ASTM Publication Code Number (PCN): 04-0122410-08.
- Berger, E.& Huege, F., ( 2004), " The Use of Hydrated Lime in Hot Mix Asphalt" Chemical Lime Company-Lhoist, TXUSA
- Brown, E. R., Kandhal, P. S., & Zhang, J. (2001) "Performance Testing for Hot Mix Asphalt (Executive Summary)". Report 01-05A, National Center for Asphalt Technology (NCAT), Auburn.
- Christopher, R.W. ,2004," Development of Laboratory Performance Test Procedures and Trial Specifications for Hot Mix Asphalt" Final Report, Michigan Technological University,
- Huang, B., Xiang, S., and Xinwei, C., (2007)"Effects of Mineral Fillers on Hot-Mix Asphalt Laboratory Measured Properties", International Journal of Pavement Engineering, Volume 8, No. 1, USA.
- Hugo, B., Rodrigo, M., Felix, P.J., and Adriana, H.M., (2007) "Effect of Calcareous Fillers on Bituminous Mix Aging", Transportation Research Record, Journal of the Transportation Research Board, Volume 1998, USA,

- Ishai, I. and Craus, J. (1977). "Effect of the Filler on Aggregate-Bitumen Adhesion Properties in Bituminous Mixtures" Journal of the Association of Asphalt Paving Technologists, Vol. 46, pp. 228-258.
- Johansson L. (1998) "Bitumen Ageing and Hydrated Lime", Ph.D. Dissertation, TRITA-IP FR 98-38, Royal Institute of Technology, Stockholm, Sweden.
- Kandhal, P. S., & Mallick, R. B. (1998). Open-Graded Asphalt Friction Course: State of the Practice. Report 98-07 for the National Center for Asphalt Technology (NCAT). Auburn.
- Kandhal, P.S., C.Y. Lynn, and F. Parker, Jr., (1998), "Characterization Tests for Mineral Fillers Related to Performance of Asphalt Paving Mixtures". NCAT Report No.98-2. Auburn University, AL., January.
- Kavussi, A. and Hicks, R.G. (1997). "Properties of Bituminous Mixtures Containing different Fillers" Journal of the Association of Asphalt Paving Technologists, Vol. 66, pp. 153-186.
- Lesueur, D. and Little, D. N., (2003) "Effect of Hydrated Lime on Rheology, Fracture and Ageing of Bitumen", Transportation Research Record, No. 1661, pp. 93-105.
- Little, D.N. and Petersen, J.C. (2005). "Unique Effects of Hydrated Lime Filler on the Performance-Related Properties of Asphalt Cements: Physical and Chemical Interactions Revisited", Journal of Materials in Civil Engineering, Vol. 17, No. 2, pp. 207-218.
- McGennis, R.B., Shuler, S., Bahia, H.U, (1994) "Background of SUPERPAVE ASPHALT BINDER TEST METHODS", Publ no. FHWA-SA-94-069. Federal Highway Administration, Washington, D.C.
- Mogawer WS, Stuart KD (1996), Effects of mineral fillers on properties of stone matrix asphalt mixtures. Transportation Research Record 1530, Transportation Research Board, National Research Council, Washington DC, USA. TBR86-94.
- OLADAPO, S.A. and ADETORO, A.E, Comparative Analysis of Effects of Filler Materials on Performance of Asphalt, International Journal of Engineering and Innovative Technology (IJEIT)Volume 4, May 2015, Ado-Ekiti, Nigeria
- Petersen, J.C., Plancher, H. and Harnsberger, P.M. (1987). "Lime Treatment of Asphalts to Reduce Age Hardening and Improve Flow Properties", Journal of the Association of Asphalt Paving Technologists, Vol. 56, pp. 632-653.
- Petersen, J.C., Robertson, R.E., Branthaver, J.F., Harnsberger, P.M., Duvall, J.J., Kim, S.S., Anderson, D.A., Christiansen, D.W., and Bahia, H.U. "Binder charactericzation and evaluation, Volume 1." SHRP-A-367, Strategic Highway Research Program, National Research Council, Washington, D.C. 1994.
- Plancher, H., Green, E.L. and Petersen, J.C. (1976). "Reduction of oxidative hardening of asphalts by treatment with hydrated lime – a mechanistic study." Asphalt Paving Technology.
- Puzinauskas VP (1969), "Filler in asphalt mixtures", The Asphalt Institute Research Report 69-2, Lexington, Kentucky.

- R Muniandy*, E Aburkaba and R Taha(2013), "Effect of Mineral Filler Type and Particle Size on the Engineering Properties of Stone Mastic Asphalt Pavements", Univerity Putra Malaysia,
- Tangella, S. C. S., Craus, J, Deacon, J. A., & Monismith, C. L. (1990) Summary report on Fatigue Response of Asphalt Mixtures. Report SHRP-A-312, Strategic Highway Research Program.National Research Council, Washington, D.C.
- Traxler, R.N. and Miller, J.S. (1936). "Mineral Powders, Their Physical Properties and Stabilizing Effects", Proceedings of the Association of Asphalt Paving Technologies, Vol. 7.
- Tunnicliff, D.G. (1962). "A Review of Mineral Filler", Journal of the Association of Asphalt Paving Technologies, Vol. 31, pp. 119-147.
- Tunnicliff, D.G. (1967). "Binding Effects of Mineral Filler", Journal of the Association of Asphalt Paving Technologies, Vol. 36, pp. 114-156.
- Witczak, M. W., Kaloush, K., Pellinen, T., Basyouny, M. E., & Quintus, H. V. (2002), "Simple Performance Test for Superpave Mix Design". Report NCHRP-465, National Cooperative Highway Research Program. National Research Council, Washington, D.C
- Wojciech, G., and Jaroslaw, W., (2008), "The Structure of Mineral Fillers and Their Stiffening Properties in Filler-Bitumen Mastics", Journal of Materials and Structures, Volume 41, No. 4, USA,
- Whiteoak, C. D., (1990), The Shell Bitumen Handbook. Surrey, UK: Shell Bitumen, Hastead, W. J., (1985), "Relation of Asphalt Chemistry to Physical Properties and Specifications" Proceedings of the Association of Asphalt Paving Technologists, vol. 54, pp. 91-117,

## APPENDIX A- Material quality test result

***Table A-1:-*** physics properties of asphalt binders

| Types of Test | Test Trials | Test Replication | | Average |
|---|---|---|---|---|
| Penetration at 25°C , 100g,5s (0.1mm) | Trial -1 | 67.1 | 66.2 | |
| | Trial -2 | 68.2 | 67.6 | |
| | Trial -3 | 65.5 | 66.5 | |
| | Average | **66.9** | **66.8** | **66.9** |
| Ductility at 25°C(mm) | Brucket-1 | 155 | 155 | |
| | Brucket-2 | 155 | 155 | |
| | Brucket-3 | 155 | 155 | |
| | Average | **155** | **155** | **155.0** |
| Softening point (°C) | Ring-1 | 50.5 | 50.1 | |
| | Ring-2 | 50.5 | 50.3 | |
| | Average | **50.5** | **50.2** | **50.4** |
| Flash & Fire Point | Trial -1 | 307 | 305 | |
| | Trial -2 | 305 | 304 | |
| | Average | **306** | **304.5** | **305.3** |

***Table A-2:-*** Bitumen quality test result

| I. No | Test description | Test method | ERA specification | Test result |
|---|---|---|---|---|
| 1 | Ductility,5cm/min at 25°c | AASHTO T-51 | Min. 100 | 100+cm |
| 2 | Penetration,100gm,5sec at 25°c | AASHTO T-49 | 60-70 | 66.9 |
| 3 | Flash point, °c | AASHTO T-48 | 232°C (450°F) | 305°C(586°F) |
| 4 | Specific Gravity | AASHTO T228 | - | 1.015 |
| 5 | Softening point | AASHTO T-053 | | 50.4$^{o}$C(123$^{o}$F) |

***Table A-3:-***aggregate quality test result

| I. N | Test description | Test Method | Specification (ERA, 2002) | Test Result |
|---|---|---|---|---|
| 1 | Particle shape, Flakiness, % | BS 812, Part 105 | < 45 | 17 |
| 2 | Los Angeles Abrasion, % | AASHTO T96 | < 30 | 14 |
| 4 | Aggregate Crushing Value, ACV, % | BS 812, Part 110 | < 25 | 19 |
| 6 | Water absorption, % | ASTM C 127 | < 2 | 1.8 |
| 7 | Specific Gravity (Bulk) | | | |
| | i. Coarse Aggregate | AASHTO T85 | - | 2.70 |
| | ii. Fine Aggregate | AASHTO T84 | - | 2.65 |

## APPENDIX B –Amplitude Sweep Test (AST) test result

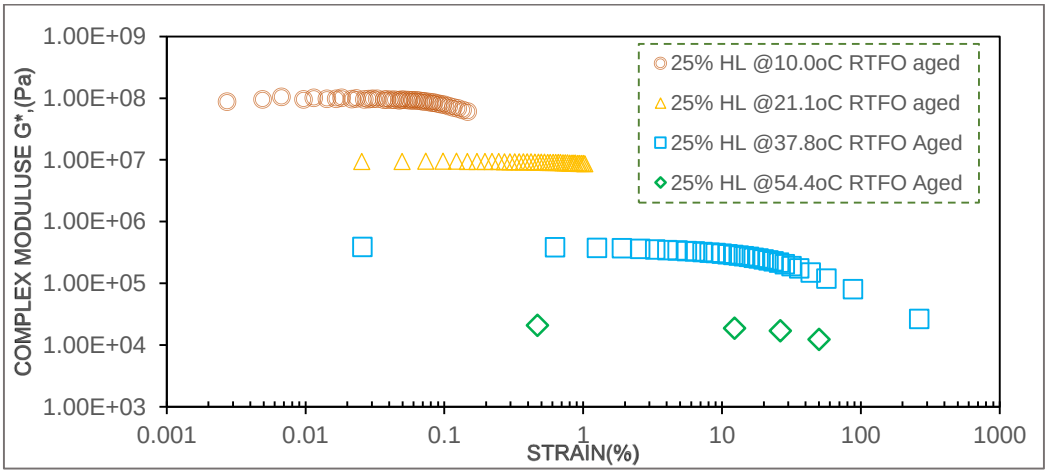


***Figure B-1:- :-*** *Effect of temperature on LVER for 25%HL Aged mastic*

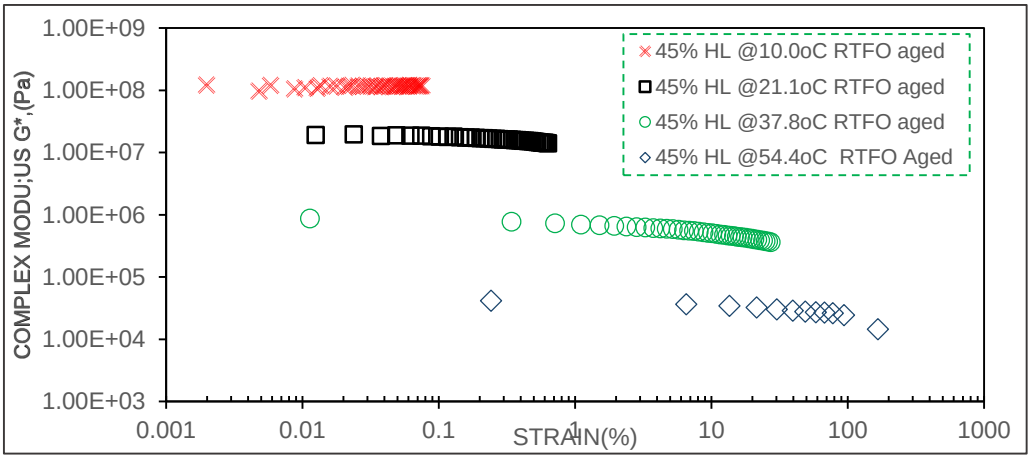


***Figure B-2:-*** *Effect of temperature on LVER for 45%HL Aged mastic*

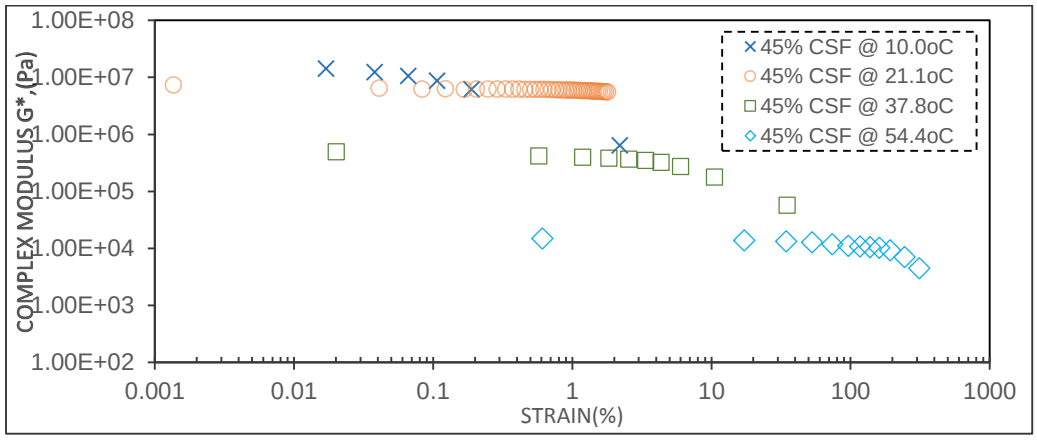


***Figure B-3:-*** *Effect of temperature on LVER for 45% CSF Unaged mastic*

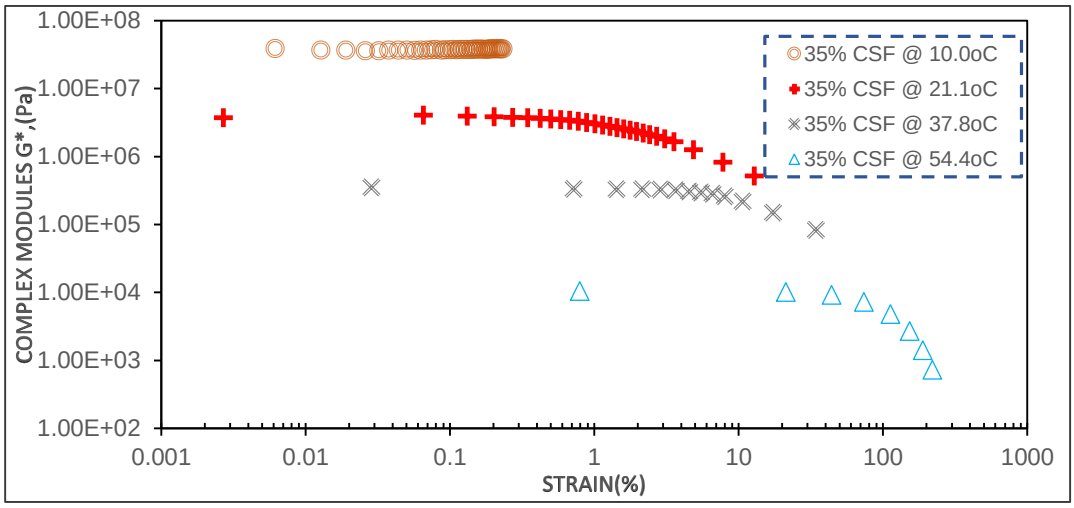


***Figure B-4:-****Effect of temperature on LVER for 35% CSF Unaged mastic*

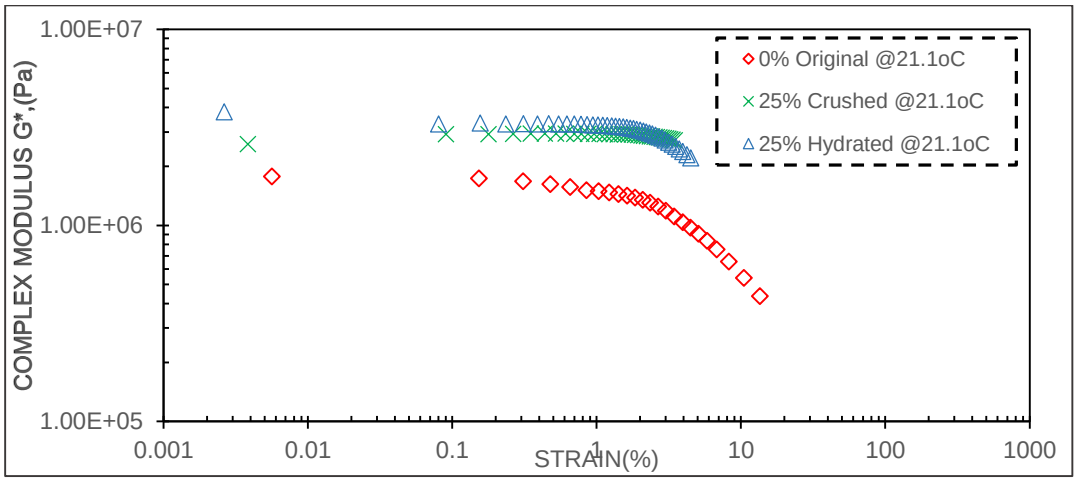


***Figure B-5:-*** *Effect of filler type on LVER for CSF & HL Unaged mastic at 21.1°C*

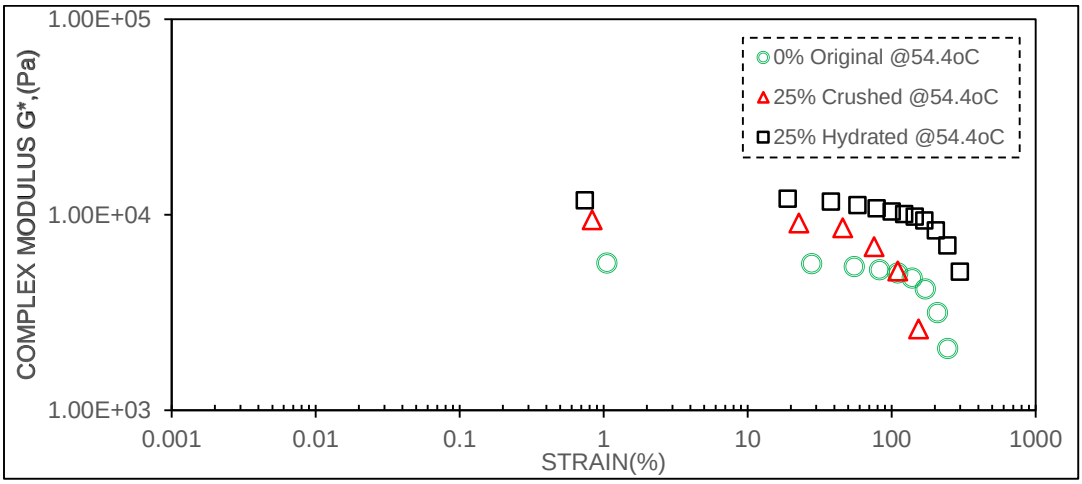


***Figure B-5:-****Effect of filler type on LVER for CSF & HL Unaged mastic at 54.4°C*

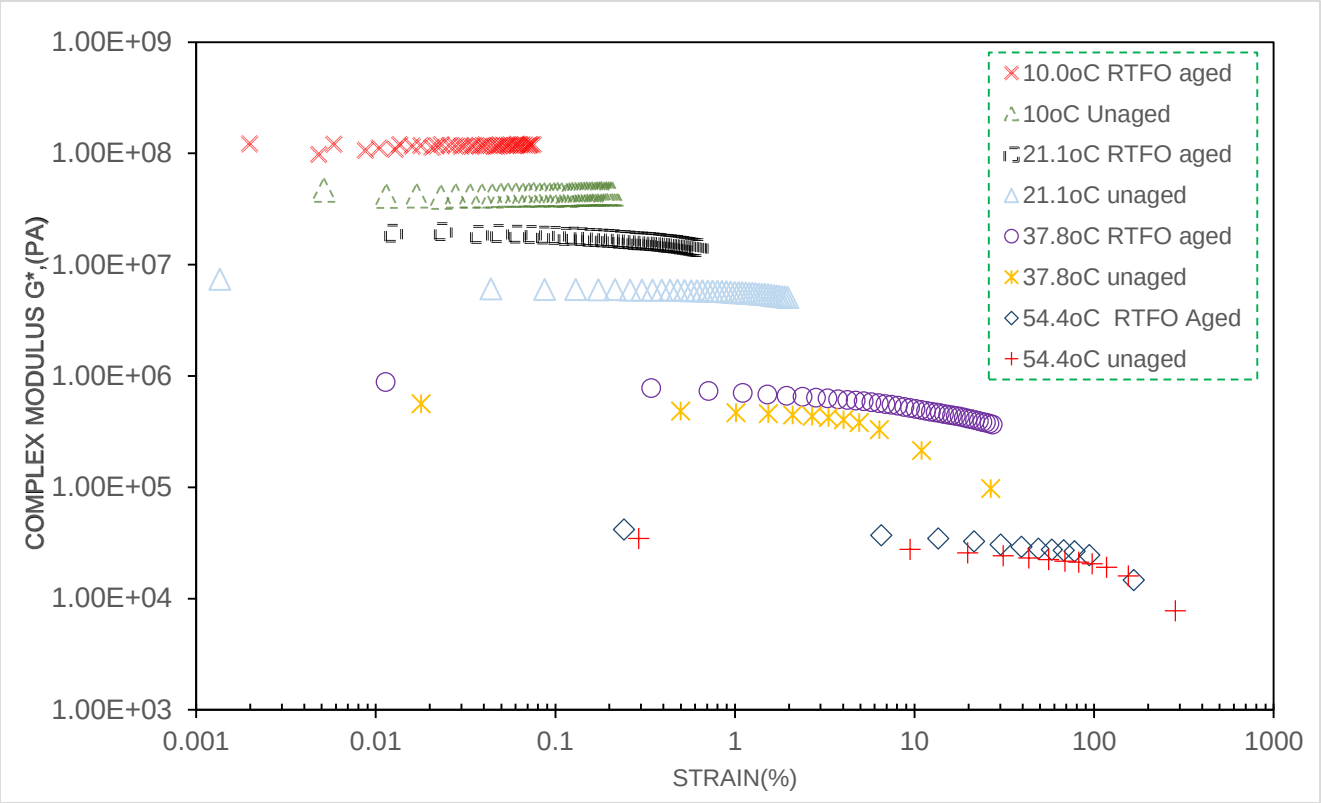


***Figure B-5:-****Effect of aging on LVER for 45%HL mastic*

## APPENDIX C – Frequency Sweep Test (FST) test result

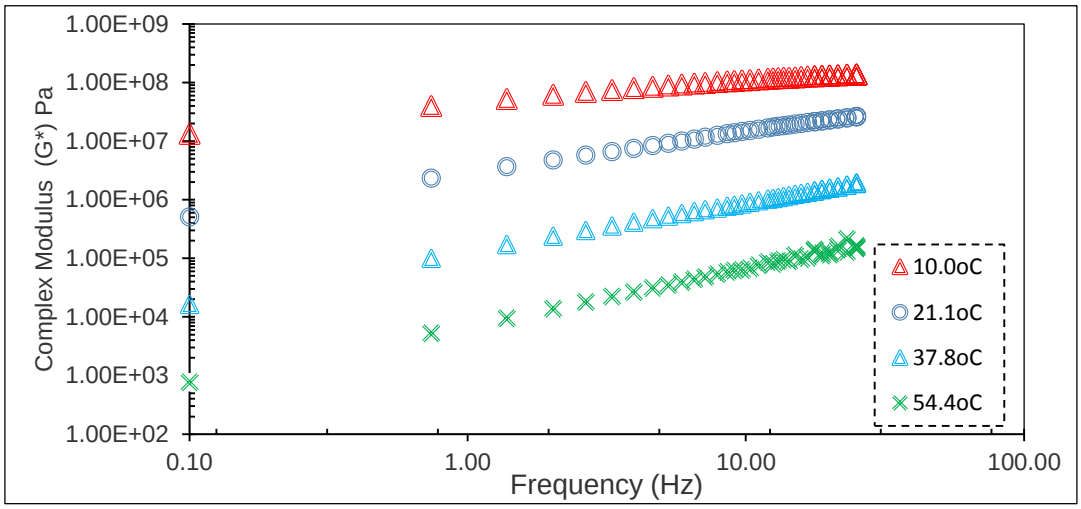


***Figure C-1:-*** *Effect of temperature on Complex modulus result for 35% HL mastics*

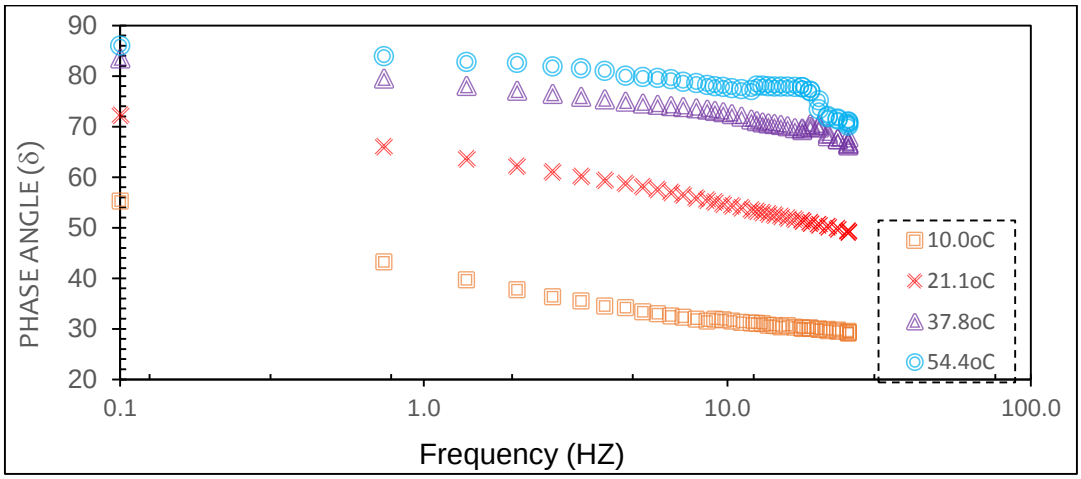


***Figure C-2:-*** *Effect of temperature on Phase angle result for 35% HL mastics*

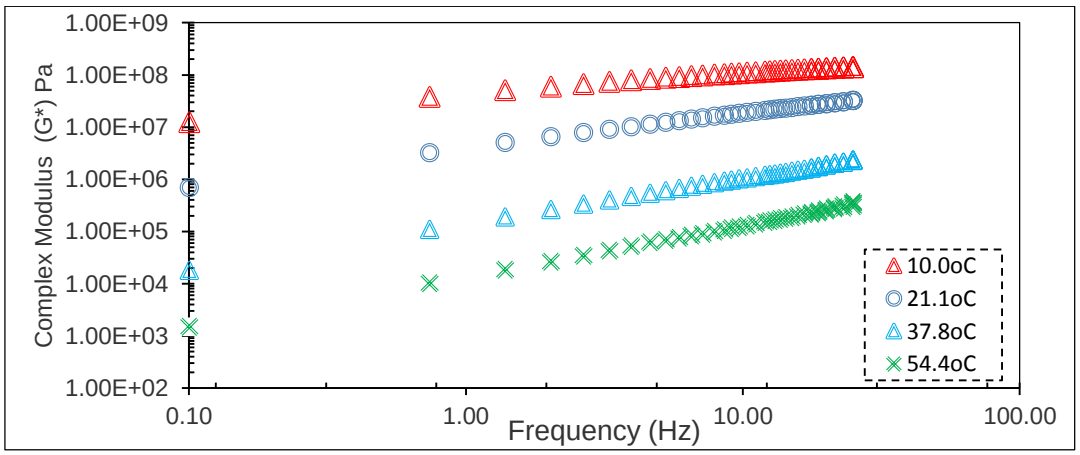


***Figure C-3:-*** *Effect of temperature on Complex modulus result for 45% CSF mastics*

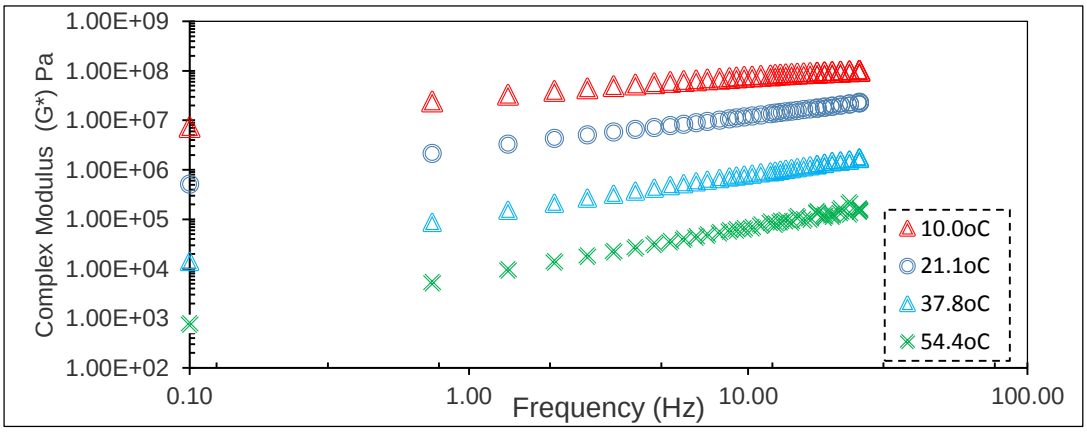


***Figure C-4:-*** *Effect of temperature on Phase angle result for 35% CSF mastics*

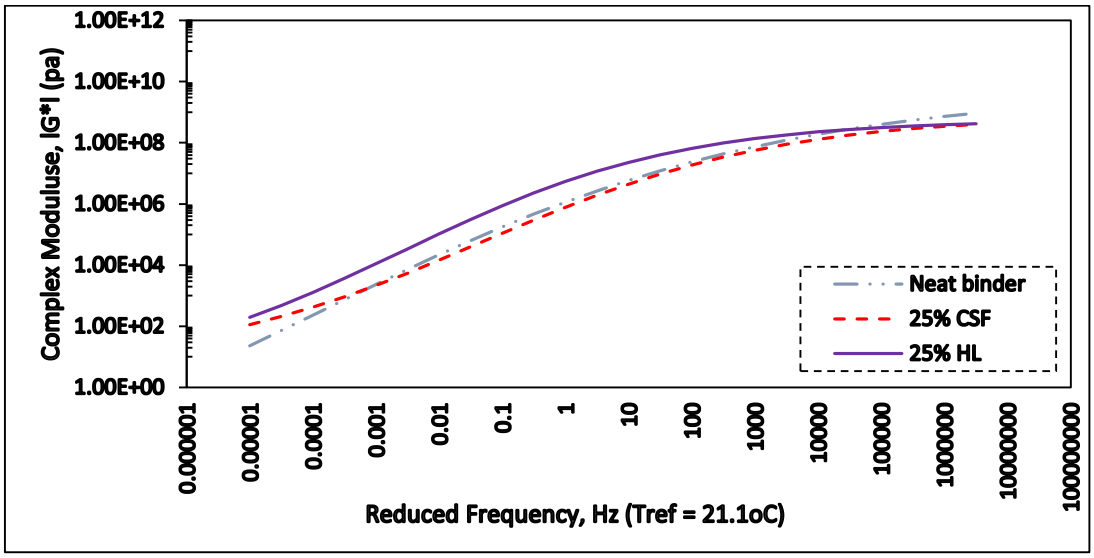


***Figure C-5:-*** *Effect of filler type on Stiffness Master Curve for mastics at 25%*

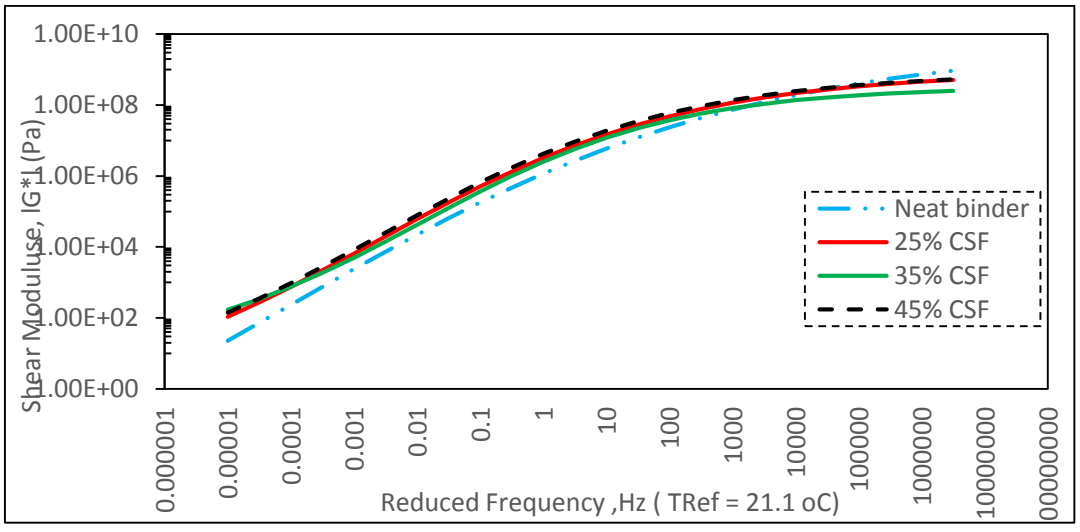


***Figure C-6:-*** *FST Stiffness Master Curve for mastics with Crushed stone*

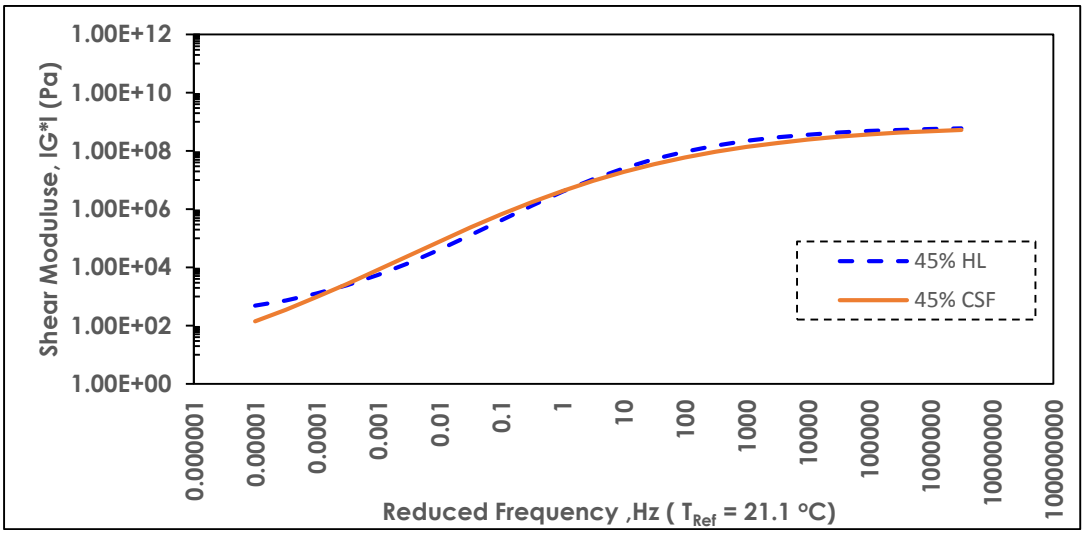


***Figure C-7:-*** *FST Stiffness Master Curve for 45% HL and CSF mastics*

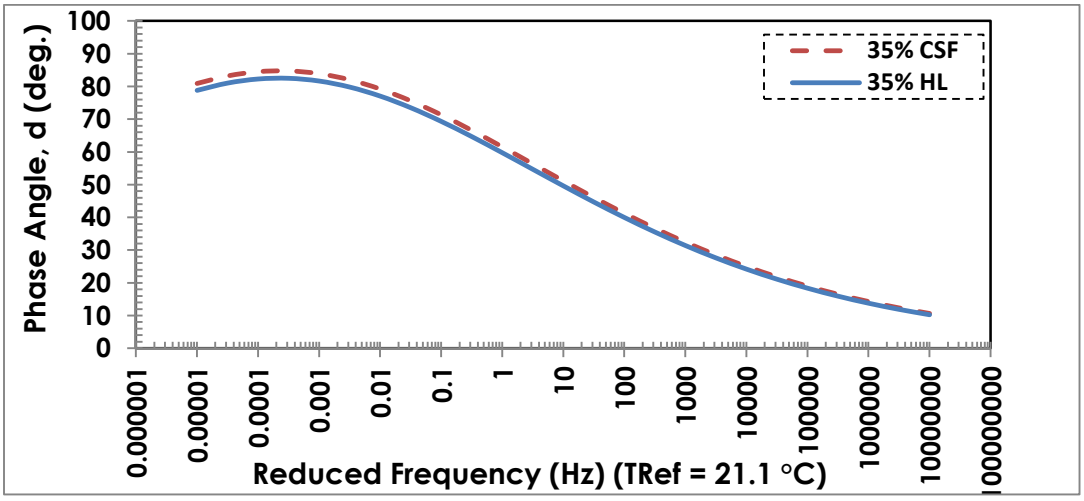


***Figure C-8:-*** *FST Phase angle Master Curve for 35% HL and CSF mastics*

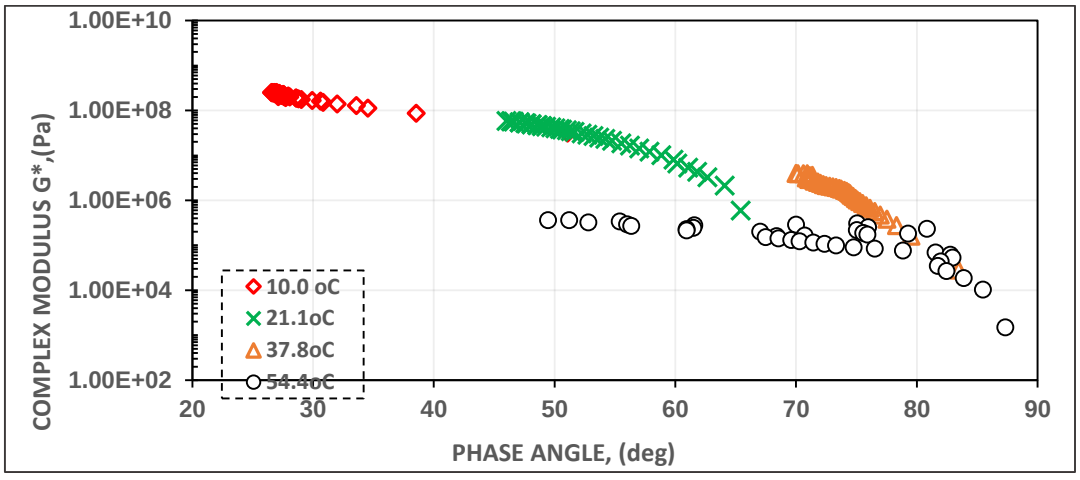


***Figure C-9:-*** *FST Black space Diagram for 45% HL*

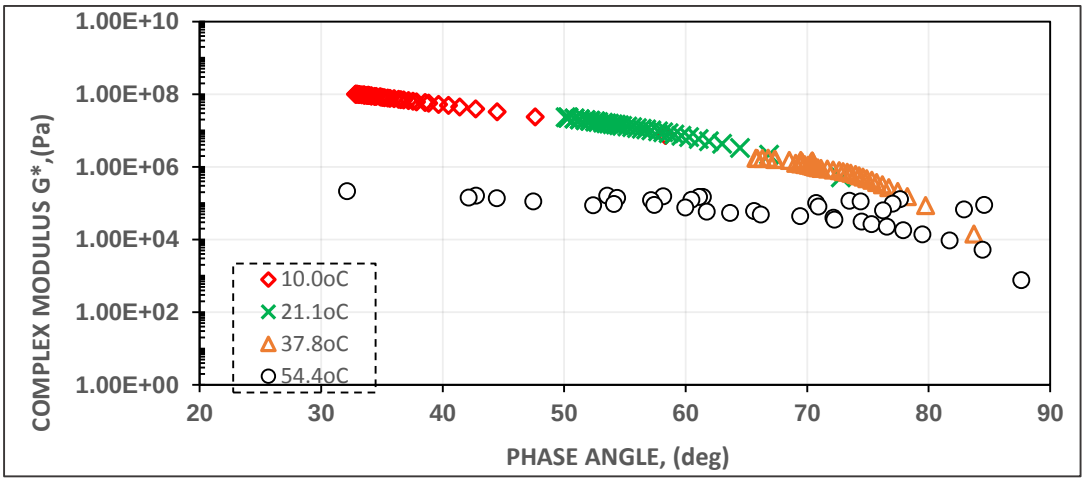


***Figure C-10:-*** *FST Black space Diagram for 35% CSF*

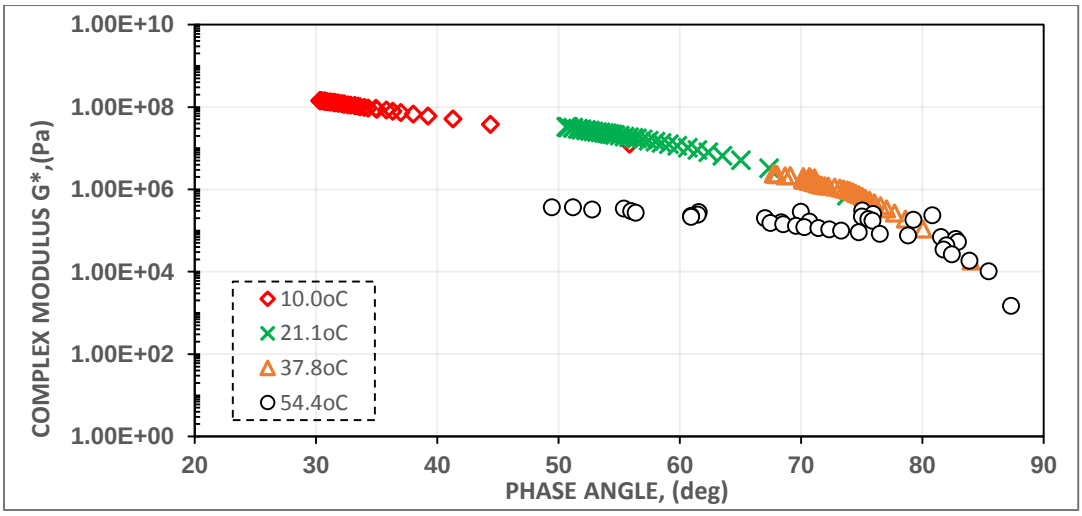


***Figure C-11:-*** *FST Black space Diagram for 45% CSF*

## APPENDIX D – Statically Analysis using ANOVA (using MS-EXCEL)

***Table D-1:-***summary of random sample taken from FST result for analysis of variance (ANOVA)

| Frequency | Filler percentage in asphalt | | | |
|---|---|---|---|---|
| | 0% | 25% | 35% | 45% |
| 1.00E-05 | 2.29E+01 | 1.97E+02 | 1.09E+02 | 4.82E+02 |
| | 7.25E+01 | 4.80E+02 | 2.76E+02 | 7.38E+02 |
| 1.00E+00 | 2.69E+06 | 2.31E+06 | 1.32E+06 | 1.33E+06 |
| | 5.90E+06 | 5.47E+06 | 3.21E+06 | 3.98E+06 |
| 1.00E+06 | 7.30E+08 | 3.92E+08 | 4.55E+08 | 5.70E+08 |
| | 9.35E+08 | 4.24E+08 | 5.10E+08 | 6.00E+08 |

***Table D-2:-***Statistical analysis for FST at f = $10^{-5}$ Hz using ANOVA method of treatment

SUMMARY

| *Groups* | *Count* | *Sum* | *Average* | *Variance* |
|---|---|---|---|---|
| Column 1 | 2 | 9.54E+01 | 4.77E+01 | 1.23E+03 |
| Column 2 | 2 | 6.77E+02 | 3.38E+02 | 4.02E+04 |
| Column 3 | 2 | 3.85E+02 | 1.92E+02 | 1.40E+04 |
| Column 4 | 2 | 1.22E+03 | 6.10E+02 | 3.26E+04 |

ANOVA

| *Source of Variation* | *SS* | *df* | *MS* | *F* | *P-value* | *F crit* |
|---|---|---|---|---|---|---|
| Between Groups | 345771.5 | 3 | 115257.2 | 5.237547 | 0.071764 | 4.19086 |
| Within Groups | 88023.77 | 4 | 22005.94 | | | |
| | | | | | | |
| Total | 433795.2 | 7 | | | | |

***Table D-3:-***Statistical analysis for FST at f = 10 Hz using ANOVA method of treatment

SUMMARY

| *Groups* | *Count* | *Sum* | *Average* | *Variance* |
|---|---|---|---|---|
| Column 1 | 2 | 8.59E+06 | 4.29E+06 | 5.15E+12 |
| Column 2 | 2 | 7.77E+06 | 3.89E+06 | 5E+12 |
| Column 3 | 2 | 4.53E+06 | 2.27E+06 | 1.79E+12 |
| Column 4 | 2 | 5.31E+06 | 2.66E+06 | 3.53E+12 |

ANOVA

| *Source of Variation* | *SS* | *df* | *MS* | *F* | *P-value* | *F crit* |
|---|---|---|---|---|---|---|
| Between Groups | 5.63E+12 | 3 | 1.88E+12 | 0.485082 | 0.710683 | 4.19086 |
| Within Groups | 1.55E+13 | 4 | 3.87E+12 | | | |
| | | | | | | |
| Total | 2.11E+13 | 7 | | | | |

***Table D-4:-***Statistical analysis for FST at f = $10^{+6}$ Hz using ANOVA method of treatment

SUMMARY

| *Groups* | *Count* | *Sum* | *Average* | *Variance* |
|---|---|---|---|---|
| Column 1 | 2 | 1.67E+09 | 8.33E+08 | 2.1E+16 |
| Column 2 | 2 | 8.16E+08 | 4.08E+08 | 4.94E+14 |
| Column 3 | 2 | 9.65E+08 | 4.83E+08 | 1.49E+15 |
| Column 4 | 2 | 1.17E+09 | 5.85E+08 | 4.44E+14 |

ANOVA

| *Source of Variation* | *SS* | *df* | *MS* | *F* | *P-value* | *F crit* |
|---|---|---|---|---|---|---|
| Between Groups | 2.06E+17 | 3 | 6.86E+16 | 11.68026 | 0.018997 | 4.19086 |
| Within Groups | 2.35E+16 | 4 | 5.87E+15 | | | |
| | | | | | | |
| Total | 2.29E+17 | 7 | | | | |

## APPENDIX D – Performance Grade (PG) test result

***Table E-1:-*** PG determination for Unaged Neat binder

| Test Temperature | Phase Angle (δ) | Complex Modulus(G*) | Elastic Modulus(G′) | Viscous Modulus(G″) | G*/Sind ≥ 1kPa | Remark |
|---|---|---|---|---|---|---|
| (°C) | (°) | (Pa) | (Pa) | (Pa) | (Pa) | |
| 64.04 | 85.83 | 2.66E+03 | 1.94E+02 | 2.66E+03 | 2.67E+03 | Pass |
| 69.95 | 87.03 | 1.21E+03 | 6.24E+01 | 1.20E+03 | 1.21E+03 | Fail |
| Pass Fail Temp.(°C) | 65.5 | | | | | |
| Grade | 64 | | | | | |

***Table E-2:-*** PG determination for Aged Neat binder

| Test Temperature | Phase Angle (δ) | Complex Modulus(G*) | Elastic Modulus(G′) | Viscous Modulus(G″) | G*/Sind ≥ 2.2kPa | Remark |
|---|---|---|---|---|---|---|
| (°C) | (°) | (Pa) | (Pa) | (Pa) | (Pa) | |
| 57.99 | 86.81 | 3.43E+03 | 1.91E+02 | 3.42E+03 | 3.43E+03 | Pass |
| 63.93 | 87.82 | 1.53E+03 | 5.80E+01 | 1.53E+03 | 1.53E+03 | Pass |
| 69.97 | 88.61 | 7.22E+02 | 1.75E+01 | 7.21E+02 | 7.22E+02 | Fail |
| Pass Fail Temp.(°C) | 67.3 | | | | | |
| Grade | 64 | | | | | |

***Table E-3:-*** PG determination for Unaged 25%CSF mastic

| Test Temperature | Phase Angle (δ) | Complex Modulus(G*) | Elastic Modulus(G′) | Viscous Modulus(G″) | G*/Sind ≥ 1kPa | Remark |
|---|---|---|---|---|---|---|
| (°C) | (°) | (Pa) | (Pa) | (Pa) | (Pa) | |
| 58.04 | 86.71 | 5.49E+03 | 3.15E+02 | 5.48E+03 | 5.50E+03 | Pass |
| 64.07 | 87.81 | 2.25E+03 | 8.57E+01 | 2.25E+03 | 2.25E+03 | Pass |
| 70.06 | 88.61 | 1.05E+03 | 2.55E+01 | 1.05E+03 | 1.05E+03 | Pass |
| 75.89 | 89.22 | 5.50E+02 | 7.50E+00 | 5.50E+02 | 5.50E+02 | Fail |
| Pass Fail Temp.(°C) | 71.34 | | | | | |
| Grade | 70 | | | | | |

***Table E-4:-*** PG determination for Aged 25%CSF mastic

| Test Temperature | Phase Angle (δ) | Complex Modulus(G*) | Elastic Modulus(G′) | Viscous Modulus(G″) | G*/Sind ≥ 2.2kPa | Remark |
|---|---|---|---|---|---|---|
| (°C) | (°) | (Pa) | (Pa) | (Pa) | (Pa) | |
| 64.04 | 85.83 | 2.66E+03 | 1.94E+02 | 2.66E+03 | 2.67E+03 | Pass |
| 69.95 | 87.03 | 1.21E+03 | 6.24E+01 | 1.20E+03 | 1.21E+03 | Fail |
| Pass Fail Temp.(°C) | 65.5 | | | | | |
| Grade | 64 | | | | | |

## APPENDIX F - MSCR test result

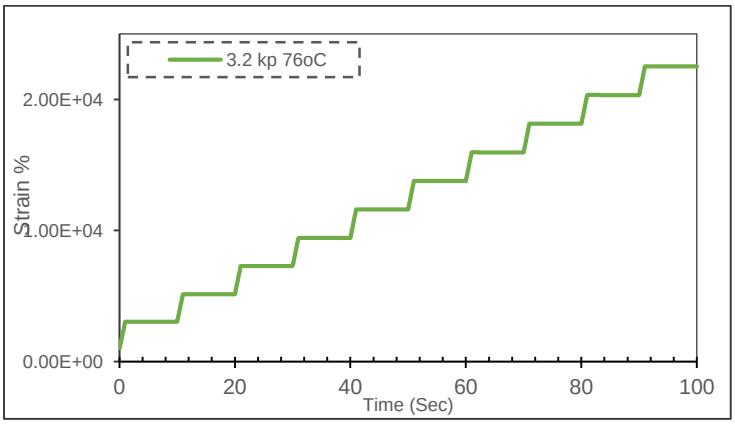


***Figure F-1:-*** *35%HL at 76°C at stress 3200Pa*

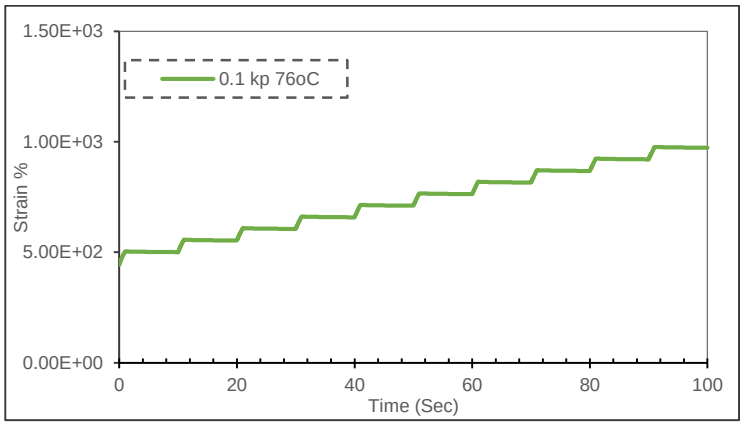


***Figure F-2:-*** *35%HL at 76°C at stress 100Pa*

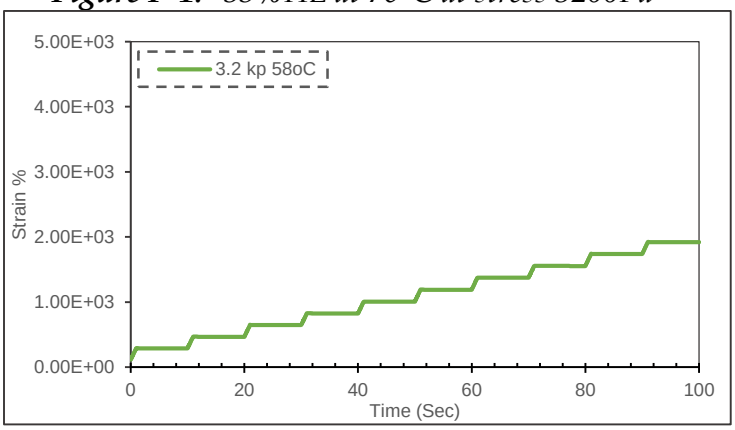


***Figure F-3:-****35%HL at 58°C at stress 3200Pa*

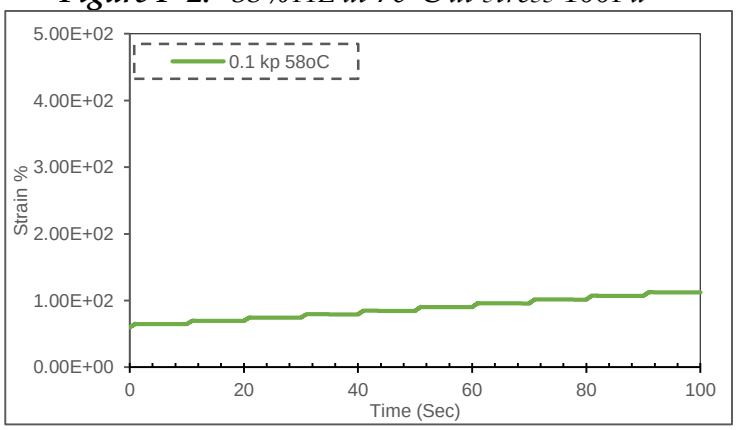


***Figure F-4:-*** *35%HL at 58°C at stress 100Pa*

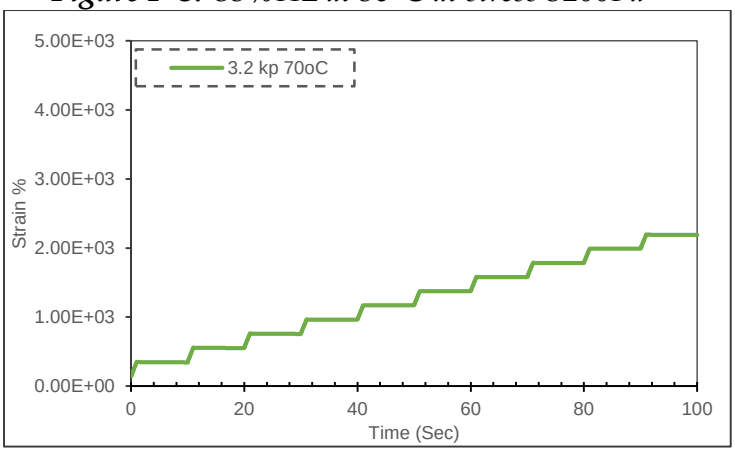


***Figure F-5:-*** *45%HL at 70°C at stress 3200Pa*

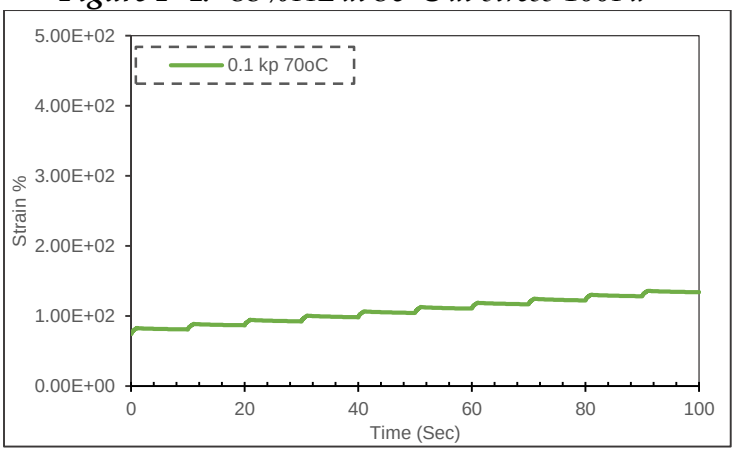


***Figure F-6:-*** *45%HL at 70°C at stress 100Pa*

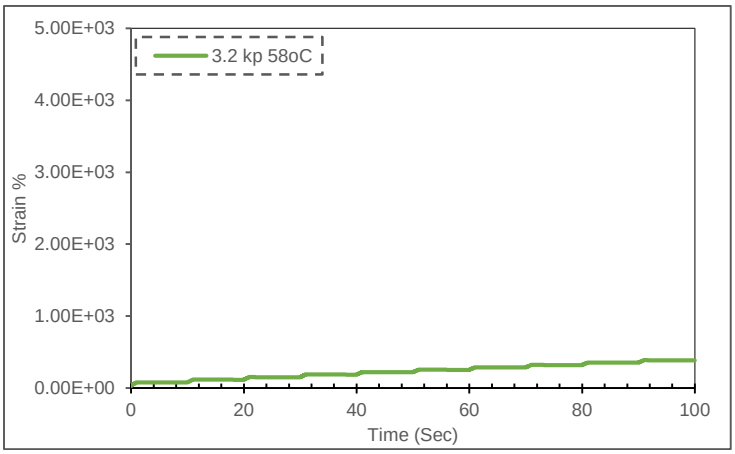


***Figure F-7:-*** *45%HL at 58°C at stress 3200Pa*

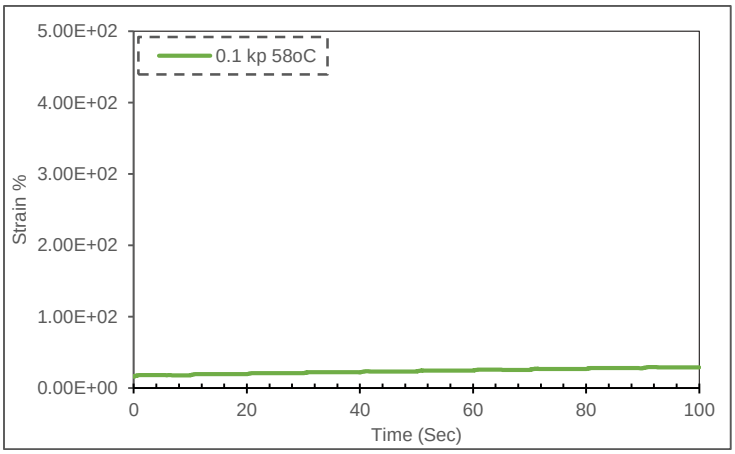


***Figure F-8:-*** *45%HL at 58°C at stress 100Pa*

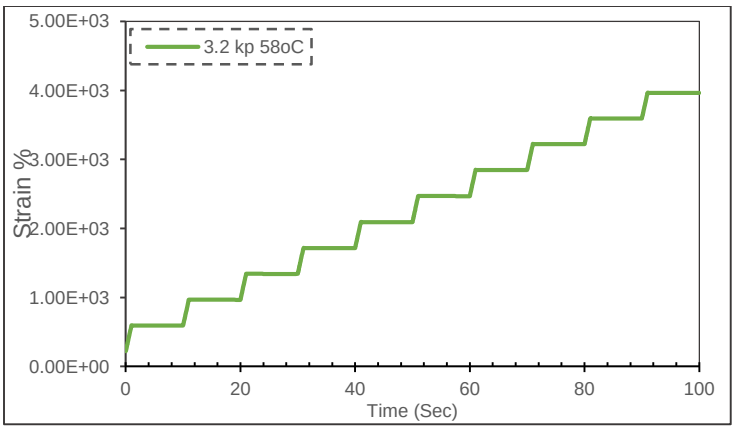


***Figure F-9:-*** *25%HL at 58°C at stress 3200Pa*

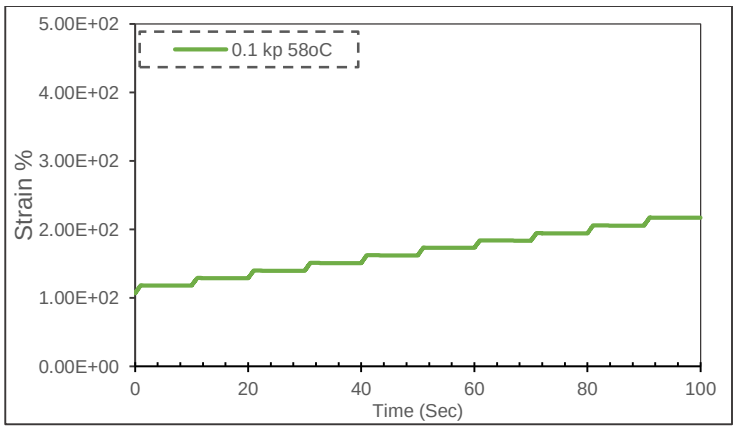


***Figure F-10:-*** *25%HL at 58°C at stress 100Pa*

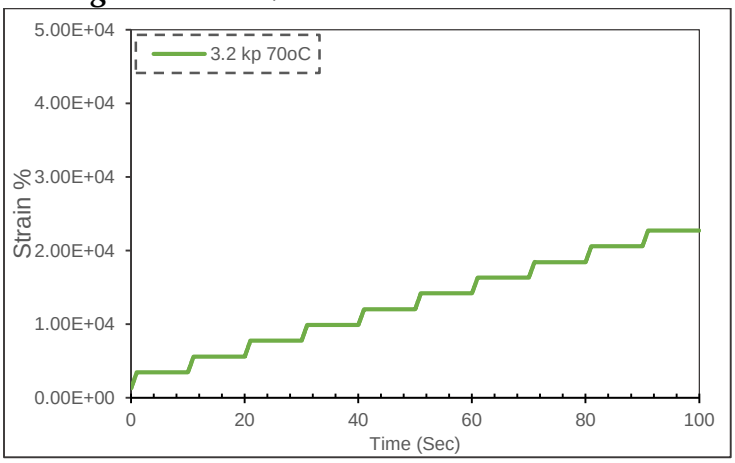


***Figure F-11:-*** *25%HL at 70°C at stress 3200Pa*

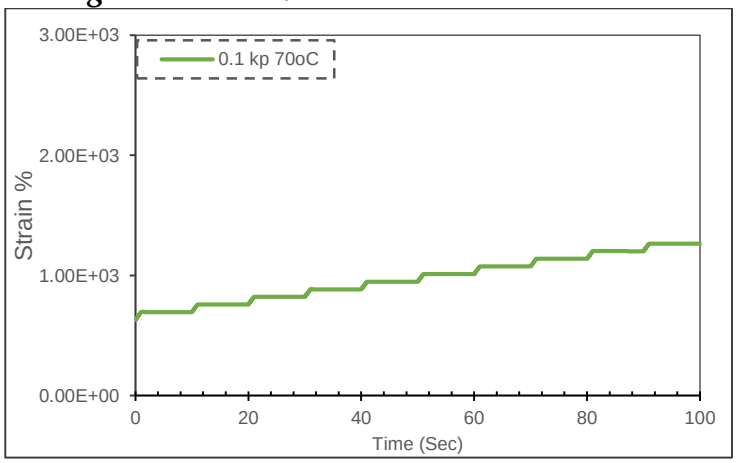


***Figure F-12:-*** *25%HL at 70°C at stress 100Pa*

***Table F-1:-*** MSCR ($J_{nr}$) and %( R) Computation for 25% HL mastics at temperature 70°C

| Stress cycle | Initial strain | Strain at the end of creep (1 sec) | Total strain for 1 sec creep time | Strain at end of 9 sec) Recovery | Total unrecovered strain @ 1sec | Percent of recovery | Jnr, Kpa$^{-1}$ |
|---|---|---|---|---|---|---|---|
| **0.1 kPa** | **a** | **b** | **c=b-a** | **$d=a_{i+1}$** | **e=d-a** | **%R=(d-b)/c** | **$J_{nr}$=e/0.1kPa** |
| 1 | 6.31E+02 | 6.95E+02 | 6.41E+01 | 6.95E+02 | 6.36E+01 | 1% | 6.36 |
| 2 | 6.96E+02 | 7.59E+02 | 6.30E+01 | 7.58E+02 | 6.24E+01 | 1% | 6.24 |
| 3 | 7.59E+02 | 8.22E+02 | 6.28E+01 | 8.21E+02 | 6.22E+01 | 1% | 6.22 |
| 4 | 8.22E+02 | 8.84E+02 | 6.22E+01 | 8.84E+02 | 6.17E+01 | 1% | 6.17 |
| 5 | 8.85E+02 | 9.47E+02 | 6.24E+01 | 9.47E+02 | 6.19E+01 | 1% | 6.19 |
| 6 | 9.47E+02 | 1.01E+03 | 6.30E+01 | 1.01E+03 | 6.24E+01 | 1% | 6.24 |
| 7 | 1.01E+03 | 1.07E+03 | 6.32E+01 | 1.07E+03 | 6.27E+01 | 1% | 6.27 |
| 8 | 1.07E+03 | 1.14E+03 | 6.38E+01 | 1.14E+03 | 6.33E+01 | 1% | 6.33 |
| 9 | 1.14E+03 | 1.20E+03 | 6.32E+01 | 1.20E+03 | 6.27E+01 | 1% | 6.27 |
| 10 | 1.20E+03 | 1.27E+03 | 6.30E+01 | 1.26E+03 | 6.25E+01 | 1% | 6.25 |
| **Temperature** | | **70°C** | | | | 1% | **6.25** |
| | | | | | **Average** | | **6.2526** |
| | | | | | **Minimum** | | **6.1652** |
| | | | | | **Maximum** | | **6.3596** |

***Table F-2:-*** MSCR ($J_{nr}$) and %( R) Computation for 25% HL mastics at temperature 70°C

| Stress cycle | Initial strain | Strain at the end of creep (1 s) | Total strain for 1 sec creep time | Strain at end of 9s )Recovery | Total unrecovered strain @ 1sec | Percent of recovery | Jnr, Kpa-1 |
|---|---|---|---|---|---|---|---|
| **3.2 kPa** | **a** | **b** | **c=b-a** | **d=ai+1** | **e=d-a** | **%R=(d-b)/c** | **Jnr=e/3.2kPa** |
| 1 | 1.29E+03 | 3.43E+03 | 2.13E+03 | 3.43E+03 | 2.14E+03 | 0% | 6.68 |
| 2 | 3.46E+03 | 5.58E+03 | 2.12E+03 | 5.58E+03 | 2.12E+03 | 0% | 6.63 |
| 3 | 5.61E+03 | 7.73E+03 | 2.12E+03 | 7.74E+03 | 2.13E+03 | 0% | 6.64 |
| 4 | 7.76E+03 | 9.87E+03 | 2.11E+03 | 9.87E+03 | 2.11E+03 | 0% | 6.59 |
| 5 | 9.90E+03 | 1.20E+04 | 2.12E+03 | 1.20E+04 | 2.12E+03 | 0% | 6.63 |
| 6 | 1.21E+04 | 1.42E+04 | 2.12E+03 | 1.42E+04 | 2.12E+03 | 0% | 6.64 |
| 7 | 1.42E+04 | 1.63E+04 | 2.10E+03 | 1.63E+04 | 2.10E+03 | 0% | 6.56 |
| 8 | 1.63E+04 | 1.84E+04 | 2.10E+03 | 1.84E+04 | 2.10E+03 | 0% | 6.56 |
| 9 | 1.85E+04 | 2.06E+04 | 2.10E+03 | 2.06E+04 | 2.10E+03 | 0% | 6.58 |
| 10 | 2.06E+04 | 2.27E+04 | 2.13E+03 | 2.27E+04 | 2.13E+03 | 0% | 6.66 |
| **Temperature** | | **70°C** | | | | 0% | **6.62** |
| | | | | | **Average** | | **6.6165** |
| | | | | | **Minimum** | | **6.5597** |
| | | | | | **Maximum** | | **6.6800** |

| Stress cycle | Initial strain | Strain at the end of creep (1 sec) | Total strain for 1 sec creep time | Strain at end of 9 sec Recovery | Total unrecovered strain @ 1sec | Percent of recovery | Jnr, Kpa$^{-1}$ |
|---|---|---|---|---|---|---|---|

| 0.1 kPa | a | b | c=b-a | d=ai+1 | e=d-a | %R=(d-b)/c | Jnr=e/0.1kPa |
|---|---|---|---|---|---|---|---|
| 1 | 8.59E+02 | 9.47E+02 | 8.78E+01 | 9.44E+02 | 8.54E+01 | 3% | 8.54 |
| 2 | 9.45E+02 | 1.03E+03 | 8.80E+01 | 1.03E+03 | 8.54E+01 | 3% | 8.54 |
| 3 | 1.03E+03 | 1.12E+03 | 8.71E+01 | 1.12E+03 | 8.46E+01 | 3% | 8.46 |
| 4 | 1.12E+03 | 1.20E+03 | 8.53E+01 | 1.20E+03 | 8.31E+01 | 3% | 8.31 |
| 5 | 1.20E+03 | 1.29E+03 | 8.83E+01 | 1.29E+03 | 8.62E+01 | 2% | 8.62 |
| 6 | 1.29E+03 | 1.38E+03 | 8.72E+01 | 1.37E+03 | 8.49E+01 | 3% | 8.49 |
| 7 | 1.38E+03 | 1.46E+03 | 8.69E+01 | 1.46E+03 | 8.48E+01 | 2% | 8.48 |
| 8 | 1.46E+03 | 1.55E+03 | 8.70E+01 | 1.55E+03 | 8.48E+01 | 3% | 8.48 |
| 9 | 1.55E+03 | 1.64E+03 | 8.78E+01 | 1.63 E+03 | 8.58E+01 | 2% | 8.58 |
| 10 | 1.63E+03 | 1.72E+03 | 8.77E+01 | 1.72E+03 | 8.56E+01 | 2% | 8.56 |
| **Temperature** | | **70°C** | | | | 2.6% | **8.51** |

| | |
|---|---|
| **Average** | **8.5069** |
| **Minimum** | **8.3117** |
| **Maximum** | **8.6180** |

**Table F-3:-** MSCR ($J_{nr}$) and %( R) Computation for 25% CSF mastics at temperature 70°C

**Table F-4:-** MSCR ($J_{nr}$) and %( R) Computation for 25% CSF mastics at temperature 70°C

| Stress cycle | Initial strain | Strain at the end of creep (1 sec) | Total strain for 1 sec creep time | Strain at end of 9 sec Recovery | Total unrecovered strain @ 1sec | Percent of recovery | Jnr, $Kpa^{-1}$ |
|---|---|---|---|---|---|---|---|
| 3.2 kPa | a | b | c=b-a | d=ai+1 | e=d-a | %R=(d-b)/c | Jnr=e/3.2kPa |
| 1 | 1.76E+03 | 4.71E+03 | 2.96E+03 | 4.72E+03 | 2.96E+03 | 0% | 9.26 |
| 2 | 4.76E+03 | 7.76E+03 | 3.01E+03 | 7.77E+03 | 3.01E+03 | 0% | 9.42 |
| 3 | 7.81E+03 | 1.08E+04 | 3.03E+03 | 1.08E+04 | 3.04E+03 | 0% | 9.50 |
| 4 | 1.09E+04 | 1.39E+04 | 3.02E+03 | 1.39E+04 | 3.03E+03 | 0% | 9.48 |
| 5 | 1.40E+04 | 1.69E+04 | 2.95E+03 | 1.69E+04 | 2.96E+03 | 0% | 9.25 |
| 6 | 1.70E+04 | 1.99E+04 | 2.98E+03 | 1.99E+04 | 2.99E+03 | 0% | 9.33 |
| 7 | 2.00E+04 | 2.30E+04 | 3.03E+03 | 2.30E+04 | 3.04E+03 | 0% | 9.49 |
| 8 | 2.30E+04 | 2.61E+04 | 3.03E+03 | 2.61E+04 | 3.04E+03 | 0% | 9.51 |
| 9 | 2.61E+04 | 2.92E+04 | 3.03E+03 | 2.92E+04 | 3.04E+03 | 0% | 9.49 |
| 10 | 2.92E+04 | 3.21E+04 | 2.91E+03 | 3.21E+04 | 2.92E+03 | 0% | 9.12 |
| **Temperature** | | **70°C** | | | | 0% | **9.39** |

| | |
|---|---|
| **Average** | **9.3850** |
| **Minimum** | **9.1228** |
| **Maximum** | **9.5096** |

# APPENDICES